# BOVINE INOSITOL MONOPHOSPHATASE : STRUCTURAL AND FUNCTIONAL STUDIES

A thesis submitted to the
Department of Biochemistry
University of Southampton

for the degree of
Doctor of Philosophy

by
Karen Joan Rees-Milton

August 1994

University of Southampton

Abstract

Faculty of Science

Biochemistry

Doctor of Philosophy

# Bovine inositol monophosphatase : Structural and functional studies

By Karen Rees-Milton

Inositol monophosphatase is the putative target of $Li^+$ therapy for manic depression and occupies a pivotal role in the recycling of inositol within the brain. Inositol monophosphatase is involved in both the de-novo synthesis of inositol and the recycling of inositol by the hydrolysis of inositol monophosphate esters derived from the phosphatidylinositol cycle . The uncompetitive nature of $Li^+$ inhibition and the fact that inositol only very poorly crosses the blood-brain barrier, means that $Li^+$ therapy is specific for manic depression. The $\Delta G$ between folded and unfolded inositol monophosphatase is only average, but the $E_a$ for unfolding is high and probably accounts for the high thermostability of the enzyme. It is possible that charge-aromatic interactions between histidine and tryptophan residues make important contributions to the stability of bovine inositol monophosphatase. The N-terminus of inositol monophosphatase is important for activity (Greasley et al., 1993) and near-UV CD and limited proteolysis studies demonstrate a change in the environment of the aromatic amino acids when $Mg^{2+}$ binds, possibly signalling a conformational change at the N-terminus of the enzyme upon $Mg^{2+}$ binding and dissociation. A combination of site directed mutagenesis and chemical modification with diethylpyrocarbonate demonstrates that His-217 is located near the active site.

## ACKNOWLEDGEMENTS

I am indebted to Dr. M.G. Gore for his guidance and advice on all aspects of this work. I must also thank Dr. P. Greasley for his help on numerous occasions over the years and in particular for the preparation of all mutant enzymes used.

I would like to thank all involved in the Gore group over the years for their friendship and assistance: Karen, Steve, the three Nickis, Oliver and Lawrence. Good luck to Mark in continuing the project.

Special thanks to members of Glen and Chamberlain SCR: Kath, Òrla, Carol, Irene, John, Bernard and Kit: with whom I have enjoyed a drink or two during my years in Southampton, for helping to make my time here so enjoyable.

Finally, I would like to thank my parents, Ray and Joan, for all the help and encouragement. This thesis is dedicated to you both.

To my parents, Ray and Joan

# TABLE OF CONTENTS

## FIGURES AND TABLES

## ABBREVIATIONS

| | |
|---|---|
| A | Adenine |
| ALA | Alanine |
| AnalaR | Analytical grade |
| 2'AMP | 2'adenosine monophosphate |
| APS | Ammonium persulphate |
| ASP | Aspartic acid |
| ATP | Adenosine triphosphate |
| CD | Circular dichroism |
| cDNA | Complementary deoxyribonucleic acid |
| CYS | Cys |
| DEPC | Diethylpyrocarbonate |
| $dH_2O$ | Distilled water |
| $ddH_2O$ | Distilled deionised water |
| DMF | Dimethyl formamide |
| DMSO | Dimethyl sulfoxide |
| DNA | Deoxyribonucleic acid |
| DNaseI | Deoxyribonuclease I |
| DTNB | 5,5'-dithiobis (2-nitrobenzoic acid) |
| $E_a$ | Activation energy |
| E.COLI | Escherichia Coli |
| EDTA | Ethylenediaminetetraacetic acid |
| EGTA | Ethylene-bis(oxyethylenenitrilo) tetraacetic acid |
| EMTS | An ethyl derivative of MMTS |
| $\Delta G$ | Conformational energy difference |
| Glc(6)P | Glucose-6-phosphate |
| GLN | Glutamine |
| GLU | Glutamic acid |
| GLY | Glycine |
| 2'GMP | 2'guanidine monophosphate |
| GuHCl | Guanidine hydrochloride |
| HIS | Histidine |
| HPLC | High performance liquid chromatography |

| | |
|---|---|
| Ins(1)P | Inositol(1)phosphate |
| Ins(2)P | Inositol(2)phosphate |
| $Ins(1,4,5)P_3$ | Inositol(1,4,5)trisphosphate |
| IPMTS | An isopropyl derivative of MMTS |
| IPTG | Isopropyl-ß-D-thiogalactoside |
| $K_d$ | Dissociation constant |
| LB | Luria broth |
| LYS | Lysine |
| MES | 2-[N-morpholino] ethane sulfonic acid |
| MMTS | Methylmethanethiosulphonate |
| NEM | N-ethylmaleimide |
| $NTB^{2-}$ | p-Nitrothiobenzoate |
| OD | Optical density |
| $P_i$ | Inorganic phosphate |
| PTH | Phenylthiohydantoin derivative of amino acid |
| RNase | Ribonuclease A |
| SDS | Sodium dodecyl sulphate |
| SDS-PAGE | Sodium dodecyl sulphate polyacrylamide gel electrophoresis |
| SER | Serine |
| T | Absolute temperature |
| TEMED | N,N,N',N'-tetramethylethylenediamine |
| THR | Threonine |
| TNBS | trinitrobenzene sulphonic acid |
| TRIS | Tris(hydroxymethyl)aminomethane |
| TRP | Tryptophan |
| UV | Ultraviolet |

# CHAPTER 1

# INTRODUCTION

# Chapter 1

# Introduction

## 1.1 The phosphatidylinositol cycle and the clinical relevance of inositol monophosphatase

Inositol monophosphatase occupies a pivotal role in the recycling of inositol for the synthesis of the phosphatidylinositol phospholipids in the phosphatidylinositol second messenger signalling pathway of the brain [figure 1.1a]. Inositol monophosphatase is involved both in the de-novo synthesis of inositol from glucose-6-phosphate via Ins(1)P and the breakdown of the inositol monophosphate esters derived from the phosphatidylinositol pathway [figure 1.1a]. Inositol crosses the blood-brain barrier only very poorly (Berridge *et al.*, 1989), hence dietary inositol is not a source of inositol in the brain and inhibition of inositol monophosphatase effectively prevents inositol recycling in the brain. It has been proposed that the effects of lithium in the treatment of manic depression are due to modulation of the phosphatidylinositol cycle second messenger signalling pathway (Berridge *et al.*, 1982, and Nahorski *et al.*, 1991). More specifically, lithium has been shown to inhibit inositol monophosphatase at therapeutically relevant levels (0.5-1.5mM), (Hallcher *et al.*, 1980, and Gee *et al.*, 1988).

The action of lithium is specific for manic depression for two reasons. Firstly, the fact that inositol very poorly crosses the blood-brain barrier means that dietary inositol is not a source of inositol in the brain and secondly, lithium is an uncompetitive inhibitor of inositol monophosphatase. An uncompetitive inhibitor will only bind the enzyme-substrate or enzyme-intermediate complex, it will not bind the free enzyme. Hence, the overactive neurones of manic depression will be preferentially inhibited over the normal neurones.

Unfortunately, the therapeutic use of lithium can only occur under careful medical supervision; lithium has considerable systemic toxicity effects (cardiovascular, renal,

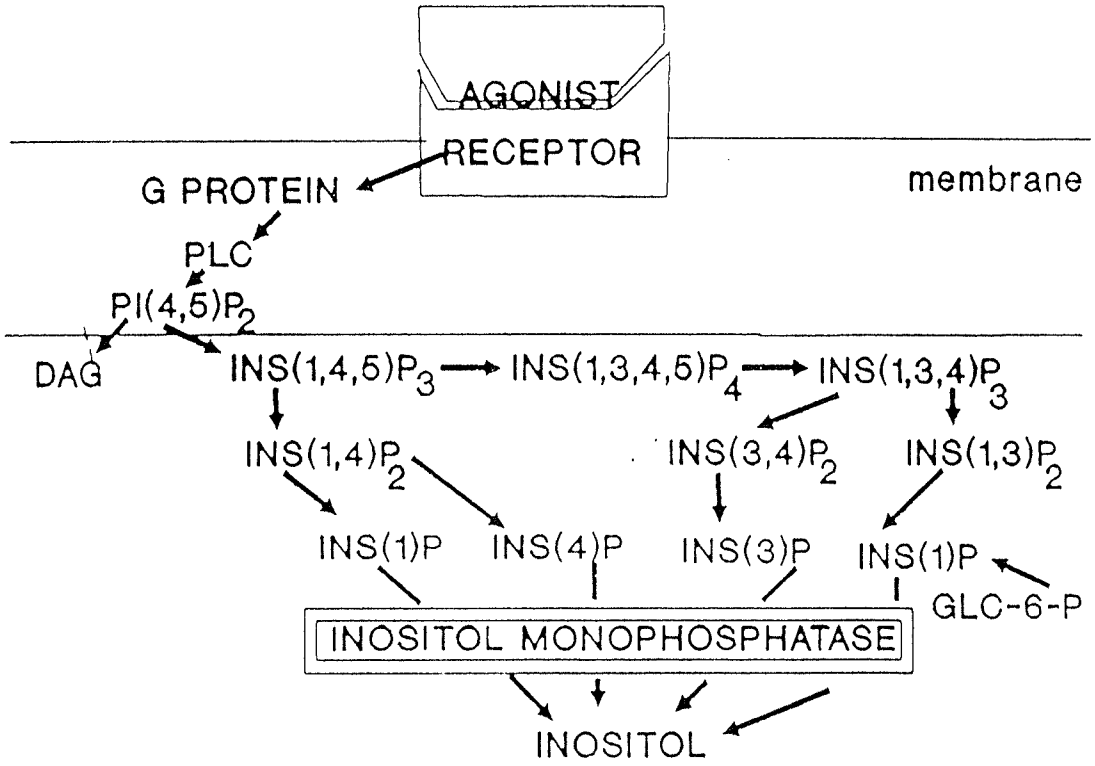


Figure 1.1a: The phosphatidylinositol cycle (adapted from Shears, 1989).

endocrine, gastrointestinal and muscular), which are associated with the chronic use of lithium therapy, (Schrauzer, 1991). Hence, characterisation of inositol monophosphatase, the putative target of lithium therapy, is essential if alternatives are to be found for the treatment of manic depression.

## 1.2 The phosphatidylinositol cycle

The phosphatidylinositol cycle [figure 1.1a], (Shears, 1989), can be viewed more simply from a functional point of view. Upon agonist binding at receptors, phosphatidylinositol-4,5-bisphosphate is hydrolysed by phospholipase C to generate via G-proteins two second messengers, inositol(1,4,5)trisphosphate and 1,2-diacylglycerol. The rest of the pathway serves three functions. The first function of the pathway is to terminate the second messenger activity of $Ins(1,4,5)P_3$ (Downes *et al.*, 1990). The second function of the pathway is to generate further signal molecules, for example, Ins(1,3,4,5)tetrakisphosphate, which together with $Ins(1,4,5)P_3$, is involved in the mobilisation of $Ca^{2+}$ from intracellular stores (Downes *et al.*, 1990). The final function of the pathway is to recycle inositol for the resynthesis of the phosphatidylinositol phospholipids (Downes *et al.*, 1990).

## 1.3 Properties of inositol monophosphatase

Inositol monophosphatase is composed of two identical subunits (Mr 30,055), (Diehl *et al.*, 1990). The enzyme has an absolute requirement for $Mg^{2+}$ for activity (Hallcher *et al.*, 1980), with a $K_m$ of 2mM (Gee *et al.*, 1988). Higher concentrations of $Mg^{2+}$ inhibit the enzyme (Hallcher *et al.*, 1980).The inhibition by $Mg^{2+}$ varies considerably with substrate structure and pH. Using Ins(1)P, the $K_i$ for $Mg^{2+}$ is 4mM at pH 8.0 and 37°C (Ganzhorn *et al.*, 1990), whereas when 4-methylumbelliferyl phosphate is the substrate, concentrations of $Mg^{2+}$ as high as 100mM do not inhibit the enzyme (Gore *et al.*, 1992).

Inositol monophosphatase, isolated from a number of sources, demonstrates a broad substrate specificity. It dephosphorylates all monophosphate esters of inositol except

Ins(2)P, where the ester linkage is in the axial position relative to the ring. Studies have shown that the 2' and the 6' hydroxyl groups of Ins(1)P are independently associated with substrate binding and the mechanism of hydrolysis. The enzyme has been shown to dephosphorylate substrate analogues such as 2'AMP, 2'GMP, glycerol-3-phosphate, as well as a number of other monophosphate esters (Gee *et al.*, 1988, Hallcher *et al.*, 1980, Roth *et al.*, 1981, Takimoto *et al.*, 1985, Baker *et al.*, 1989, and Attwood *et al.*, 1988). The maximal velocities with a number of different substrates depend upon the nature of the phosphate ester and the presence of adjacent hydroxyl groups allows hydrolysis to occur more readily (Gore *et al.*, 1992, and Ganzhorn *et al.*, 1990).

The broad specificity of inositol monophosphatase has been exploited in a continuous assay for enzyme activity using the substrate 4-methylumbelliferyl phosphate (Gore *et al.*, 1992). The hydrolysis of the phosphate group from this compound can be readily detected by a resultant large shift in the emission spectrum from 390nm to 450nm.

## 1.4 Mechanism of inositol monophosphatase

The mechanism of inositol monophosphatase, as proposed by Leech *et al.*, (1993), is shown in figure 1.4a. The mechanism indicates ordered binding of $Mg^{2+}$ and Ins(1)P, with Ins(1)P binding first. At this stage, it was postulated that only a single $Mg^{2+}$ was needed for activity. $Mg^{2+}$ is released after Ins(1)P hydrolysis, before the first product, inositol, is released, followed by $P_i$. $Li^+$ binds to the enzyme/product complex only and not to the free enzyme.

The mechanistic implications of the near-UV CD ligand binding data discussed in chapter 5, together with limited proteolysis (Whiting *et al.*, 1990, Greasley *et al.*, 1993, Gee *et al.*, 1991), X-ray crystallography (Bone *et al.*, 1994, Pollack *et al.*, 1993, Pollack *et al.*, 1994), equilibrium dialysis (Greasley *et al.*, 1993), stopped flow fluorescence and fluorescence labelling studies (Greasley *et al.*, 1994) will be discussed in chapter 4 and a refined mechanism proposed.

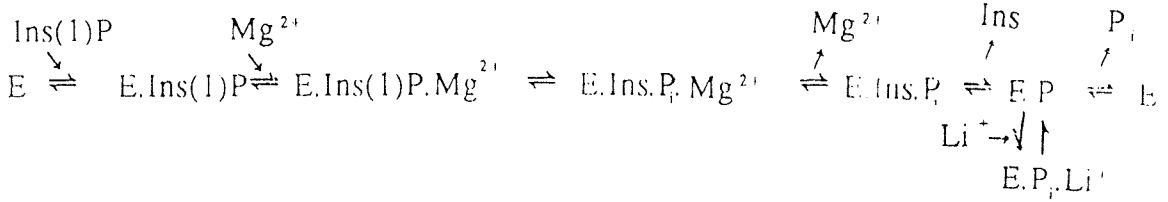


Figure 1.4a : Mechanism of inositol monophosphatase, as proposed by Leech *et al.*, (1993).

There are two alternative mechanisms for phosphatases; either the attack of an enzyme nucleophile, or the direct attack of water, on the substrate phosphoryl group (Bone *et al.*, 1992). Nucleophilic attack by an active site amino acid side chain proceeds through covalent phosphoenzyme intermediates (Knowles *et al.*, 1980); enzymes which involve a phosphorylenzyme intermediate include acid and alkaline phosphatase (Fersht, 1985).

Histidine is a frequently used catalytic residue for phosphate ester cleaving enzymes, for example, acid phosphatase (Van Etten *et al.*, 1977), phosphoglycerate mutase (Rose, 1970), and glucose-6-phosphatase (Feldman *et al.*, 1969). The catalytic mechanism of the tyrosine phosphatases involves the nucleophilic attack by a cysteine residue to form a thiol-phosphate intermediate, and phosphate displacement by a water molecule (Tanier *et al.*, 1994).

All attempts to trap a phosphoenzyme species with inositol monophosphatase have failed (Leech *et al.*, 1993). Hence, the current mechanism proposed for inositol monophosphatase involves the direct attack of the phosphate ester by water, in which $Mg^{2+}$ ion(s) may be involved in activating water for nucleophilic attack, in substrate binding and/or the Lewis acid stabilisation of the oxyanion leaving group (Pollack *et al.*, 1994). These roles for metal ions in an enzyme catalysed reaction are consistent with observations that metal ions catalyse non-enzyme phosphate ester hydrolysis by stabilising the negative charge on the leaving group (Herschlag *et al.*, 1987) and by enhancing the nucleophilicity of water through coordination.

It has now been shown that inositol monophosphatase requires two metal ions for activity (Greasley *et al.*, 1993), similarly to alkaline phosphatase (Kim *et al.*, 1990) and fructose-1,6-bisphosphatase (Zhang *et al.*, 1993). Possible metal binding and catalytic residues of inositol monophosphatase include Lys36, Glu70, Asp90, Ile92, Asp93, Thr95, His217, Cys218 and Asp220 (Bone *et al.*, 1992, Pollack *et al.*, 1994). One of the metal binding sites exhibits the feature of poor cation selectivity common to other $Mg^{2+}$ enzymes, for example the phosphorylation activated signalling protein CheY, which arises because one hemisphere of the cation is coordinated by solvent

(Needham *et al.*, 1993).

Metallo-chemistry is often explained by the hard / soft acid base theory (Pearson, 1963). This theory classifies metal ions as acids since they tend to accept electron "donation" and their ligands tend to "donate" electrons. The Lewis acidity of a metal ion is determined by its charge to mass ratio; the greater this value, the greater its ability to polarise ligands. However, the Lewis acidity of a metal can be modulated by its ligands; the extent of modification is affected differently for hard and soft metals. If the Lewis acidity remains unaffected by ligation the metals are termed hard acids, for example $Mg^{2+}$, whereas, the Lewis acidity of a soft metal (soft acid) can be reduced by certain ligands. In general, hard acids tend to have small ionic radii and high oxidation states, for example, $Mg^{2+}$, $Fe^{3+}$, $Co^{3+}$ and $Li^{+}$ and soft acids tend to have low oxidation states, large ionic radii and accessible vacant orbitals of low energy, for example, $Cu^{+}$, $Ag^{+}$, $Hg^{2+}$, $Pb^{2+}$ and $Cd^{2+}$. The ability of a particular ligand to alter the Lewis acidity of a metal is also classified as hard or soft. In general, hard ligands tend to have small radii, high electronegativities and accessible vacant orbitals of high energy, for example, F, O and N; hence, carboxylates are frequent ligands for $Mg^{2+}$. Whereas, soft ligands tend to have large radii, low electronegativities and accessible vacant orbitals of low energy, for example, S and P.

There is a conserved arginine residue in the structurally homologous inositol monophosphatase (Arg191) and fructose-1,6-bisphosphatase (Arg243), which belongs to the neighbouring chain in or near the active site (Zhang *et al.*, 1993). In fructose-1,6-bisphosphatase, this arginine is part of the active site domain where the 6-phosphate group is bound; inositol monophosphatase is inactivated by the modification of a single arginine residue by phenylglyoxal (Jackson et al., 1989). Arg191 may be part of the same anion-binding loop (the P-loop), involved in recognition, orientation and stabilisation of the bound phosphate in the protein tyrosine phosphatases (Stuckey *et al.*, 1994). The sequence of the anion binding loop in *Yersinia* protein tyrosine phosphatase ( 403 **CRAGVGRTA** 411) shows close sequence homology to the sequence of inositol monophosphatase around Arg191

(189 GIRGVGTA 196), (Diehl *et al.*, 1990). A similar anion binding loop is also found in fructose-1,6-bisphosphatase (Zhang *et al.*, 1993), Rhodanese (Stuckey *et al.*, 1994), and human placenta PTP1B (protein tyrosine phosphatase), (Stuckey *et al.*, 1994). Despite the similarities seen in the phosphate binding sites, there are sharp differences in the design of the catalytic sites of human placenta PTP1B and *Yersinia* protein tyrosine phosphatase (Stuckey *et al.*, 1994). It is possible that inositol monophosphatase uses the P-loop motif for anion binding and transfer.

## 1.5 Inositol monophosphatase: X-ray crystallographic structure

The crystallographic structure of human inositol monophosphatase has been determined (Bone *et al.*, 1992). The sequence of the bovine enzyme, which displays 79% sequence homology to the human enzyme (McAllister *et al.*, 1992) has been successfully mapped onto the human structure (C. Ragan, personal communication).

The secondary structural elements can be visualised in figure 1.5a which shows both subunits. The different elements of secondary structure are coloured in one subunit for ease of identification; the other subunit is identical. The enzyme is composed of a five layered sandwich of alternating α-helices and ß-sheets. There is a pair of α-helices at the N-terminus, C-terminus and at the subunit core. These three pairs of α-helices are separated by layers of, predominantly anti-parallel, ß-sheets. The remainder of the structure is composed of two small α-helices, of approximately two turns each, and several regions of irregular structure.

The active site cleft of each subunit of the enzyme can be visualised in the X-ray crystallographic structure shown in chapter 5 and is located at the base of the two central α-helices near the dimer interface [figure 5.1a]. It does not appear that the active site is shared between subunits (Bone *et al.*, 1992). The precise location of the active site amino acid side chains cannot be viewed from the X-ray crystallographic structure, however, the X-ray crystallographic structure does provide a framework for the design of experiments to determine active site residues.

Figure 1.5a: X-ray crystallographic structure of inositol monophosphatase (only the carbon backbone is shown for clarity). The various elements of secondary structure are coloured differently in one of the subunits for ease of identification: α-helices (shown in purple), ß-sheets (shown in yellow).

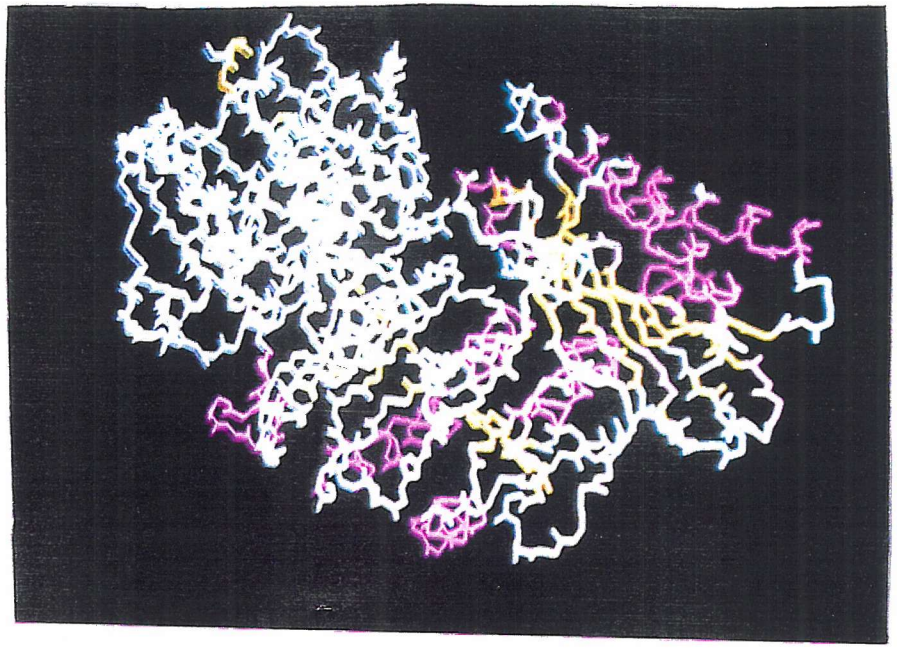

Figure 1.5a

From figure 1.5a, which shows the X-ray crystallographic structure of the two associated subunits, each of which has two separate domains (Bone *et al.*, 1992), it can be seen that the subunit interface is extensive and involves interactions distributed throughout the chain: 10% of the surface area on each subunit is buried upon dimer formation (Bone *et al.*, 1992) and 17% of the residues on each subunit are close enough to participate in the exclusion of solvent from the interface (Connelly, 1983). The dimer is further stabilised by the formation of 18 hydrogen bonds between the subunits (Bone *et al.*, 1992).

## 1.6 Inositol monophosphatase: Sequence and structural homologies

The cDNA coding for the bovine inositol monophosphatase has been inserted into a T7 polymerase bacterial expression vector, pRSET5a (Diehl *et al.*, 1990) and the recombinant enzyme, bovine inositol monophosphatase, has been expressed in E.Coli (Diehl *et al.*, 1990).

Analysis of the protein sequence, reveals that it is moderately hydrophillic, with no unusual regions of hydrophobic character. No consensus sequences were identified for phosphorylation, calcium binding sites, ATP binding sites, or any other recognizable regulatory sequences (Diehl *et al.*, 1990). However, the sequence of inositol monophosphatase is highly conserved between species with 79% homology between bovine, rat and human enzymes (McAllister *et al.*, 1992), [Figure 1.6a]

Sequence similarity has been noted between inositol monophosphatase and the inferred products of several diverse genes (Diehl *et al.*, 1990, and Neuwald *et al.*, 1991) including the products of the *suhB* and *amtA* genes of *E.Coli*, the *qa-x* gene of *Neurospora crassa* and the *qutG* gene of *Aspergillus nidulans*. Based on the homology with inositol monophosphatase and evidence implicating these genes in the regulation of cellular processes (Yano *et al.*, 1990, Fabiny *et al.*, 1991, Geever *et al.*, 1989, Hawkins *et al.*, 1988, and Giles *et al.*, 1991), it was suggested that these genes act by enhancing the synthesis or degradation of phosphorylated messenger

**Figure 1.6a:** Aligned amino acid sequences of bovine, human and xenopus inositol monophosphatase.

```
            1                                                    50
Myop_Bovin  MADPWQECMD Y.AVTLAGQA GEVVREALKN EMNIMVKSS. .PADLVTATD
Myop_Human  MADPWQECMD Y.AVTLARQA GEVVCEAIKN EMNVMLKSS. .PVDLVTATD
Myop_Xenla  MEDRWQECMD FLAVSIARKA GSVVCAALKE DVSIMVKTSL APADLVTATD

            51                                                   100
Myop_Bovin  QKVEKMLITS IKEKYPSHSF IGEESVAAGE KSILTDNPTW IIDPIDGTTN
Myop_Human  QKVEKMLISS IKEKYPSHSF IGEESVAAGE KSILTDNPTW IIDPIDGTTN
Myop_Xenla  QKVEEMIISS IKEKYPSHSF IGEESVAAGA GSTLTDNPTW IIDPIDGTTN

            101                                                  150
Myop_Bovin  FVHGFPFVAV SIGFVVNKKM EFGIVYSCLE DKMYTGRKGK GAFCNGQKLQ
Myop_Human  FVHRFPFVAV SIGFAVNKKI EFGVVYSCVE GKMYTARKGK GAFCNGQKLQ
Myop_Xenla  FVHRFPFVAV SIGFAVHKQV EFGVVYSCVE DKMYTGRKGK GSFCNGQKLQ

            151                                                  200
Myop_Bovin  VSHQEDITKS LLVTELGSSR TPETVRII.L SNIERLLCLP IHGIRGVGTA
Myop_Human  VSQQEDITKS LLVTELGSSR TPETVRMV.L SNMEKLFCIP VHGIRSVGTA
Myop_Xenla  VSGQKDITKS MIITELGSNR NPEFIKTVSL SNMERLLCIP IHGIRAVGTA

            201                                                  250
Myop_Bovin  ALNMCLVAAG AADAYYEMGI HCWDVAGAGI IVTEAGGVLL DVTGGPFDLM
Myop_Human  AVNMCLVATG GADAYYEMGI HCWDVAGAGI IVTEAGGVLM DVTGGPFDLM
Myop_Xenla  AVNMCLVATG GADAYYEMGL HCWDMAAASV IVTEAGGTIL DATGGLFDLM

            251                                  285
Myop_Bovin  SRRVIASSNK TLAERIAKEI QIIPLQRDDE D....
Myop_Human  SRRVIAANNR ILAERIAKEI QVIPLQRDDE D....
Myop_Xenla  SCRIISASSR EIAERIAKEL QIIPLERDDG KSTNS
```

molecules (Neuwald *et al.*, 1991).

In mapping the aligned sequences of these genes onto the phosphatase structure, patterns of residue hydrophobicity are maintained in the structural core, while insertions and more dramatic sequence variations occur in irregular segments, turns or solvent-exposed residues. It is very striking that the residues from which the metal and phosphate binding sites are formed are conserved in the sequences from these diverse genes (Bone *et al.*, 1992). From these observations, it appears that the phosphatase, *suhB, amtA, qa-x and qutG* are members of a structural family and have a conserved metal binding site (Bone *et al.*, 1992). In addition, the possibility that the products of *suhB, amtA, qa-x and qutG* have phosphatase activities (Neuwald *et al.*, 1991) is strengthened.

Inositol polyphosphate-1-phosphatase, the other enzyme inhibited by $Li^+$ in the phosphatidylinositol cycle, has also been cloned (bovine), sequenced and expressed in *E.Coli* (York *et al.*, 1990). Although the enzyme appears to have no overall sequence homology with inositol monophosphatase, an alignment of the two protein sequences is possible in two regions (York *et al.*, 1990, and Neuwald *et al.*, 1991). These regions include most of the residues from which the metal and phosphate binding sites are constructed (Bone *et al.*, 1992). Uncompetitive inhibition of both enzymes by $Li^+$ and the possibility that both enzymes have the same metal/phosphate binding site suggests that $Li^+$ binding involves components of this site.

Fructose-1,6-bisphosphatase is a key regulatory enzyme catalysing the hydrolysis of fructose-1,6-bisphosphate to fructose-6-phosphate and inorganic phosphate in the gluconeogenesis pathway (Benkovic *et al.*, 1982, and Tejwani *et al.*, 1983). Inositol monophosphatase and fructose-1,6-bisphosphatase share very little sequence homology (Zhang *et al.*, 1993). Ribbon structures of inositol monophosphatase and fructose-1,6-bisphosphatase based upon the X-ray crystallographic data are shown in figures 1.6c and 1.6d. Recent work has highlighted the similarity between inositol monophosphatase and fructose-1,6-bisphosphatase (which also has a requirement for two $Mg^{2+}$ ions for activity) in terms of a conserved αßαßα tertiary structure and, in

particular, a conserved motif including an array of acidic residues known to be involved in metal ligation in fructose-1,6-bisphosphatase (Zhang *et al.*, 1993). These conserved sites have been suggested to be the putative $Mg^{2+}$ binding site in inositol monophosphatase (Greasley *et al.*, 1993).

In fructose-1,6-bisphosphatase, the binding of phosphate requires the presence of $Mg^{2+}$ (Tejwani, 1983). This observation is in agreement with data presented in Greasley *et al.*, 1992.

The active site of both enzymes is located in a hydrophillic cleft near the dimer interface. From the structures of inositol monophosphatase and fructose-1,6-bisphosphatase, it could be reasonably concluded that the conserved residues between residues 68 and 125 (numbers refer to the fructose-1,6-bisphosphatase sequence) are part of a metal binding site (Zhang *et al.*, 1993). All but one of the metal binding residues are conserved in the two enzymes. These residues are Asp-74, Glu-98, Asp-118 and Glu-280 in fructose-1,6-bisphosphatase and residues Asp-47, Glu-70, Glu-71, Asp-90, Asp-93 and Asp-220 in inositol monophosphatase (Zhang *et al.*, 1993).

There is a conserved arginine residue (243 in fructose-1,6-bisphosphatase and 191 in inositol monophosphatase) which belongs to the neighbouring chain in or near the active site (Zhang et al., 1993). This arginine residue may have a structural role in forming the dimer interface, especially in inositol monophosphatase.

Fructose-1,6-bisphosphatase also shares other features with inositol monophosphatase, for example, it too is inhibited by $Li^{+}$, contains a highly susceptible proteolytic site (Lys36-Ser37 in inositol monophosphatase (Gee *et al.*, 1991) and Thr66-Gly67 in fructose-1,6-bisphosphatase (Botello *et al.*, 1977)) and, like inositol monophosphatase, undergoes a structural change during catalysis (Ke *et al.*, 1990).

**Figure 1.6c**: X-ray crystallographic structure of inositol monophosphatase. The structure is represented as a ribbon structure so that the various elements of secondary structure can be easily visualised.

**Figure 1.6d** : X-ray crystallographic structure of fructose-1,6-bisphosphatase. The structure is represented as a ribbon structure so that the various elements of secondary structure can be visualised.

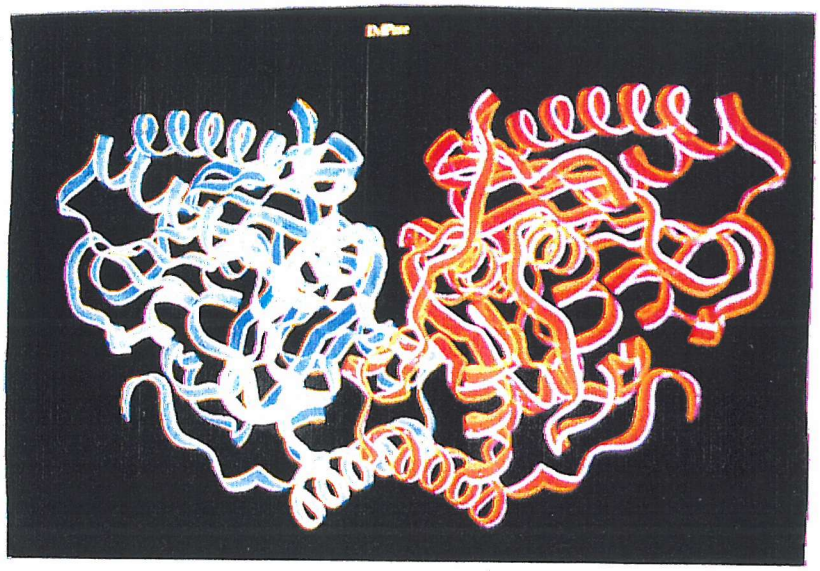

Figure 1.6c

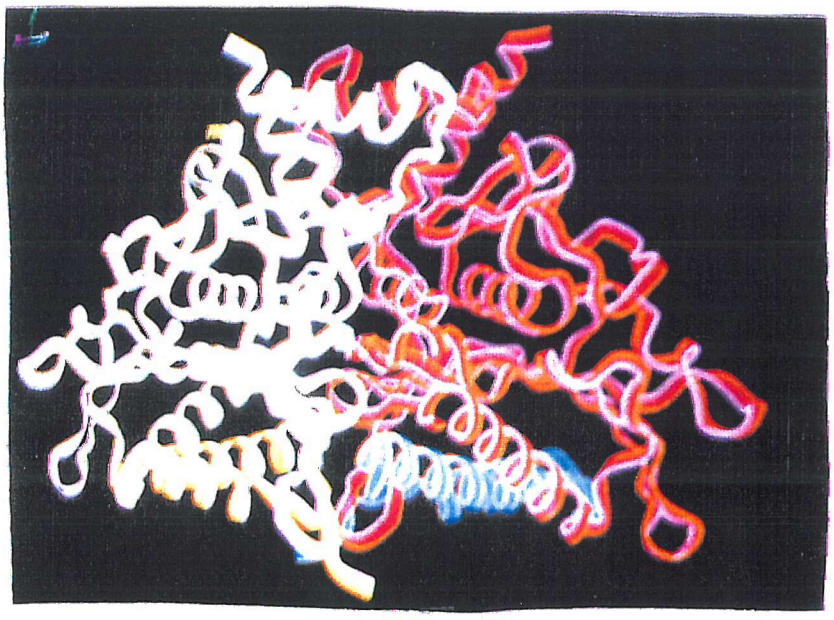

Figure 1.6d

## 1.7 Inositol monophosphatase: Conformational changes during catalysis

The X-ray crystallographic structure [figure 5.1a] suggests that the N-terminal α-helix of inositol monophosphatase is relatively exposed to solvent. This X-ray crystallographic structure is taken in the absence of substrate. Upon substrate binding, it is postulated that the N-terminal α-helix moves over the active site of the enzyme; this movement is important for catalysis.

Experimental evidence for this conformational change has been obtained from limited proteolysis experiments (Gee *et al.*, 1989). When bovine inositol monophosphatase is incubated with endoprotease Lys-C, there is a loss of enzyme activity and a concurrent decrease in Mr of each subunit from 30 to 28kDa. The decrease in Mr is due to cleavage at a single bond, Lys36-Ser37, in the solvent exposed N-terminal α-helix. This data suggests that the 36 amino acids in this N-terminal α-helix are important for activity in some way. In the presence of substrate, endoprotease Lys-C does not cleave inositol monophosphatase and there is no inactivation of the enzyme. This would be the case if upon substrate binding the N-terminal α-helix moved over the active site during catalysis. Binding of a monoclonal antibody to the Cys8 region of the protein results in up to 83% inhibition of enzyme activity (Gee *et al.*, 1989), suggesting that antibody binding can prevent the N-terminal α-helix conformational change.

## 1.8 Project aims

The overall aim of my post-graduate research involves structural and functional studies of bovine inositol monophosphatase. To determine the amino acid residues essential for activity and the structure of the enzyme. These studies include the examination of residues essential for activity and structure; the interaction of metal ions with the structure; and the stability of the protein. The Experiments were designed using X-ray crystallographic data (Bone *et al.*, 1992), which allows localisation of the enzyme active site, together with previous published work on inositol monophosphatase which more precisely localises amino acid residues located

at or near the active site; for example, the chemical modification and site directed mutagenesis studies of Knowles *et al.*, (1992), have shown that Cys218 is located near the active site. Mechanistic interpretations from experiments were proposed by comparison with other phosphatase enzymes with well established catalytic mechanisms.

# CHAPTER 2

# MATERIALS AND METHODS

# Chapter 2

# Materials and Methods

## 2.1 Materials

Most chemicals were obtained from BDH Ltd., Dorset, or Sigma Chemical Company Ltd., Poole. More specialist reagents were obtained from the following sources: Boehringer Manheim UK Ltd., Lewes, East Sussex: DNase I, RNase A.

Dynatech Laboratories Ltd., Billinghurst, Sussex: microtitre plates.

Lablogic, Sheffield: protogel.

Lab. M., Bury, Lancs.: tryptone, yeast extract, agar no.1.

Northumbria Biologicals Ltd., Cramlington, Northumberland: ampicillin, IPTG.

Pharmacia AB, Uppsala, Sweden: agarose (NA grade).

Promega, Chilworth, Hants., Plasmid DNA magic miniprep resin and columns.

The substrate D,L-Ins(1)P was a gift from Merck Sharpe and Dohme Research Laboratories.

The derivatives of MMTS were synthesised at The University of Southampton by Dr. R. Sharma.

Dansylcamphor-10-sulphonic acid was synthesised at The University of Southampton by Dr. R. Sharma.

## 2.2 Microbial methods

### 2.2.1 Bacterial strains

| STRAIN | *E. Coli* CJ236 | *E. Coli* DH5α | *E. Coli* BL21(DE3) |
|---|---|---|---|
| GENOTYPE | dut1, ung1, thi-1, relA1/PCJ105(Cam$^r$ F') | supE44,Δ lacU169($\phi$ 80 lacZΔM15), hsdR17, recA1, endA1, gyrA96, thi-1, relA1. | hsd5gal, (λIts857 ind1 5 am 7 nun5 lacUV5-T7 gene1) |
| REFERENCE | Kunkel *et al.*, (1987) | Hanahan, (1983) | Studier, (1986) |

### 2.2.2 Bacterial growth medium

Luria Broth (LB)(g/l)

Tryptone (10); yeast extract (5); NaCl (5).

Recombinant proteins and plasmid DNA were produced by the growth of bacteria in LB. Where necessary, the media was supplemented by the aseptic addition (after autoclaving and cooling) of ampicillin (50μg/ml). LB was solidified for the production of plates by the addition of 1.1 % w/v agar no.1.

### 2.2.3 Sterilisation

All media, stock solutions, pipette tips and microfuge tubes were sterilised by autoclaving at 120°C and 15 psi for 20 minutes. Stock solutions of heat labile chemicals, such as antibiotics and IPTG, were sterilised by filtration through disposable 0.45μM filters.

### 2.2.4 Bacterial strain storage

Bacterial strains were stored short term as streaks on LB plates and were restreaked every four weeks. For longer term storage, 10ml cultures were grown in LB and at the mid-log phase of growth, cells were pelleted, resuspended in 850µl LB, added to 150µl sterile glycerol in sterile cryotubes, mixed and stored at -70°C. These stocks were replaced every 12 months.

## 2.3 Molecular biology methods

### 2.3.1 Production of competent cells for transformation

*E. coli* were rendered competent for the uptake of plasmid DNA by the calcium chloride method (Cohen *et al.*, 1972). An overnight culture of the host strain in LB was taken and diluted 1:100 into fresh LB and incubated with shaking until mid-log growth was attained ($OD_{600nm}$ = 0.6). The culture was left on ice for 10 minutes before being pelleted by centrifugation for ten minutes in a bench top centrifuge and resuspended in half original culture volume volume of sterile $CaCl_2$ at 4°C. The cells were left on ice for 30 minutes and then repelleted as above. The cells were then resuspended in one tenth volume of sterile $CaCl_2$ at 4°C and refrigerated until required. Cells were optimally used after 4 hours.

### 2.3.2 Transformation of competent cells with plasmid DNA

1µl of plasmid DNA (typically 2-10ng) was added to 20µl of competent cells. The cells were incubated on ice for 60 minutes, heat shocked at 42°C for 90 seconds and then returned to ice for a further 3 minutes. The cells were then plated out on LB plates containing ampicillin and left overnight at 37°C.

### 2.3.3 Preparation of double stranded plasmid DNA

Plasmid DNA was prepared using Promega Magic Miniprep columns. The cells from 3ml of an overnight culture were pelleted and resuspended in 200µl of cell resuspension solution. To this was added 200µl cell lysis solution. 200µl neutralisation solution was then added. After mixing by inversion, the resulting precipitate was pelleted in a microfuge. The supernatant was transferred to a fresh tube and 1ml of miniprep resin added. The mixture was then applied to a miniprep column and washed with 2ml of column wash. The resin on the column was spun dry in a microfuge and the DNA eluted by the addition of 50µl of TE buffer, pH 7.5, at 65°C and recentrifugation for 30 seconds in a microfuge. The yield and quality of the plasmid DNA prepared was determined by agarose gel electrophoresis.

Cell resuspension solution: 10mM EDTA; 50mM Tris.HCl, pH 7.5; 100µg/ml RNaseA.
Cell lysis solution: 0.2M NaOH; 2 % w/v SDS.
Neutralisation solution: 2.55M potassium acetate.
Column wash solution: 200mM NaCl; 5mM EDTA; 20mM Tris.HCl, pH 7.5. (Dilute when required 1:1 with 99.9 % v/v ethanol).

### 2.3.4 Agarose gel electrophoresis

Submerged horizontal agarose mini-gels were used for the routine analysis of double and single stranded plasmid DNA (Maniatis, 1982). The agarose was used at 0.8 to 2 % w/v in 1XTBE (10XTBE: 108g Tris, 55g boric acid, 9.3g EDTA, per litre distilled water) and required boiling to form a solution. When the temperature had dropped to approximately 50°C, ethidium bromide was added to a final concentration of 0.1µg/ml. 20ml of this solution was poured onto a gel plate with a comb and allowed to set. The gel was submerged in a tank containing 1XTBE and samples prepared by the addition of 1µl 6Xgel loading buffer (6Xgel loading buffer: 0.25 % w/v bromophenol blue, 30 % v/v glycerol) to 5µl DNA. 6µl of each sample was loaded into the wells and the gel run at 100V for 20 minutes. The bands on the gel

were visualised on an UV transilluminator.

## 2.4 Protein biochemistry methods

### 2.4.1 Expression and purification of inositol monophosphatase: Growth of bacterial cultures for the expression of recombinant inositol monophosphatase

The gene for both bovine and human inositol monophosphatase was provided by Dr. C.I. Ragan (Merck Sharpe and Dohme Research Laboratories) in the pRSET 5a vector. The vector was transformed into *E.coli* BL21(DE3) and a single colony used to innoculate 10ml LB media containing 50μg/ml of ampicillin. The culture was grown overnight at 37°C with shaking and then diluted 100 fold into fresh LB containing 50μg/ml of ampicillin. The cells were shaken at 100rpm and 37°C until an OD of approximately 1.2 was attained and then IPTG was added to a final concentration of 0.4mM. The cells were vigorously shaken at 200rpm and 37°C for a further 12 hours before being harvested.

### 2.4.2 Expression and purification of inositol monophosphatase: Extraction of recombinant inositol monophosphatase from *E.coli* BL21(DE3)

The cells from 8l of LB were pelleted in a Sorvall RC-3B refrigerated centrifuge. The cells were spun at 5,500rpm for 30 minutes at 4°C. The pelleted cells were resuspended in 30ml 50mM Tris.HCl, 0.1mM EGTA, pH 8.0, and transferred to a 50ml Oakridge tube. Lyzozyme was added to a final concentration of 0.1mg/ml and the cells left on ice for 30 minutes before sonication using a MSE Soniprep 150 for 6X30 seconds with a 15 second break in between. Triton X100 (0.5 % v/v) and DNase I (to a final concentration of 0.1mg/ml) were added and subsequently left on ice for a further 30 minutes. The insoluble cell debris was removed by centrifuging the sonicate for 30 minutes at 4°C and 18.000rpm using a Beckman J2-21 centrifuge and an 8X50ml rotor. The supernatant was separated from the pellet and returned to

ice.

### 2.4.3 Expression and purification of inositol monophosphatase: Purification of recombinant inositol monophosphatase from *E.coli* BL21(DE3)

The supernatant (from 2.4.2) was placed in a water bath at 60°C for 1 hour. The denatured protein was removed by centrifugation at 10,000rpm and 4°C for 30 minutes using a Beckman J2-21 and an 8X50ml rotor. The supernatant was then applied to a Q-Sepharose anion exchange column pre-equilibrated in 30mM Tris.HCl, 30mM NaCl, pH 8.0 (buffer A) (flow rate = 2ml/min). A linear gradient of buffer A and buffer B (30mM Tris.HCl, 300mM NaCl, pH 8.0) was run using a Bio-rad Econo system and 5ml fractions collected. The column was washed with 30mM Tris.HCl, 2M NaCl, pH 8.0, before re-use. The elution of the protein was monitored at 280nm and each peak was assayed for inositol monophosphatase using the continuous fluorescence assay of Gore *et al.*, (1992). 5µl of the fractions covering the peak of enzyme activity were run on a 12 % SDS PAGE gel. The fractions were pooled according to the purity. Inositol monphosphatase was routinely found to be greater than 95 % pure.

### 2.4.4 Measurement of enzyme activity by the fluorescence assay of Gore *et al.*, ( 1992)

Inositol monophosphatase was assayed by monitoring the rate of hydrolysis of 4-methylumbelliferyl phosphate; the product (4-methylumbelliferone) fluorescesces intensely at 450nm.

### 2.4.5 Polyacrylamide gel electrophoresis

The discontinuous Tris.glycine method of Laemmli, (1970), was used for the separationof proteins:

The solutions are detailed below:

The main separating gel: (volumes are in ml unless otherwise stated).

Running gel:

| % acrylamide: | 9 | 12 | 15 | 18 |
|---|---|---|---|---|
| water (distilled, deionised) | 14.58 | 11.58 | 8.58 | 5.58 |
| protogel (30% acrylamide/ 0.8 % bis-acrylamide) | 9 | 12 | 15 | 18 |
| 1.875M Tris.HCl, pH 8.8 | 6 | 6 | 6 | 6 |
| 10 % SDS | 0.3 | 0.3 | 0.3 | 0.3 |
| TEMED | 0.1 | 0.1 | 0.1 | 0.1 |
| APS | 0.15 | 0.15 | 0.15 | 0.15 |

Stacking gel:

| | |
|---|---|
| water (distilled, deionised) | 11.29 |
| 0.875M Tris.HCl, pH 6.8 | 2.5 |
| 10 % SDS | 0.125 |
| TEMED | 75$\mu$l |
| APS | 0.1 |

5Xrunning buffer: (per l): Tris (15.15g); glycine(72g); SDS (5g).

Samples were diluted in an equal volume of 2Xsample buffer, boiled for 5 minutes and then loaded onto the gels.

2Xsample buffer: 0.625M Tris.HCl, pH 6.8 (2ml); 10 % w/v SDS (4ml); glycerol (2ml); mercaptoethanol (1ml); distilled, deionised water (1ml); trace of bromophenol blue dye

Stain solution: methanol (454ml); acetic acid (92ml); distilled deionised water (454ml); Coomassie Brilliant Blue (2.5g).

Destain solution: methanol (250ml); acetic acid (375ml); distilled deionised water (4375ml).

### 2.4.6 Determination of protein concentration

Protein concentration was determined either by the Bicinchoninic acid protein assay (Smith *et al.*, 1975) or the Bradford assay (Bradford, 1976) using bovine serum albumin as the standard.

### 2.4.7 Diethylpyrocarbonate modification

A solution of 25μM enzyme (Mr 30,055) in 20mM MES, pH 6.5, at 25°C, was incubated with 4mM diethylpyrocarbonate taken from a stock of 1M diethylpyrocarbonate dissolved in anhydrous ethanol. The effective concentration of the diethylpyrocarbonate solution was determined using the imidazole method (Miles, 1977). The modification was repeated in the presence of 2mM Ins(1)P, 20mM $MgCl_2$ and 100mM LiCl. 25μM wild type enzyme and H217Q, in MES, pH 6.5 at 25°C, were incubated with 29mM diethylpyrocarbonate to allow the modification of all histidine residues.

Since the extinction coefficient for diethylpyrocarbonate modified histidine depends on the environment (Miles, 1977), it was determined in the buffer system employed in these experiments (20mM MES, pH 6.5), by the addition of excess diethylpyrocarbonate (4mM) to known concentrations of L-histidine (0-200μM) in 20mM MES, pH 6.5, at 25°C. The stoichiometry of the reaction was monitored by following the increase in absorbance at 240nm ($\varepsilon_{240nm}$ = 2727$M^{-1}cm^{-1}$) using an Hitachi U-2000 spectrophotometer.

Diethylpyrocarbonate is very unstable in aqueous solution. Therefore, any accurate determination of the rates of modification or inactivation needs to consider the rate of autohydrolysis of diethylpyrocarbonate in 20mM MES, pH 6.5, at 25°C. 1.5ml reaction mixes were set up with 0.8, 2.0, 4.0 and 8mM diethylpyrocarbonate in 20mM MES, pH 6.5, at 25°C. Periodically, 90μl aliquots were removed and added to 10μl excess histidine (1M), in 20mM MES, pH 6.5, 25°C. 10μl of this diluted aliquot was added to 990μl 20mM MES, pH 6.5, and the absorbance measured at 240nm.

The integrity of the dimeric nature of the enzyme after modification with diethylpyrocarbonate was determined by the use of a Gilson hplc system equipped with a 250mmX7.5mm TOSOH-TSK G3000SW gel permeation column equilibrated with 20mM MES, pH 6.5.

### 2.4.8 Modification by MMTS and its derivatives

8.3μM enzyme (Mr 30,055), in 50mM Tris.HCl, pH 8.0, at 25°C, was modified by MMTS and its derivatives EMTS and IPMTS, taken from a 100mM stock (MMTS and its derivatives were first solubilised in DMF before dilution with ethanol such that the final stock DMF concentration was 10 %v/v). The final DMF concentration never rose above 1%v/v, which was shown to have no effect on the enzyme. The reaction was monitored by following the decrease in protein fluorescence at 340nm after excitation at 290nm. For the determination of stoichiometry, the unreacted reagent was removed by passing the modified enzyme down a G-10 Sephadex

column equilibrated in 50mM Tris.HCl, pH 8.0. The number of residues which had not reacted with MMTS or its derivatives was determined by modification with 1mM DTNB in the presence of 1 % w/v SDS. Inactivation was followed by periodically removing aliquots for assay by the fluorescence assay of Gore *et al.*, (1992). The modification was repeated in the presence of 100mM LiCl, 10mM $MgCl_2$ and 2mM 2'AMP.

### 2.4.9 DTNB modification

Inositol monophosphatase, in 50mM Tris.HCl, pH 8.0 at 25°C, was modified by 1mM DTNB in the presence of 1 % w/v SDS. The DTNB was taken from a 10mM stock prepared in 50mM Tris.HCl, pH 8.0 (DTNB was first solubilised in ethanol before adding 50mM Tris.HCl and then adjusting the pH to 8.0 with NaOH; the final ethanol concentration was 10%v/v). The final ethanol concentration never rose above 1%v/v, which was shown to have no effect on the enzyme. The production of $NTB^{2-}$ was followed at 412nm ($\varepsilon_{412nm}$ = 13,600$M^{-1}cm^{-1}$) using an Hitachi U-2000 spectrophotometer.

### 2.4.10 Modification by eosin-maleimide and fluorescein-maleimide

The 100mM eosin-maleimide and fluorescein-maleimide stocks were freshly prepared in 50mM Tris.HCl, pH 8.0 (eosin-maleimide and fluorescein-maleimide were first solubilised in DMF and then the volume made up with 50mM Tris.HCl, pH 8.0, to give a final concentration of 0.2 % v/v DMF) and stored on ice, in the dark, before use. 16.6μM enzyme (Mr 30,055), in 50mM Tris.HCl, pH 8.0, was incubated with 166μM eosin-maleimide or fluorescein-maleimide overnight, at 25°C, in the dark. The reaction was stopped by the addition of 144mM ß-mercaptoethanol. Excess eosin-maleimide and fluorescein-maleimide were removed by passing the modified enzyme down a G-10 Sephadex column, previously equilibrated in 50mM Tris.HCl, pH 8.0. The number of cysteine residues modified can be quantitated spectrophotometrically in the presence of 1 % w/v SDS ($\varepsilon_{524nm}$ (eosin-maleimide) = 89,389$M^{-1}cm^{-1}$ and $\varepsilon_{495nm}$ (fluorescein-maleimide) = 62,562$M^{-1}cm^{-1}$) . The

modification reaction was repeated in the presence of 2mM AMP, 100mM LiCl and 10mM $MgCl_2$. The C218A mutant was also modified by eosin-maleimide and fluorescein-maleimide.During the first two hours of the modification reaction of the wild type enzyme, 50µl aliquots were periodically removed and assayed by the fluorescence assay of Gore *et al.*, (1992). Also, 1ml aliquots were removed during the first two hours, the reaction was stopped, excess reagent was removed and the number of residues modified determined.

### 2.4.11 TNBS modification

20µM enzyme (Mr 30,055), in 50mM $NaHCO_3$, pH 8.5, at 25°C, was incubated with 100mM TNBS (from a 1M stock prepared in 50mM Tris.HCl, pH 8.5). Periodically, aliquots were removed and the reaction stopped by the addition of 1M ß-mercaptoethanol. Excess TNBS was removed by dialysis against 50mM Tris.HCl, pH 8.5. The stoichiometry of modification was determined by measuring the absorbance at 420nm ($\varepsilon_{420nm}$ = 19,200 $^{-1}cm^{-1}$). The activity was measured by the fluorescence assay of Gore *et al.*, (1992). The amino terminus of the protein was analysed for TNBS modification using an Applied Biosystems 477A sequencer with on line 120A HPLC for identification of the PTH-amino acids released at each cycle.

### 2.4.12 Phenylglyoxal modification

36µM bovine inositol monophosphatase (Mr 30,055), in 50mM $NaHCO_3$, pH 7.8 at 25°C, was incubated with various final concentrations of phenylglyoxal (taken from a 500mM stock in ethanol and DMSO: phenylglyoxal was first dissolved in DMSO and then diluted with ethanol such that DMSO was at a final stock concentration of 10%v/v). The final DMSO concetration never rose above 1%v/v, which was shown to have no effect on the enzyme.

The modification was also followed with time by periodically removing 50µl aliquots and assaying by the fluorimetric assay of Gore *et al.*, (1992).

### 2.4.13 1-pyreneglyoxal modification

Quantitative modification of arginine residues in proteins can be achieved with chromophoric reagents such as 1-pyreneglyoxal. Arginine residues modified with 1-pyreneglyoxal can be quantitated by measuring their absorbance at 360nm ($\varepsilon_{360nm}$ = 16,000$M^{-1}cm^{-1}$). The reaction with 1-pyreneglyoxal can be followed by monitoring the fluorescence at 453nm, upon excitation at 360nm.

Since 1-pyreneglyoxal is only poorly soluble in aqueous solution, 36μM bovine inositol monophosphatase (Mr 30,055), in 50mM $NaHCO_3$, pH 7.8 at 25°C, was incubated with an equimolar concentration of 1-pyreneglyoxal (taken from a 20mM stock in ethanol and DMSO: 1-pyreneglyoxal was first dissolved in DMSO and then diluted with ethanol such that DMSO was at a final stock concentration of 10% v/v).

The modification was also followed with time by periodically removing 50μl aliquots and assaying by the fluorimetric assay of Gore *et al.*, (1992).

### 2.4.14 Modification by dansyl camphor-10-sulphonic acid

36μM bovine inositol monophosphatase (Mr 30,055), in 50mM $NaHCO_3$, pH 7.8 at 25°C, was incubated with dansyl camphor-10 sulphonic acid (taken from a 500mM stock in ethanol and DMSO: camphor-10-sulphonic acid was first dissolved in DMSO and then diluted with ethanol such that DMSO was at a final stock concentration of 10%v/v).

The modification was also followed with time by periodically removing 50μl aliquots and assaying by the fluorimetric assay of Gore *et al.*, (1992).

### 2.4.15 Pyrene-maleimide modification

30 μM bovine inositol monophosphatase (Mr 30,055) in 50mM Tris.HCl, pH 8.0, at

25°C, was incubated for 90minutes with 30μM pyrene-maleimide (prepared as a 1mM stock: the pyrene-maleimide was solubilised in DMSO before dilution with ethanol, such that the final DMSO concentration in the stock was 10% v/v). The stoichiometry of modification was determined by measuring the OD at 338nm ($\varepsilon_{338nm}$ = 23,000 $M^{-1}cm^{-1}$). Resonance energy transfer, in the presence and absence of $Mg^{2+}$, was measured using an excitation wavelength of 292nm and an emission wavelength of 272nm.

### 2.4.16 Fluorescence: Correction for quenching by the inner filter effect

Protein fluorescence was corrected for the inner filter effect using the equation: $F_{corrected} = F_{observed} \times 10^{0.5OD}$, where the OD was determined at the excitation wavelength.

### 2.4.17 Denaturation studies

The enzyme was dialysed against 50mM Tris.HCl, pH 8.0. 7M guanidium hydrochloride and 10M urea (prepared in 50mM Tris.HCl, pH 8.0) and 50mM Tris.HCl, pH 8.0, solutions were adjusted to pH 8.0 and filter sterilised. Enzyme was incubated in increasing concentrations of denaturant at 25°C. The degree of denaturation with increasing concentrations of denaturant was followed by several means: protein fluorescence; enzyme activity (Gore *et al.*, 1992); circular dichroism.

### 2.4.18 Preparation of enzyme for kinetic studies

Bovine inositol monophosphatase was dialysed against 5l 50mM Trizma.HCl, 1mM EGTA, 1mM EDTA and 1mM 1,10-phenanthroline, pH 8.0, at 4°C, to remove all metal ions before dialysis against 2X5l 50mM Trizma.HCl, pH 8.0. All glassware was previously washed with dilute sulphuric acid and analaR water. All solutions were prepared with analR water. The fluorescence assay of Gore *et al.*, (1992), was used for kinetic studies.

### 2.4.19 Fluorescence studies

All fluorescence measurements were made using a thermostated Hitachi-2000 fluorimeter. Protein (excitation at 292nm) fluorescence (scans and fixed wavelength measurements) were performed at 25°C using 5nm slit widths.

### 2.4.20 Circular dichroism studies

Enzyme was prepared for circular dichroism studies by dialysis against 5l 50mM Trizma.HCl, pH 8.0, at 4°C (1mM EGTA, 1mM EDTA and 1mM 1,10-phenanthroline were added to the enzyme prior to dialysis to remove all metal ions and all glassware previously washed with dilute sulphuric acid and analaR water for ligand binding studies). All solutions were prepared with analR water, filter sterilised and degassed prior to use. The dialysed enzyme was filtered prior to circular dichroism. Near UV-studies were performed in the range 240-320nm (using a 1cm path length cell and 0.5mg/ml enzyme) and far-UV studies in the range 185-250nm (using a 0.1cm path length cell and 0.2mg/ml enzyme). For maximal signal to noise ratio, each spectra printed was an accumulation of three runs at 20nm/min (for $Mg^{2+}$ titration work, a slower scan speed, 5nm/min, and wavelength range, 270-280nm, was used. Other measurement parameters were response (0.125sec), band width (1.0nm), slit width (500μm). All CD spectra were converted to molar residue ellipticity (obtained by dividing the enzyme concentration in g/l by 110, the average molecular weight of an amino acid).

### 2.4.21 Data analysis

Conversion of CD spectra to molar residue ellipticity and determination of α-helical content of inositol monophosphatase were both performed using Jasco software. All other data was analysed by ENZFIT, FIGP (linear regression) and manual calculation.

# CHAPTER 3

# CHEMICAL MODIFICATION

# Chapter 3

# Chemical modification studies

## 3.1 Introduction

Chemical modification is a technique, coupled with additional approaches, which can lead to an understanding of the structure and function of enzymes in solution (Lundblad *et al.*, 1970, and Means *et al.*, 1971). For those proteins whose total conformation is known from X-ray crystallographic studies, no major discrepancies have been noted between the results of chemical modifications and X-ray diffraction, indeed they mutually supplement each other, indicating that the structure deduced by X-ray crystallography bears a very close correspondence to that found in solution. The interactions between protein side chains revealed by X-ray diffraction have allowed greater insight into the factors governing side chain reactivity. Chemical modification, a technique involving the covalent binding of a reagent to an amino acid side chain, is rarely absolutely specific for a certain side chain and is greatly influenced by the microenvironment of amino acid side chains; that is, polarity, hydrogen-bonding effects, electrostatic effects, steric effects by other side chains and experimental conditions (including pH and buffer nature). The different chemical properties of the various side chains provide a basis for their differential chemical modification. At the active site of enzymes, which is in a less polar environment, amino acids often show a markedly different $pK_a$ than that of the same free amino acid. These amino acids are often more reactive, thus increasing the selectivity with which they may be labelled by group specific reagents.

The investigation of relationships between biological properties and specific residues is one of the most active applications of chemical modification of proteins and a correlation of the degree of modification with a change in a biological property (for example, enzyme activity) is essential if one wishes to ascribe a function to the modified residue and to exclude non-specific modification. The assignment of function to modified amino acids is difficult on the basis of chemical modification

alone, but in combination with protection experiments can give valuable information. Finally, to confirm the function assigned to a modified residue, it is very important to determine if the alteration caused by the modification is due to a steric effect. A good approach here is to transform the putative essential residue into another amino acid of similar size and general properties by site directed mutagenesis.

## 3.2 Chemical modification of histidine residues

### 3.2.1 Introduction

At neutral pH, histidine can be uncharged or positively charged, depending on its local environment. Histidine residues are often found at the active site of enzymes, where its imidazole ring can readily switch between these states [figure 3.2.1a] to catalyse the making and breaking of bonds:

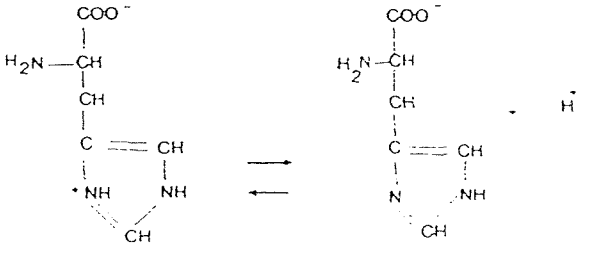

Figure 3.2.1a: Ionisation of the imidazole side chain of histidine.

The typical $pK_a$ for the imidazole group in proteins is 6.5, but the actual $pK_a$ value will depend on the temperature, ionic strength and the microenvironment of the ionizable group.

Chemical modification of histidine residues can be achieved by photo-oxidation in the presence of sensitisers (methylene blue or rose bengal), (Schneider, 1978); by azo-coupling (Schneider, 1978); by alkylation (especially with α-haloacids), (Gurd,

1967); or diethylpyrocarbonate (Miles *et al.*, 1977). Chemical modification by diethylpyrocarbonate is the favoured method of chemical modification of histidine residues, since it can be used under mild conditions and is considerably more specific for histidine residues than either of the other two methods. Diethylpyrocarbonate rapidly inactivates several enzymes, for example, ribonuclease and trypsin (Rosen, 1966).

Ovadi *et al.*, (1967), proposed that diethylpyrocarbonate should be selective for histidine residues in proteins around pH 6.0 and showed this to be the case for several proteins. Diethylpyrocarbonate reacts with histidine residues to yield a N-carbethoxyhistidyl derivative [figure 3.2.1b], (Miles, 1978):

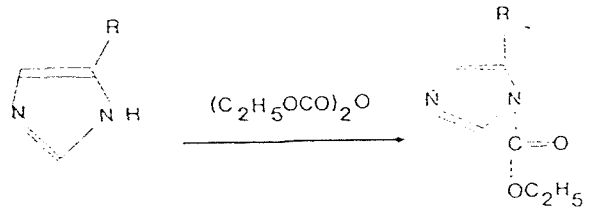


**Figure 3.2.1b**: Diethylpyrocarbonate modification of the amino acid histidine.

This reaction may be followed spectrophotometrically by monitoring the increase in absorbance at 240nm, (Roosemont, 1978). Excess diethylpyrocarbonate is hydrolysed by water [figure 3.2.1c], (Miles, 1977). Indeed the carbethoxyhistidyl product is also unstable and is hydrolysed (Melchior *et al.*, 1970).

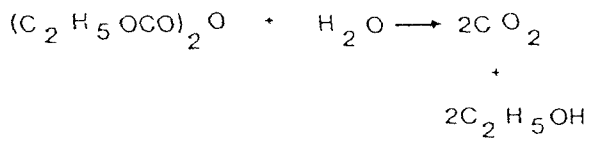


**Figure 3.2.1c**: Hydrolysis of excess diethylpyrocarbonate.

Pelton *et al.*, (1992), showed that all five histidine residues of bovine inositol monophosphatase can be modified with diethylpyrocarbonate at pH 6.0. The modification occurred in at least two identifiable phases; two equivalents reacting rapidly with no effect on activity and three more equivalents at a slower rate. The site of action was not identified, but the total loss of activity did not occur until all five histidine residues had been modified.

### 3.2.2 Results and Discussion

#### 3.2.2.1 Diethylpyrocarbonate inactivates inositol monophosphatase

Preliminary studies using diethylpyrocarbonate to inactivate inositol monophosphatase, showed that the use of a lower concentration of the reagent than used by Pelton and Ganzhorn, (1992), permits approximately 70% inactivation of the enzyme without total modification of all five histidine residues.

When inositol monophosphatase is incubated with 4mM diethylpyrocarbonate at pH 6.5, it is approximately 63% inactivated [figure 3.2.2a] with a second order rate constant of 14.1 ± 1.6 $M^{-1}min^{-1}$ (n = 3) [table 3.2.2a]. Analysis of the stoichiometry of modification, monitored by the change in absorbance at 240nm ( $\varepsilon_{240nm} = 2727M^{-1}cm^{-1}$) [figure 3.2.2b], shows that under these conditions, three equivalents of histidine per subunit are modified [table 3.2.2a].

The data analysis was carried out as described in Dominici *et al.*, (1985), and compensates for the hydrolysis of the reagent during the time of incubation with the enzyme. Diethylpyrocarbonate is readily hydrolysed in aqueous solution, its half-life being dependent on temperature, pH, concentration and buffer composition (Berger, 1975). The first order rate constant for the autohydrolysis of diethylpyrocarbonate in 20mM MES, pH 6.5, at 25°C, is $0.022min^{-1}$ [figure 3.2.2c].

Two equivalents react with a second order rate constant of 224 ± 17 $M^{-1}min^{-1}$ and a third equivalent reacts at a slower rate of 19.4 ± 1.8 $^{-1}min^{-1}$, which is

**Figure 3.2.2a**: Inactivation of 25$\mu$M bovine inositol monophosphatase (Mr 30,055) by diethylpyrocarbonate (4mM), in 20mM MES, pH 6.5, at 25°C: The activity was determined by periodically taking 50$\mu$l aliquots and assaying by the fluorescence assay of Gore *et al.*, (1992). The curves shown represent incubations of DEP with wild type inositol monophosphatase (○) or mutated enzymes C218A (▼), H217Q (●) and inositol monophosphatase in the presence of 2mM Ins(1)P, 20mM $Mg^{2+}$ and 100mM $Li^{+}$ (▲).

**Figure 3.2.2b**: Determination of the extinction coefficient at 240nm for diethylpyrocarbonate modified histidine residues in 20mM MES, pH 6.5, at 25°C. The extinction coefficient determined under these conditions is 2727$M^{-1}cm^{-1}$.

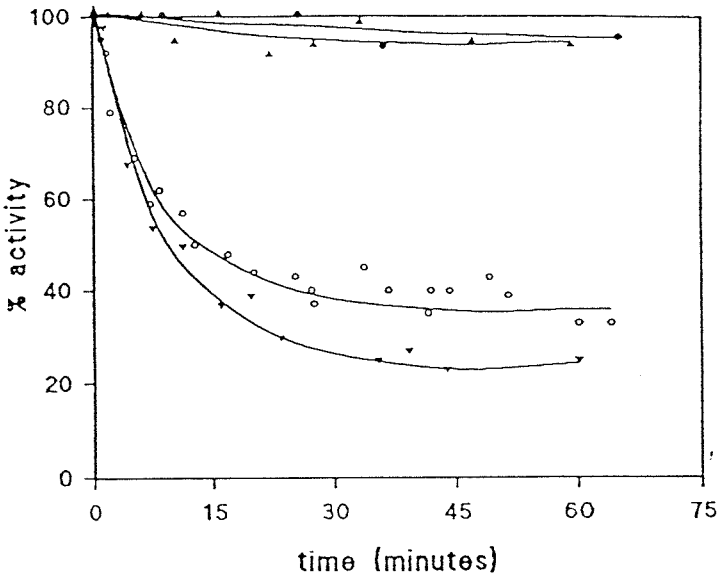


Figure 3.2.2a

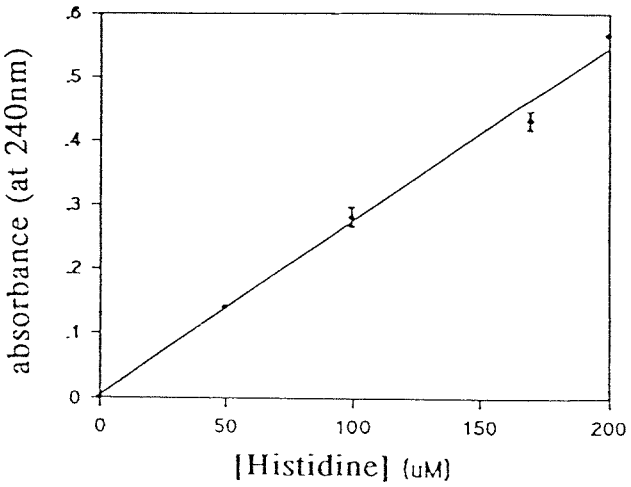


Figure 3.2.2b

**Table 3.2.2a** : Modification of inositol monophosphatase by diethylpyrocarbonate (DEP). The table shows the total % activity lost, the rate of loss of activity ($K_{inact}$) and the total number of sites modified (in the presence and absence of 2mM Ins(1)P, 20mM $Mg^{2+}$ and 100mM $Li^{+}$) and mutant enzymes (H217Q and C218A), in 20mM MES, pH 6.5. The modification of the wild type enzyme and the mutant enzyme (H217Q) in the presence of 29mM DEP is also detailed. The stoichiometry of modification was determined by measuring the absorbance at 240nm ($\epsilon_{240nm}$ = 2727 $M^{-1}cm^{-1}$) and the activity was determined by the fluorescence assay of Gore *et al.*, (1992).

| ENZYME | % LOSS OF ACTIVITY | $K_{inact}$ $M^{-1}min^{-1}$ | NUMBER OF EQUIVALENTS MODIFIED |
|---|---|---|---|
| WILD TYPE (4mM DEP) | 63.3 ± 0.60 | 14.1 ± 1.60 | 2.95 ± 0.24 |
| WILD TYPE (29mM DEP) | 64.9 ± 9.20 | - | 4.80 ± 0.20 |
| WILD TYPE(+ins(1)P + $Li^+$) | 7.00 ± 3.50 | 0.23 ± 0.08 | 1.90 ± 0.20 |
| His-217→Gln (4mM DEP) | 6.00 ± 1.40 | 0.27 ± 0.12 | 1.85 ± 0.26 |
| His-217→Gln (29mM DEP) | 5.00 ± 4.10 | - | 4.00 ± 0.20 |
| Cys-218→Ala | 69.0 ± 8.50 | 14.1 ± 0.50 | 2.81 ± 0.20 |

Table 3.2.2a

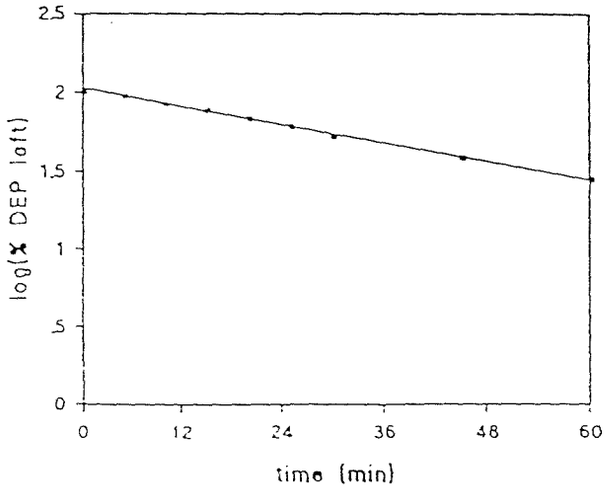


**Figure** 3.2.2c : Determination of the rate of autohydrolysis of diethylpyrocarbonate (k) at 25°C, in 20mM MES, pH 6.5 ($k = 0.022 min^{-1}$.

with the reagent. This mutant was still inactivated [figure 3.2.2a] at approximately the same rate as the wild type enzyme [table 3.2.2a] and approximately three equivalents of histidine were modified per subunit [table 3.2.2a], the same as for the wild type enzyme. Again two sites were modified quickly and one at a slower rate. It can be concluded, therefore, that it is not the modification of Cys-218 by diethylpyrocarbonate that inactivates the enzyme.

Furthermore, the addition of 1M hydroxylamine to the modified and inactivated enzyme led to the regain of all control activity indicating that histidinyl residues had been modified by diethylpyrocarbonate; hydroxylamine reverses the chemical modification of histidine but not lysine, arginine or cysteine residues by diethylpyrocarbonate (Miles *et al.*, 1977).

Therefore, modification of a histidine residue by diethylpyrocarbonate causes inactivation of inositol monophosphatase; suggesting that a histidine residue lies at or near the active site of the enzyme.

### 3.2.2.4 Identification of a histidine residue at or near the active site; design of a mutant enzyme

Bovine inositol monophosphatase contains five histidine residues. The positions of these residues are shown in the X-ray crystallographic structure [figure 3.2.2e].

The reagent diethylpyrocarbonate reacts with the unprotonated side chains of histidine and, therefore, the rate of the reaction will depend upon both the accessibility of the site to be modified and the $pK_a$ of the group. Previous studies on the enzyme from human brain have shown that the $pK_a$ of His-217 is higher than would be expected (approximately 7.5), (Greasley *et al.*, 1993), and might, therefore, be relatively unreactive to the reagent and, hence, have a slower rate of modification. His-217 might, therefore, be the slow reacting residue in the above studies.

Comparison of the sequence of the enzyme from the bovine, human and rat brain

Figure 3.2.2e: X-ray crystallographic structure of inositol monophosphatase. The two subunits are shown in different colours and the histidine residues in white (at positions 65, 100, 188 and 217). This is the X-ray structure for human inositol monophosphatase. The sequence of the bovine enzyme, which has been successfully mapped onto the structure of the human enzyme, contains one extra histidine residue at position 150 (this is a glutamine residue in the human enzyme).

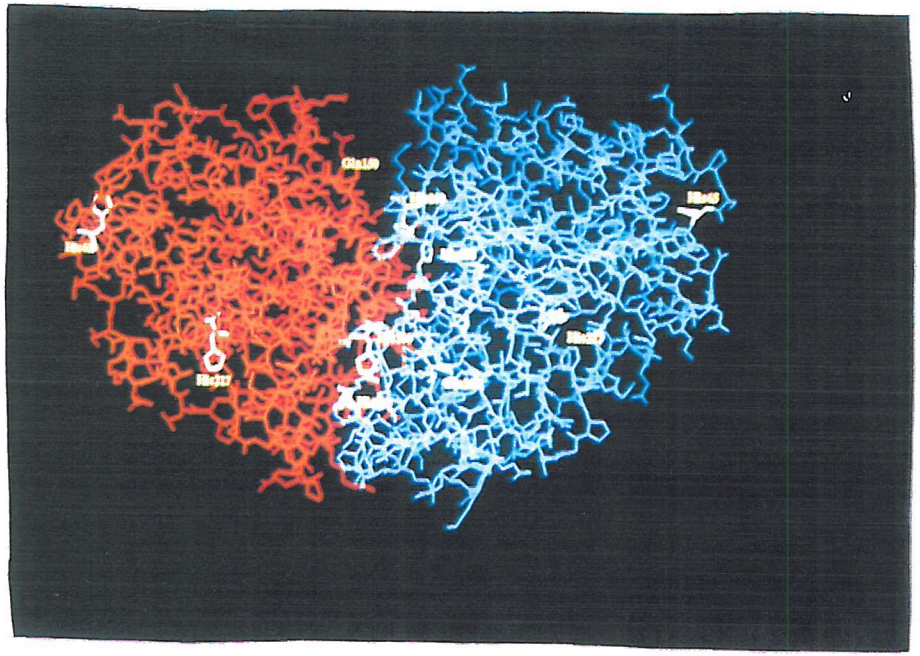

Figure 3.2.2e

(McAllister *et al.*, 1992), show that His-150 is unlikely to be catalytically important since it is not conserved in the human or rat enzymes which have a Gln replacement.

Previous labelling studies using [$^3$H]-iodoacetic acid, (Knowles *et al.*, 1992), have shown that the only histidine residue modified under the conditions used was His-65 and no loss of activity occurred. This observation suggests that His-65 is very exposed or reactive and may, therefore, be one of the fast reacting sites with diethylpyrocarbonate.

In the X-ray crystallographic structure, probable hydrogen bonds can be drawn between His-100 and His-188 located in the dimer interface. The close distance between His-100 and His-188 from each other means that a hydrogen bond between these two amino acids is very likely; such a hydrogen bond would be important in stabilising the dimer structure. The inactivation of bovine inositol monophosphatase by diethylpyrocarbonate is due to the modification of a single slow reacting residue and gel filtration studies demonstrate that there is no perturbation in the quaternary structure of the enzyme. Hence, it is unlikely that His-100 and His-188 are modified by diethylpyrocarbonate.

The data described above, together with the close proximity in the protein sequence of His-217 to Cys-218 (shown to be near the active site in N-ethylmaleimide studies of Knowles *et al.*, (1992), suggests that modification of His-217 by diethylpyrocarbonate might result in the inactivation of bovine inositol monophosphatase. This possibility was investigated by reacting another mutant of bovine inositol monophosphatase bearing a His-217→Gln replacement with diethylpyrocarbonate.

### 3.2.2.5 Identification of a histidine residue at or near the active site ; diethylpyrocarbonate modification

The mutant of the enzyme bearing a His-217→Gln replacement upon reaction with diethylpyrocarbonate is only inactivated 6% [figure 3.2.2a] at a rate of 0.23 ± 0.08

$M^{-1}min^{-1}$, which is approximately 100-fold slower than that of the wild type enzyme [table 3.2.2a]. Significantly, only two equivalents of histidine per subunit were modified [table 3.2.2a] whether substrate and $Li^+$ ions were or were not present. Thus it can be inferred that the slowest reacting of the three residues modified by diethylpyrocarbonate is the one associated with the loss of activity and that this site is His-217 in the wild type enzyme. This, in turn, implies that His-217 is located at or near the active site; a realistic possibility since Cys-218 has been suggested by other experiments to be similarly located (Knowles *et al.*, 1992).

Stoichiometry experiments show that when three equivalents are modified in the wild type enzyme, the loss of activity is only 63.3 ± 0.6 % [table 3.2.2a]. Whereas treatment of the wild type and H217Q mutant enzymes by higher concentrations of diethylpyrocarbonate (29mM) results in the modification of approximately five and four equivalents per subunit, respectively, [figure 3.2.2c], there is little further loss of activity [table 3.2.2a] than occurred when only approximately two and three equivalents, respectively, were modified.

### 3.2.2.6 His-217 is located near the active site, but is not essential for activity

Previous experiments using the human enzyme (Greasley *et al.*, 1993), have shown that the H217Q mutated enzyme is fully active, with the same $K_m$ for substrate as the native enzyme, but with an apparent $K_m$ for $Mg^{2+}$ approximately four-fold higher than that of the wild type enzyme (Greasley *et al.*, 1993). The latter data, together with the inactivation studies described above, suggest that the His-217 residue lies near to the active site of the enzyme, but is not involved in the catalytic mechanism.

### 3.2.2.7 Conclusions

Diethylpyrocarbonate modification of His-217 results in the inactivation of bovine inositol monophosphatase. A combination of the techniques of chemical modification and site directed mutagenesis have shown that His-217 lies near the active site, but

is not involved in the catalytic mechanism.

## 3.3 Chemical modification of arginine residues

### 3.3.1 Introduction

A survey of the crystal structure of numerous proteins shows that, as a rule, the positively charged arginine side chains are located on the surface of proteins, exposed to solvents and reagents (Janin *et al.*, 1979, and Sprang *et al.*, 1979). However, investigations employing α-dicarbonyls for the chemical modification of arginine residues have demonstrated that arginine residues can also play an essential role in the active site of enzymes binding anionic substrates (Riordan, 1979), since arginine residues possess a highly basic guanidino group [figure 3.3.1a] which is positively charged at neutral pH. The ionisation of the arginine side chain is shown in figure 3.3.1a, but with a $pK_a$ in water greater than 12, guanidino groups remain protonated except in strongly alkaline solution.

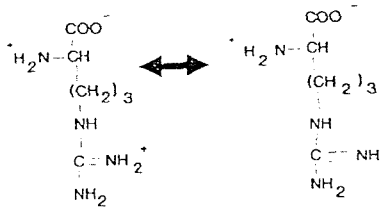

Figure 3.3.1a: Ionisation of the arginine side chain.

The various α-dicarbonyls (for example, butanedione and phenylglyoxal) have proved to be surprisingly selective modification reagents for active site arginine residues involved in the binding of anionic ligands; in most cases, activity is lost concomitant with the modification of a single arginine residue (Patthy *et al.*, 1979). Modification of arginine residues in proteins by dicarbonyl compounds involves condensation with the guanidinium group. Phenylglyoxal appears to be the most

satisfactory reagent described to date, since the reaction is restricted to arginine residues (Takahashi, 1968). At neutral pH, phenylglyoxal reacts reversibly with guanidino groups of proteins to form derivatives containing two phenylglyoxal moieties per guanidino group. Quantitative modification of arginine residues in proteins can be achieved by the use of radiolabelled phenylglyoxal (Jackson *et al.*, 1989) or with the chromophoric reagent 1-pyreneglyoxal and the fluorescent probe, dansylcamphor-10-sulphonic acid. Modification of arginine residues with 1-pyreneglyoxal can be followed by monitoring the change in fluorescence at 453nm, upon excitation at 360nm and quantitated by measuring the absorbance at 360nm ($\varepsilon_{360nm}$ = 16,000$M^{-1}cm^{-1}$). Bovine inositol monophosphatase is inactivated upon modification with phenylglyoxal due to modification of a single arginine residue (Jackson et al., 1989).

### 3.3.2 Results and Discussion

16.6μM enzyme (Mr 30,055), in 50mM $NaHCO_3$, pH 8.0, at 25°C, was incubated with various arginine specific reagents and the reaction monitored by following the decrease in activity with time [figure 3.3.2a]. The buffer, $NaHCO_3$, has been shown to allow the selective modification of arginine residues in model compounds; α-amino groups appear to be unreactive under the same conditions (Cheung *et al.*, 1979). In agreement with Jackson *et al.*, (1989), modification with phenylglyoxal causes 80-90 % inactivation of the enzyme [Figure 3.3.2a]. In the presence of $Mg^{2+}$, Ins(1)P, and $Li^+$ there is no inactivation by phenylgloxal. These data suggest that there is an arginine residue at or near the active site of the enzyme bovine inositol monophosphatase.

1-pyreneglyoxal modifies 1 residue per subunit of the enzyme (quantitated by measuring the absorbance at 360nm ($\varepsilon_{360nm}$ = 16,000$M^{-1}cm^{-1}$) with a corresponding 15 % decrease in activity, both in the presence and absence of substrate [Figure 3.3.2a]. There is an increase in fluorescence (at 453nm upon excitation at 360nm) compared to the unmodified enzyme, but no further changes in the fluorescence of the modified enzyme were detected upon subsequent substrate binding and catalysis.

The structures of two fluorescent cysteine modification reagents, eosin-maleimide and fluorescein-maleimide, are shown in figure 3.4.1a: ,

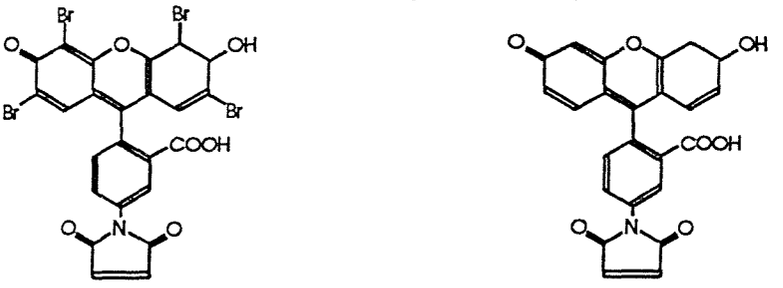

**Figure 3.4.1a :** The structures of two cysteine modification reagents, left to right. eosin-maleimide (Mr 743) and fluorescein-maleimide (Mr 427).

Quantitation of free thiol groups can be achieved by reaction with DTNB (Ellman, 1959). At pH 8.0, the reaction, one of disulphide exchange in which a mixed disulphide is formed between the enzyme and a thionitrobenzoate group, to produce a nitrobenzoate ion [figure 3.4.1b], can be quantitated spectrophotometrically by measuring the appearance of this thionitrobenzoate ion ($\varepsilon_{412}$ = 13,600$M^{-1}cm^{-1}$ at pH 8.0).

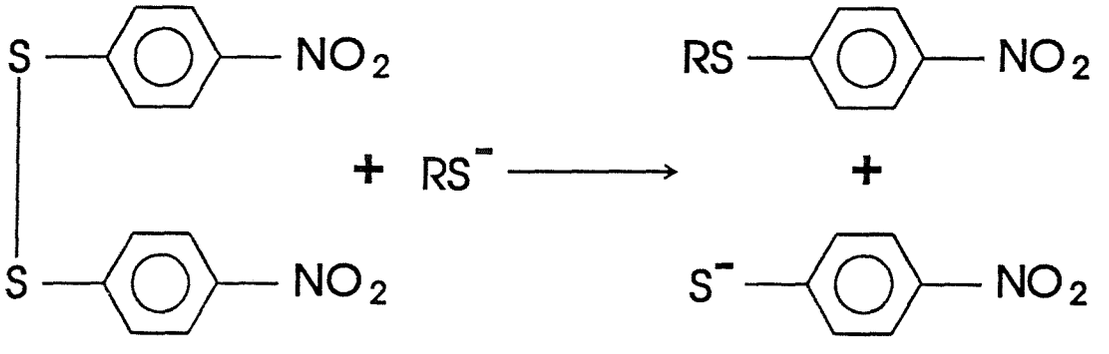

Figure 3.4.1b: Disulphide exchange reaction of free thiol groups with DTNB

The reagents MMTS (methyl methane thiosulphonate) and its derivatives are used to thioalkylate proteins, in order to investigate the role of thiol groups in catalysis. MMTS and its derivatives are composed of simple alkane thiol groups [table 3.4.1a] which can be attached onto accessible or active sulphydryl groups of proteins under conditions mild enough to preserve protein structure. The thioalkylation of sulphydryl groups by MMTS and its derivatives occurs rapidly (Smith *et al.*, 1975).

| COMPOUND | MW | FORMULA |
|---|---|---|
| MMTS | 126.2 | $C_2H_6O_2S_2$ |
| EMTS | 140 | $CH_3CH_2$-S-$SO_2$-$CH_3$ |
| IPMTS | 182.3 | $(CH_3)_2CH$-S-$SO_2$-$CH_3$ |

Table 3.4.1a: Properties of MMTS and its derivatives

Bovine inositol monophosphatase contains six cysteine residues (8, 125, 141, 184, 201, 218), (Diehl *et al.*, 1990). Cys-218 is located near the active site, but is not essential for activity (Knowles *et al.*, 1992) and Cys-8 is essential for the binding of an inhibitory monoclonal antibody (Whiting *et al.*, 1990). Cys-8 is not essential for activity since in the C8A mutant, this antibody binding is abolished, but the enzyme activity is the same as for the wild type enzyme.

### 3.4.2 Results and Discussion: Modification with fluorescein-maleimide and eosin-maleimide

16.6μM enzyme (Mr 30,055), in 50mM Tris, pH 8.0, at 25°C, was incubated overnight with 166μM fluorescein-maleimide or eosin-maleimide.

Fluorescein-maleimide modifies approximately 3 residues per subunit of bovine inositol monophosphatase with a concurrent 53.1 (± 3.4) % inactivation of the enzyme [Table 3.4.2a and figure 3.4.2a]. Two sites are modified slowly (pseudo first order rate constant = 0.00288$min^{-1}$) and one quickly (pseudo first order rate constant = 0.187$min^{-1}$), [figure 3.4.2b].

In the presence of 10mM $MgCl_2$, 1mM Ins(1)P and 10mM $Li^+$, approximately only 2 residues per subunit are modified with no decrease in enzyme activity [Table 3.4.2a].

| ENZYME | number of sites modified by fluorescein -maleimide | % decrease in activity- fluorescein -maleimide | number of sites modified by eosin- maleimide | % decrease in activity- eosin- maleimide |
|---|---|---|---|---|
| wild type | 2.68 +/-0.24 | 53.1 +/-3.4 | 2.9 +/-0.15 | 94.7 +/-1.0 |
| wild type(+S) | 1.64 +/-0.04 | 0 | 1.94 +/-0.05 | 75.2 +/-1.6 |
| C218A | 2.04 +/-0.18 | 23.3 +/-6.9 | 1.71 +/-0.11 | 65.3 +/-4.8 |

**Table 3.4.2a** : Modification of 16.6$\mu$M wild type bovine inositol monophosphatase, the mutated enzyme, C218A, (Mr 30,055) and the wild type enzyme (in the presence of 2mM 2'AMP, 10mM $Mg^{2+}$ and 100mM $Li^{+}$), in 50mM Tris.HCl, pH 8.0, at 25°C, in the dark, by 166$\mu$M fluorescein-maleimide and eosin-maleimide. The table shows the total number of sites modified and loss of activity after overnight incubation. The stoichiometry was quantitated spectrophotometrically ($\epsilon_{524nm}$ (eosin-maleimide) = 89,389 $M_{-1}cm_{-1}$ and $\epsilon_{495nm}$ (fluorescein-maleimide) = 62,562 $M^{-1}cm^{-1}$) and the activity was determined by the fluorescence assay of Gore *et al.*, (1992).

**Figure 3.4.2a** : Stoichiometry of modification of 16.6$\mu$M wild type bovine inositol monophosphatase (Mr 30,055) in 50mM Tris.HCl, pH 8.0, at 25°C, by 166$\mu$M fluorescein-maleimide. The stoichiometry of modification was determined spectrophotometrically ($\epsilon_{495nm}$ = 62,562 $M^{-1}cm^{-1}$).

**Figure 3.4.2b**: The rate of modification of 16.6$\mu$M inositol monophosphatase (Mr 30,055) in 50mM Tris.HCl, pH 8.0, at 25°C, by fluorescein-maleimide. There is a fast (○) and a slow (●) rate of modification, 0.187$min^{-1}$ and 0.00288$min^{-1}$, respectively. The y-axis intercept of 1.82 indicates that two residues are modified slowly and one quickly.

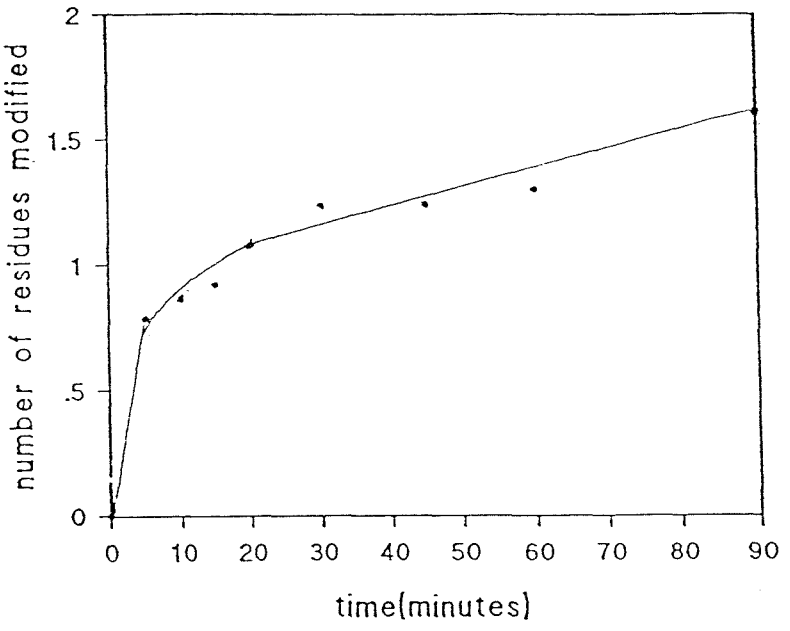


Figure 3.4.2a

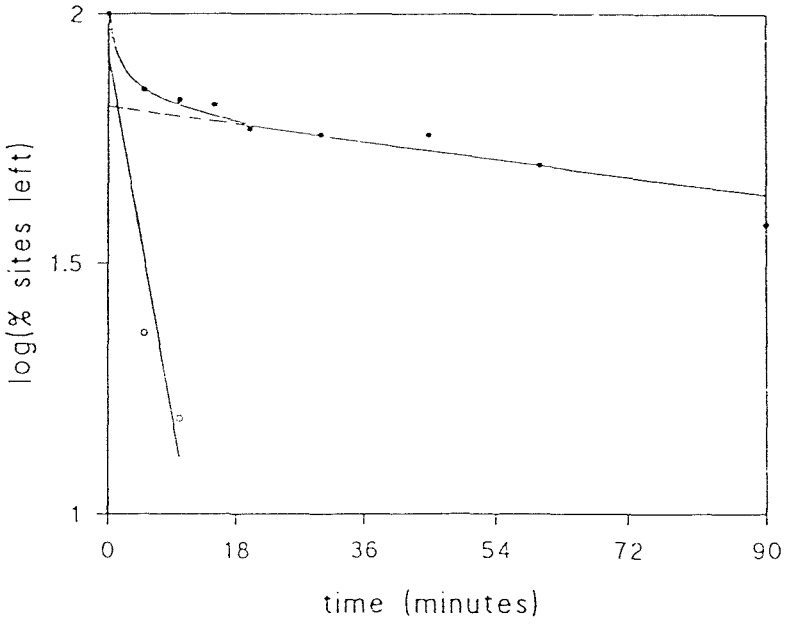


Figure 3.4.2b

Since by peptide sequencing it is only possible to identify the peptide sequence with a gap at the modified cysteine residue, a combination of site directed mutagenesis and chemical modification is employed to identify the labelled amino acids. Cys-218 is probably one of the residues modified by fluorescein-maleimide, since only approximately 2 residues are modified in the C218A mutant upon incubation with fluorescein-maleimide [Table 3.4.2a]. However, it is not the modification of Cys-218 alone that leads to inactivation of the enzyme, since modified C218A loses 26.3 (± 6.9) % activity [Table 3.4.2a].

Eosin-maleimide modifies approximately 3 residues per subunit of bovine inositol monophosphatase with a concurrent 94.7 (± 1.0) % inactivation of the enzyme [Table 3.4.2a]. In the presence of 10mM $MgCl_2$, 1mM Ins(1)P and 10mM $Li^+$, approximately 2 residues per subunit are modified with a resultant 75.2 (± 1.6) % decrease in enzyme activity [Table 3.4.2a]. Again it is probable that one of the residues modified by eosin-maleimide is Cys-218, since only 2 residues approximately are modified in the C218A mutant upon incubation with eosin-maleimide [Table 3.4.2a].

The results with fluorescein-maleimide and eosin-maleimide can be compared to those of N-ethylmaleimide by Knowles *et al.*, (1992) in which only two residues (Cys-218 and residues Cys-141 and Cys-184 in a mutually exclusive manner) were modified per subunit with a 94% inactivation of the enzyme. Long chain maleimides are sometimes more effective reagents than NEM for reaction with sulfydryl groups in apolar environments, for example, the inactivation of D-amino acid oxidase by N-octylmaleimide and several other long chain alkylmaleimides, is many fold more rapid than with hydrophilic NEM, (Fonda *et al.*, 1969). The results suggest that the third residue of bovine inositol monophosphatase modified by the less hydrophillic, longer chain maleimides described here, resides within an apolar environment.

Since modification by fluorescein-maleimide and eosin-maleimide does not totally inactivate the enzyme, it can be concluded that the residues modified are not essential for activity. The modification by these residues inactivates the enzyme due

to steric effects. The inactivation is due to the modification of more than one residue; it is possible that modification of Cys-218 sterically hinders substrate binding and if Cys-8 is modified, perhaps the closing of the N-terminal loop is prevented. Modification of Cys-218 by both reagents results in approximately 30 % inactivation of the enzyme. In the presence of substrate, one site is protected from modification by both reagents. Cys-218 has previously been shown to be located near the active site (Knowles *et al.*, 1992). The greater degree of inactivation due to modification by eosin-maleimide can be explained by its greater bulkiness providing more steric hinderance.

The fluorescence, in the presence and absence of 3mM $Mg^{2+}$, of enzyme labelled at a single site with either fluorescein-maleimide or pyrene-maleimide was compared to determine if the spectral properties of these labels can be used to indicate changes in their environment. When enzyme is labelled at a single site with pyrene-maleimide, Cys-218 (Greasley *et al.*, 1993), the enzyme has 96% activity compared with the control enzyme and the pyrene-maleimide labelled enzyme exhibits resonance energy transfer [figure 3.4.2c]. The addition of 3mM $Mg^{2+}$ to this enzyme leads to a 40% increase in resonance energy transfer [figure 3.4.2c], signalling a change in the environment of pyrene-maleimide Greasley *et al.*, 1993), which has subsequently been shown to be a conformational change occurring after $Mg^{2+}$ binding (Mark Thorne, personal communication). In contrast, labelling of the enzyme at a single site with fluorescein-maleimide leads to 80% inactivation of the enzyme and the fluorescence of fluorescein-maleimide labelled enzyme does not alter on the addition of 3mM $Mg^{2+}$ [figure 3.4.2d], suggesting that $Mg^{2+}$ may not bind the fluorescein-maleimide labelled enzyme . However, CD studies in the near-UV region with both fluorescein-maleimide and pyrene-maleimide labelled enzyme, in the presence and absence of $Mg^{2+}$, suggest that the $Mg^{2+}$ binds to the enzyme in both cases, since an increase in signal is seen in the near-UV region for both, implying that the lack of a fluorescence change upon addition of $Mg^{2+}$ to fluorescein-maleimide is not due to the inability of $Mg^{2+}$ to bind to the enzyme.

**Figure 3.4.2c:** Fluorescence changes upon addition of 3mM $Mg^{2+}$ to 1.6$\mu$M pyrene-maleimide labelled enzyme, upon excitation at 292nm. The curves drawn are unlabelled enzyme, in the presence (■) and absence (●) of 3mM $Mg^{2+}$, labelled enzyme in the absence (○) and presence (▲) of $Mg_{2+}$.

**Figure 3.4.2d:** Fluorescence changes upon addition of 3mM $Mg^{2+}$ to 1.6$\mu$M fluorescein-maleimide labelled enzyme, in the presence (○) and absence (■) of $Mg_{2+}$, and labelled enzyme in the presence (▲) and absence (●) of $Mg_{2+}$.

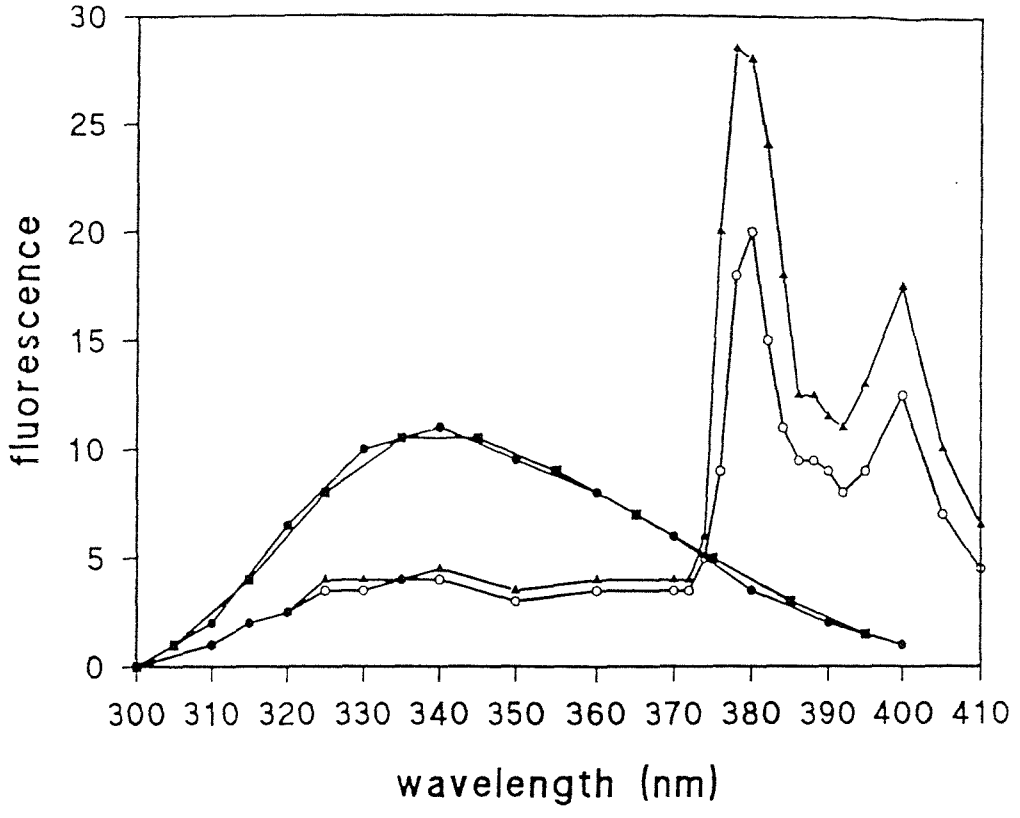


Figure 3.4.2c

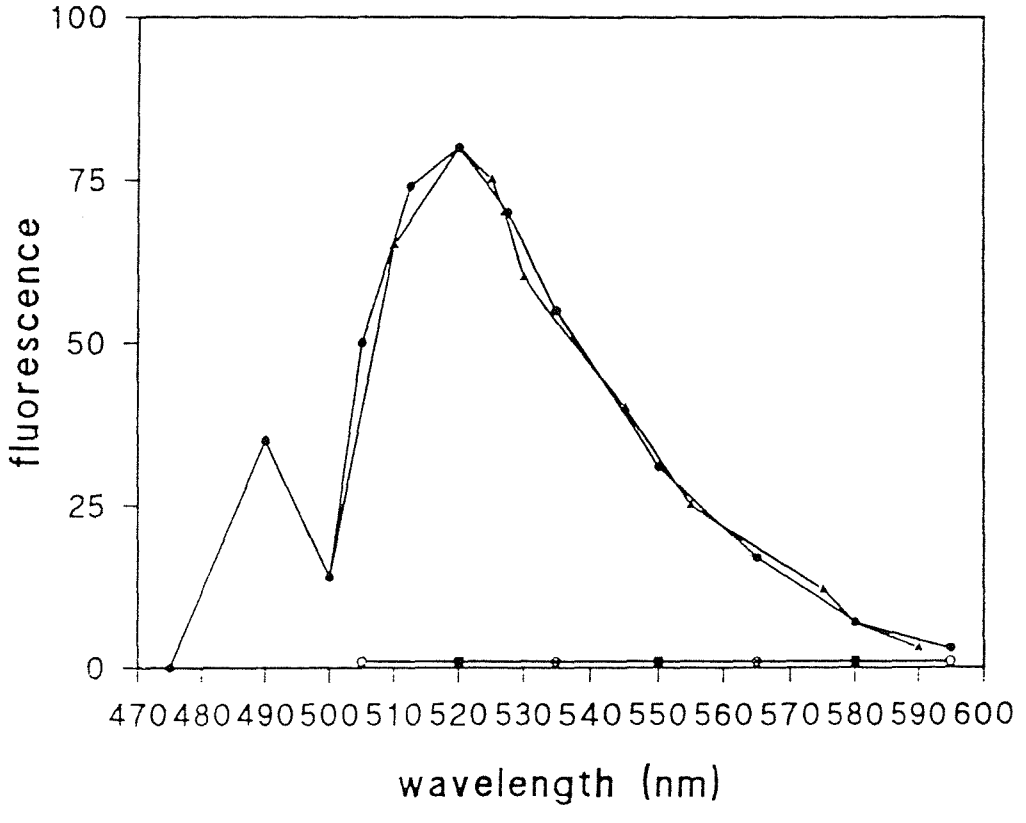


Figure 3.4.2d

| [REAGENT] (mM) | MMTS | IPMTS | EMTS |
|---|---|---|---|
| 0.05 | 10 | - | 36.5 |
| 0.1 | - | 9 | 37.8 |
| 0.125 | 30 | - | - |
| 0.25 | 55 | 21 | 56.7 |
| 0.5 | 69 | 30 | 71.6 |

**Table 3.4.3a**: Modification of 8.3$\mu$M inositol monophosphatase (Mr 30,055), in 50mM Tris.HCl, pH 8.0, at 25°C, with various concentrations of MMTS and its derivatives, EMTS and IPMTS. The table shows the % decrease in protein fluorescence (at 340nm after excitation at 290nm). 0.5mM reagent causes maximal change in fluorescence and is used in all future studies.

| ENZYME | MMTS | IPMTS | EMTS |
|---|---|---|---|
| wild type | 68.8 (±3.0) | 24.5 (±5.1) | 71.6 |
| wild type (+S) | 71 (±1.0) | 27.2 (±2.8) | 71.0 |
| C218A | 52.9 (±0.7) | 16.0 (±4.5) | 42.7 |
| C8A | 47.1 (±0.9) | 0.0 | 47.0 |

**Table 3.4.3b:** Modification of 8.3$\mu$M inositol monophosphatase (Mr 30,055) in 50mM Tris.HCl, pH 8.0, at 25°C, by 0.5mM MMTS and its derivatives (EMTS and IPMTS). The table shows the total % decrease in fluorescence (at 340nm upon excitation at 290nm) for wild type inositol monophosphatase, mutated enzymes, C218A and C8A, and inositol monophosphatase in the presence of 100mM $Li^+$, 10mM $Mg^{2+}$ and 2mM 2'AMP.

**Figure 3.4.3a**: Modification of 8.3$\mu$M inositol monophosphatase (Mr 30,055) in 50mM Tris.HCl, pH 8.0, at 25°C, by 0.5mM MMTS. The figure shows the % fluorescence (at 340nm upon excitation at 290nm) versus time of incubation with MMTS. The curves drawn are wild type inositol monophosphatase (●), mutated enzymes, C218A (▲) and C8A (○), and control (■).

**Figure 3.4.3b**: Modification of 8.3$\mu$M inositol monophosphatase (Mr 30,055) in 50mM Tris.HCl, pH 8.0, at 25°C, by 0.5mM MMTS, in the presence of 2mM 2'AMP, 10mM $Mg^{2+}$ and 100mM $Li^{+}$. The figure shows the % fluorescence (at 340nm upon excitation at 290nm) versus time of incubation with MMTS. The curves drawn are wild type inositol monophosphatase (●), mutated enzymes, C218A (▲) and C8A (○), and control (■).

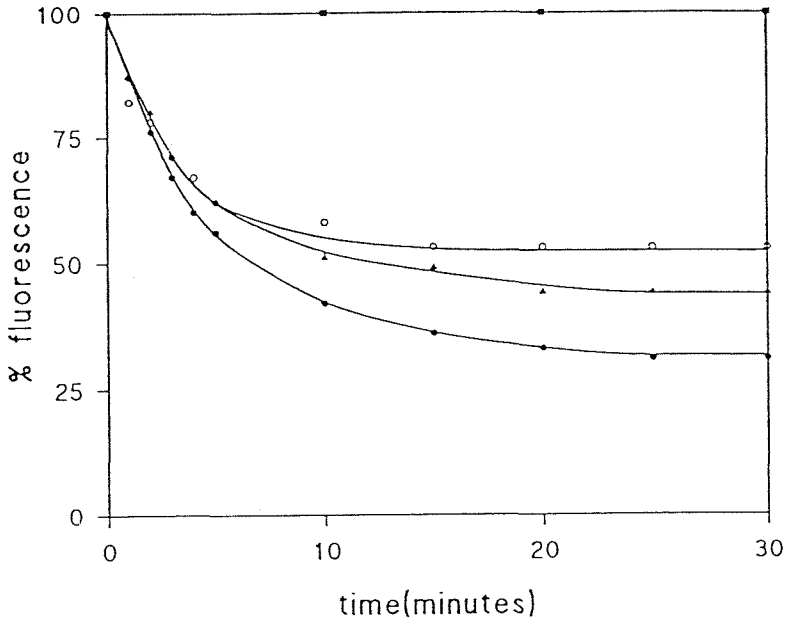


Figure 3.4.3a

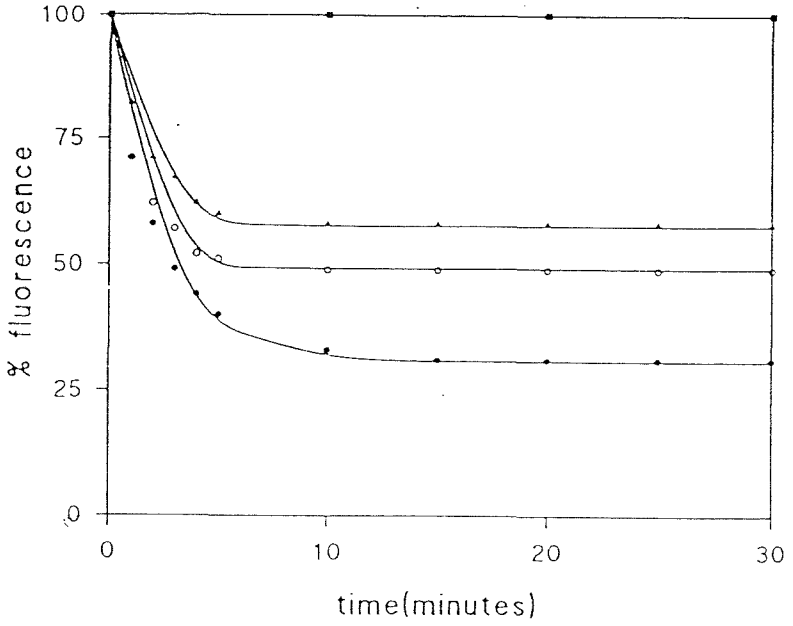


Figure 3.4.3b

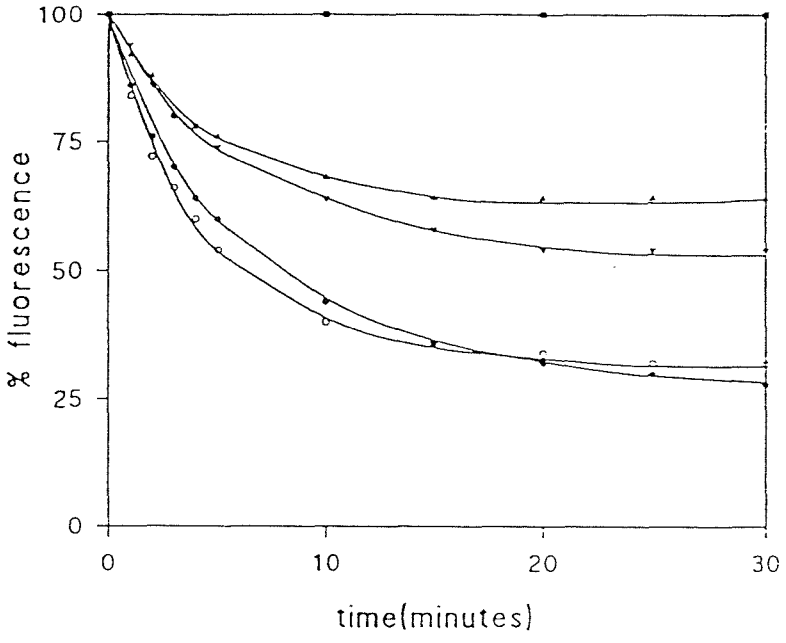


**Figure** 3.4.3c: Modification of 8.3$\mu$M inositol monophosphatase (Mr 30,055) in 50mM Tris.HCl, pH 8.0, at 25°C, by 0.5mM EMTS. The figure shows the % fluorescence (at 340nm upon excitation at 290nm) versus time of incubation with EMTS. The curves drawn are wild type inositol monophosphatase (●), mutated enzymes, C218A (▲) and C8A (▼), wild type enzyme in the presence of 2mM 2'AMP, 10mM $Mg^{2+}$ and 100mM $Li^{+}$ (○) and control (■).

| ENZYME | MMTS | IPMTS | EMTS |
|---|---|---|---|
| wild type | 4 | 3.07 | 4.19 ± 0.2 |
| wild type (+S) | 4 | 2.89 | 3.61 ± 0.12 |
| C8A | 3.12 | 1.74 | 2.92 ± 0.22 |
| C8A (+S) | 3.13 | 1.78 | - |
| C218A | 3.07 | 2.32 | 3.04 |
| C218A (+S) | 3.35 | 2.28 | - |

**Table 3.4.3c**: Modification of 8.3$\mu$M inositol monophosphatase (Mr 30,055) in 50mM Tris.HCl, pH 8.0, at 25°C, by 0.5mM MMTS and its derivatives (EMTS and IPMTS). The table shows the total number of sites modified for wild type inositol monophosphatase, and the mutated enzymes, C218A and C8A, in the presence and absence of 2mM 2'AMP, 10mM $Mg^{2+}$ and 100mM $Li^{+}$. The number of sites not modified by MMTS and its derivatives was quantitated spectrophotometrically by modification by DTNB ($\epsilon_{412nm}$ = 13,600 $M^{-1}cm^{-1}$).

| ENZYME | MMTS : % INACTIVATION (k ($M^{-1}MIN^{-1}$) | IPMTS : % INACTIVATION (k ($M^{-1}MIN^{-1}$) | EMTS : % INACTIVATION (k ($M^{-1}MIN^{-1}$) |
|---|---|---|---|
| wild type | 26 ± 0<br>(8751 ± 1042) | 13.5 ± 0.7<br>(2839) | 19.4<br>(693) |
| C218A | 11.5 ± 1.5<br>(8442 ± 704) | 0 | 14<br>(693) |
| C8A | 12.5 ± 2.5<br>(8690 ± 1254) | 12.8<br>(1922 ± 646) | 10<br>(200) |
| wild type (+S) | 23.0 ± 2.8<br>(4177 ± 440) | 13.5 ± 0.4<br>(3106 ± 622) | 18.8<br>(360) |

Table 3.4.3d: Modification of 8.3$\mu$M inositol monophosphatase (Mr 30,055) in 50mM Tris.HCl, pH 8.0, at 25°C, by 0.5mM MMTS and its derivatives (EMTS and IPMTS). The table shows the total % activity lost and the pseudo first order rate constant for inactivation (k) for wild type enzyme (in the presence and absence of 2mM 2'AMP, 10mM $Mg^{2+}$ and 100mM $Li^{+}$) and the mutated enzymes, C218A and C8A. The activity was determined by the fluorescence assay of Gore *et al.*, (1992).

**Figure** 3.4.3d: Modification of 8.3$\mu$M inositol monophosphatase (Mr 30,055) in 50mM Tris.HCl, pH 8.0, at 25°C, by 0.5mM MMTS. The figure shows the % activity versus time of incubation with MMTS for wild type inositol monophosphatase (●), the mutated enzymes, C218A (▲) and C8A (▼), and wild type inositol monophosphatase in the presence of 2mM 2'AMP, 10mM $Mg^{2+}$ and 100mM $Li^{+}$ (○). The activity was determined by periodically removing 50$\mu$l aliquots and assaying by the fluorescence assay of Gore *et al.*, (1992).

**Figure** 3.4.3e: Modification of 8.3$\mu$M inositol monophosphatase (Mr 30,055) in 50mM Tris.HCl, pH 8.0, at 25°C, by 0.5mM IPMTS. The figure shows the % activity versus time of incubation with IPMTS for wild type inositol monophosphatase (●), the mutated enzyme, C8A (▲), and wild type inositol monophosphatase in the presence of 2mM 2'AMP, 10mM $Mg^{2+}$ and 100mM $Li^{+}$ (○). The activity was determined by periodically removing 50$\mu$l aliquots and assaying by the fluorescence assay of Gore *et al.*, (1992).

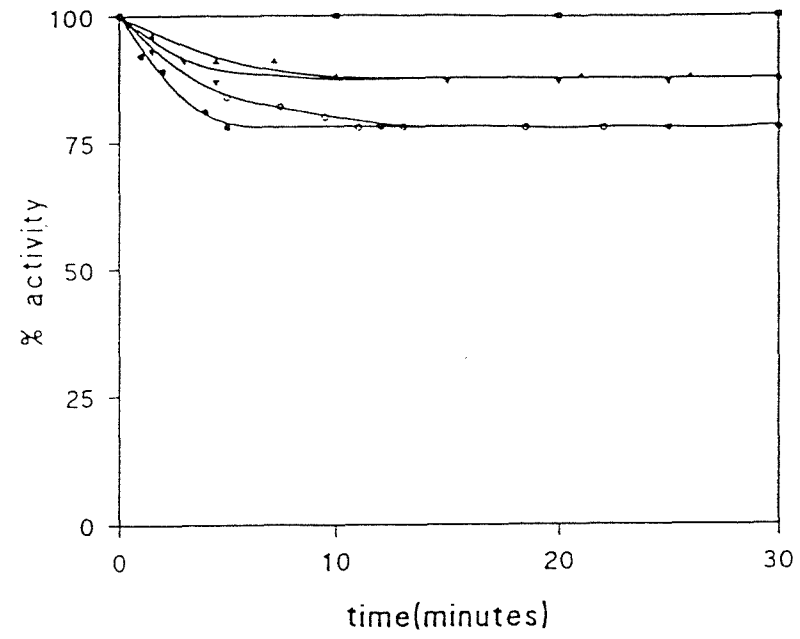


Figure 3.4.3d

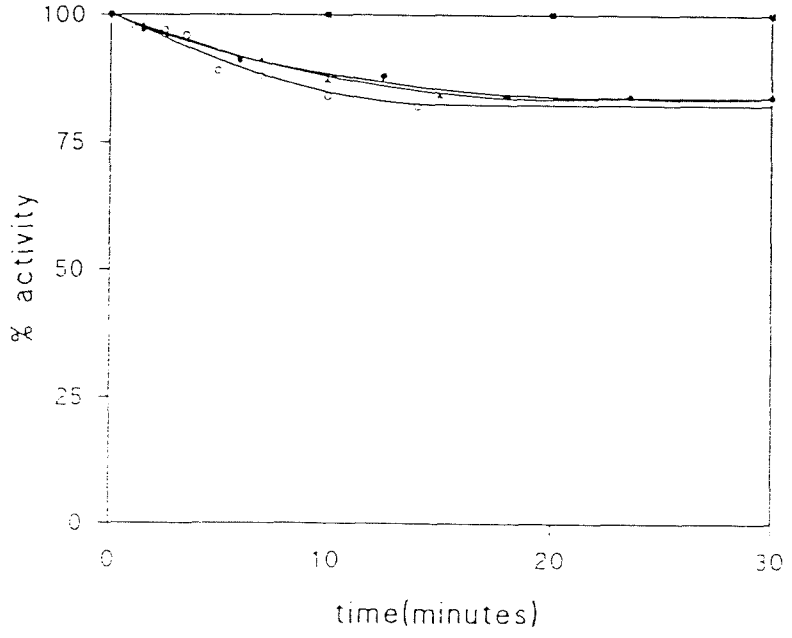


Figure 3.4.3e

hence, a combination of chemical modification and site directed mutagenesis techniques were used. In these experiments the reagent was incubated with mutant enzymes, C218A or C8A, and the reaction performed as before. These experiments suggest that Cys-218 and Cys-8 are two of the residues modified by MMTS and its derivatives since the number of groups modified in these mutant enzymes decrease by approximately one in each case [table 3.4.3c]. There is no substrate protection against modification by MMTS and its derivatives, suggesting that the modified residues are not located at or near the active site. Alternatively, the fact that MMTS and its derivatives are so small could explain the lack of total protection by substrate. The rate of inactivation in the presence of substrate is lower. However, Knowles *et al.*, (1992), demonstrated that Cys-218 is located at or near the active site by using the much larger cysteine modification reagent, NEM. By using the smaller modification reagent, MMTS, the distinction between Cys-218 being located at or simply near the active site can be made; Cys-218 is located near the active site, but is not involved in catalysis. The larger modification reagent, NEM, does not modify Cys-8 (Knowles *et al.*, (1992)). Modification of Cys-8 by the much smaller MMTS derivatives, implies that Cys-8 is only poorly accessible to the larger reagent. As seen with the cysteine modification reagents, fluorescein-maleimide and eosin-maleimide, the inactivation upon modification by MMTS and its derivative (EMTS) is due to the modification of more than one residue. For the larger derivative of MMTS, IPMTS, the inactivation is due solely to Cys-218. The inactivation seen with MMTS and EMTS is due to reaction with Cys-8 and Cys-218 which are not essential for activity.

## 3.5 Chemical modification of amino groups

### 3.5.1 Introduction

Proteins are charged molecules having characteristic numbers of both anionic and cationic residues; modification of the individual charged groups may affect their net ionic charge in a way which is disruptive to their characteristic properties. Chemical modification of ε-amino groups of the A-protein of the tobacco mosaic virus showed

that the lysine residues of the A-protein have an important role in maintaining the structure of the tobacco mosaic virus; the positive charge on Lys-53 is involved in an ion pair (Perham *et al.*, 1967).

Amino groups of proteins are basic groups (with $pK_a$ values near 8.0 for α-amino groups and 9.5 for ε-amino groups) and are positively charged except at high pH. Only the uncharged form, that which predominates at pH values greater than their $pK_a$ value, is reactive as a nucleophile. A variety of reagents have been exploited for the modification of amino groups and include: acid anhydrides for the acylation of amino groups (Lundblad, 1984); reagents for the arylation of amino groups, including fluoro- and chloro- dinitrobenzene and trinitrobenzene sulfonic acid; and carbonyl-containing reagents, for example, pyridoxal phosphate (Page *et al.*, 1968 and 1969), ß-napthoquinone and disulfonic acids (Matsushima *et al.*, 1968), glutaraldehyde (Habeeb, 1968, and Richards *et al.*, 1968): The use of many of these reagents is severely restricted by their lack of complete specificity.

TNBS exhibits fewer side reactions with other protein groups and components of solvents than other chemical modification reagents for amino groups (Means *et al.*, 1971) and so is used for studies of amino groups of bovine inositol monophosphatase described here. The reaction of TNBS (2,4,6-trinitrobenzenesulphonic acid) with α- and ε- amino groups is strongly pH dependent, since only the unprotonated amino groups react (Goldfarb, 1966, and Freedman *et al.*, 1968), and the modification converts positively charged amino groups into neutral TNP-amino acids. Lysine residues contain ε-amino groups [figure 3.5.1a]:

Figure 3.5.1a

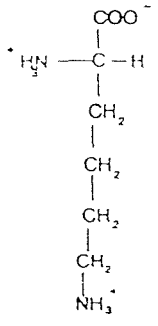

The use of TNBS for protein modification studies was originally proposed by Okuyama *et al.*, (1960). The reaction conditions for TNBS are milder than for

ninhydrin, another reagent modifying amino groups (Moore *et al.*, 1954, and Rosen, 1957), and also more specific for the modification of amino groups (Fields, 1971). In chemical modification by TNBS, sulphite is displaced from TNBS by an attacking nucleophile [Figure 3.5.1b], (Fields, 1971). The reaction can be followed by monitoring the increase in absorbance at 420nm ($\varepsilon_{420}$ = 19,200$M^{-1}cm^{-1}$), (Fields, 1971) which is remote from the region of absorbance of unreacted TNBS (Fields, 1971).

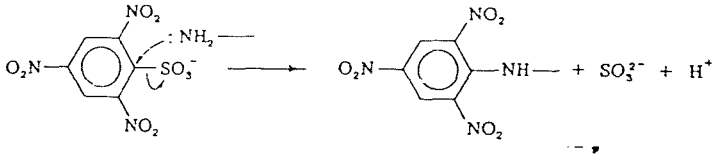

Figure 3.5.1b: Modification of amino groups by TNBS.

### 3.5.2 Results and Discussion

20μM enzyme (Mr 30,055) in 50mM $NaHCO_3$, pH 8.5, at 25°C, was incubated with 100mM TNBS. Periodically, aliquots were removed and the reaction stopped by the addition of 1M ß-mercaptoethanol. Excess adduct formed between ß-mercaptoethanol and TNBS was removed by dialysis against 5l 50mM Tris.HCl, pH 8.5. The absorption spectra of ε-TNP-lysine and α-TNP amino acids are similar in that both have absorption maxima at approximately 345nm with a broad shoulder at 420nm (Satake *et al.*, 1960). The modification of the enzyme was followed by monitoring the increase in absorbance at 420nm [Figure 3.5.2a].

The stoichiometry of modification can be calculated since at 420nm, the extinction coefficient is 19,200$M^{-1}cm^{-1}$. In the presence and absence of substrate, approximately three residues are modified [Figure 3.5.2a] with a 75% decrease in activity [Figure 3.5.2a]. Modification by TNBS is not subject to protection by the presence of

100mM LiCl, 10mM $MgCl_2$ and 2mM Ins(1)P [figure 3.5.2a], suggesting that the modified residues are not located near the active site.

The rates of modification and inactivation occur at a single rate, in the presence and absence of substrate. Modification in the presence of substrate, occurs at $0.021min^{-1}$ and in the absence of substrate at $0.023min^{-1}$. In both cases, the enzyme is inactivated with a pseudo first order rate constant of $0.011min^{-1}$.

TNBS usually reacts with lysine residues, but can react with other residues. Knowles *et al.*, (1992), have demonstrated that there is a reactive cysteine residue, Cys-218, in inositol monophosphatase and this may react with TNBS to inactivate the enzyme. This possibility was excluded since both wild type and the Cys-218→Ala mutant of inositol monophosphatase lose approximately 75% of their activity upon modification with this reagent; the pseudo first order rate constant for inactivation of C218A is $0.022min^{-1}$.

The hypothesis that TNBS modification of Lys-36 (a key residue in the amino terminal loop region of the enzyme) leads to inactivation was investigated. Limited proteolysis of the enzyme, using 0.005 % trypsin, results in cleavage of the bond between Lys-36 and Ser-37, at the N-terminus, and consequent inactivation of the enzyme (Greasley *et al.*, (1993)). If Lys-36 is modified by TNBS, the limited proteolysis, and subsequent inactivation, may not occur, since the enzymatic hydrolysis of peptide bonds depends upon recognition of the susceptible bonds by the particular enzyme. Modification of Lys-36 by TNBS could lead to inactivation of inositol monophosphatase by prevention of the conformational change at the N-terminus which is essential for activity. When incubated with trypsin, both the TNBS modified and unmodified enzyme are totally inactivated (activity expressed % relative to t = 0 incubation time with trypsin). The pseudo first order rate constant of inactivation is $0.064min^{-1}$ for the unmodified enzyme and $0.068min^{-1}$ for the TNBS-modified enzyme. This result suggests that TNBS inactivation of inositol monophosphatase is not due to modification of Lys-36 and that Lys-36 does not appear to be modified by TNBS.

When modified enzyme was taken and subjected to $NH_2$ terminal sequencing by the Edman technique (Edman, 1956) no sequence information was gained suggesting that the amino terminus was blocked. In control enzyme, unmodified by the reagent TNBS, protein sequencing could be carried out, suggesting that the N-terminus is blocked after reaction with TNBS. In conclusion, TNBS modification of bovine inositol monophosphatase leads to inactivation. The modified residue(s) important for activity are not located at or near the active site. The inactivation could be due to steric hindrance of a conformational change necessary for catalysis. Alternatively, TNBS modification of lysine residues will abolish their positive charge. It is possible that the TNBS modified enzyme is inactivated due to the abolition of surface positive charges which are necessary for a functional enzyme. Finally, the inactivation by TNBS could be due to modification of the N-terminus.

## 3.6 Modification of acidic amino acids

### 3.6.1 Introduction

There are two amino acids with strongly acidic side chains, aspartic acid and glutamic acid, which because of their low $pK_a$ values (4.4 in water), are nearly always negatively charged at physiological pH. Woodward's reagent K (N-ethyl-5-phenylisoxazolium-3-sulfonate) is a reagent used for the modification of such carboxylic acid side chains of proteins under fairly mild conditions in aqueous solution and at room temperature (Petra, 1971). The reaction results in the formation of enol-esters. The reagent is fairly unstable in aqueous solution and, therefore, must be prepared fresh and used immediately.

### 3.6.2 Results and Discussion: Evidence for an important acidic amino acid side chain

16μM inositol monophosphatase (Mr 30,055), in 50mM Tris.HCl, pH 8.0, at 25°C, was incubated with 10mM Woodward's reagent K (prepared just prior to use as a 1M stock in 50mM Tris.HCl, pH 8.0) and the modification was followed by

monitoring the decrease in activity with time by periodically removing 50µl aliquots and assaying by the fluorescence assay of Gore *et al.*, (1992) [figure 3.6.2a].

The modification was repeated in the presence of various protecting agents [figure 3.6.2a]. There is protection against inactivation by Woodward's reagent K when modification is carried out in the presence of: 1mM Ins(1)P, 10mM $Mg^{2+}$ and 100mM $Li^{+}$; or 5mM $P_i$ and 10mM $Mg^{2+}$ [figure 3.6.2a]. Protection against inactivation by Woodward's reagent K does not occur in the presence of $Mg^{2+}$ or $P_i$ alone. There is only a small degree of protection in the presence of Ins(1)P alone. There is no protection against inactivation by $P_i$ in the presence of $Li^{+}$.

The stoichiometry of modification was determined by reduction of Woodward's reagent K modified enzyme by incubation with 1mM [$^3$H] sodium borohydride (added from a 200mM stock; 500mCi/mmol) after first removing excess, hydrolysed Woodward's reagent K by gel filtration, using a G-10 Sephadex column. Excess sodium borohydride was removed by gel filtration, using a G-10 Sephadex column. The incorporated radioactivity was determined by scintillation counting. One site was modified in the unprotected enzyme and none in enzyme modified in the presence of 5mM $P_i$ and 10mM $Mg^{2+}$.

These results suggest that there is an acidic amino acid side chain located at or near the active site. Lack of protection in the absence of $Mg^{2+}$, supports the mechanism proposed in chapter 4 which proposes that there is ordered binding of substrate and $Mg^{2+}$, with $Mg^{2+}$ binding first.

A control experiment needs to be performed to verify that the reagent is not reacting with cysteine residues. Knowles *et al.*, (1992), have shown that Cys-218 is a reactive cysteine residue located near the active site of the enzyme. When 10mM Woodward's reagent K reacts with a mutant of bovine inositol monophosphatase, C218A, there is 75% inactivation of the enzyme with a pseudo first order rate constant of inhibition of 0.44 $min^{-1}$, which is comparable to that observed for the wild type enzyme, 75% inactivation with a pseudo first order rate constant of 0.456

**Figure 3.6.2a**: Inactivation of 16$\mu$M inositol monophosphatase (Mr 30,055), in 50mM Tris.HCl, pH 8.0, at 25°C, by 10mM Woodward's reagent K (N-ethyl-5-phenylisoxazolium-3-sulfonate), prepared fresh as a 1M stock in 50mM Tris.HCl, pH 8.0. The inactivation caused by Woodward's reagent K was followed by periodically removing 50$\mu$l aliquots and assaying by the fluorescence assay of Gore *et al.*, (1992). The modification was performed in the presence of various ligands: Control, no Woodward's reagent (■); no ligands (○); 1mM Ins(1)P, 10mM $Mg^{2+}$ and 100mM $Li^{+}$ (●); 10mM $Mg^{2+}$, 5mM $P_i$ (▲); 10mM $Mg^{2+}$ (□); 5mM $P_i$ (△); 1mM Ins(1)P (▽); 100mM $Li^{+}$, 5mM $P_i$ (◆).

**Figure 3.6.2b**: Inactivation of 16$\mu$M inositol monophosphatase (Mr 30,055), in 50mM Tris.HCl, pH 8.0, at 25°C, by increasing concentrations of Woodward's reagent K (prepared fresh as a 1M stock in 50mM Tris.HCl, pH 8.0). The inactivation caused by Woodward's reagent K was followed by periodically removing 50$\mu$l aliquots and assaying by the fluorescence assay of Gore *et al.*, (1992). The curves drawn are 10mM (○), 5mM (▲), 4mM (●), 3mM (▼). The pseudo first order rate constants of inhibition ($K_{app}$) for the inactivation by Woodward's reagent K can be determined from a plot of log(% activity) versus time: 10mM ($0.456min^{-1}$), 5mM ($0.223min^{-1}$), 4mM ($0.179min^{-1}$) and 3mM ($0.161min^{-1}$).

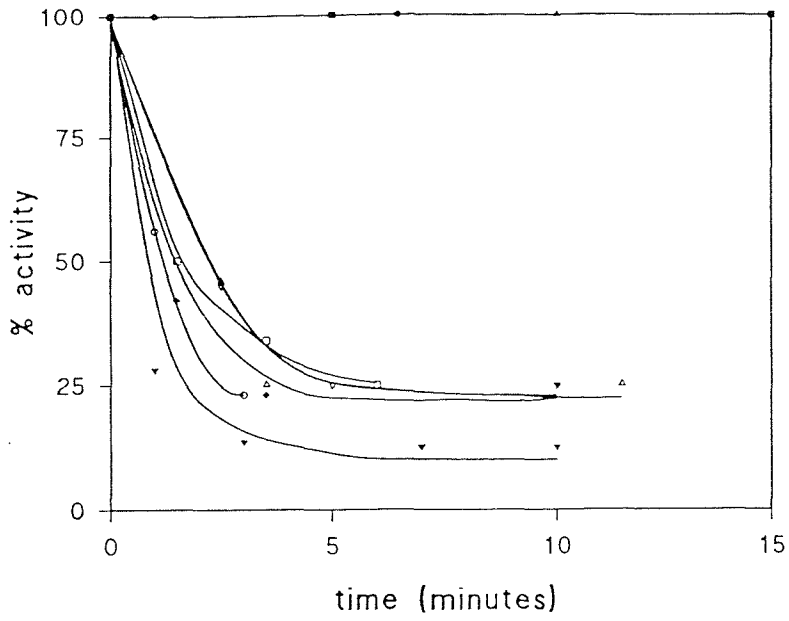


Figure 3.6.2a

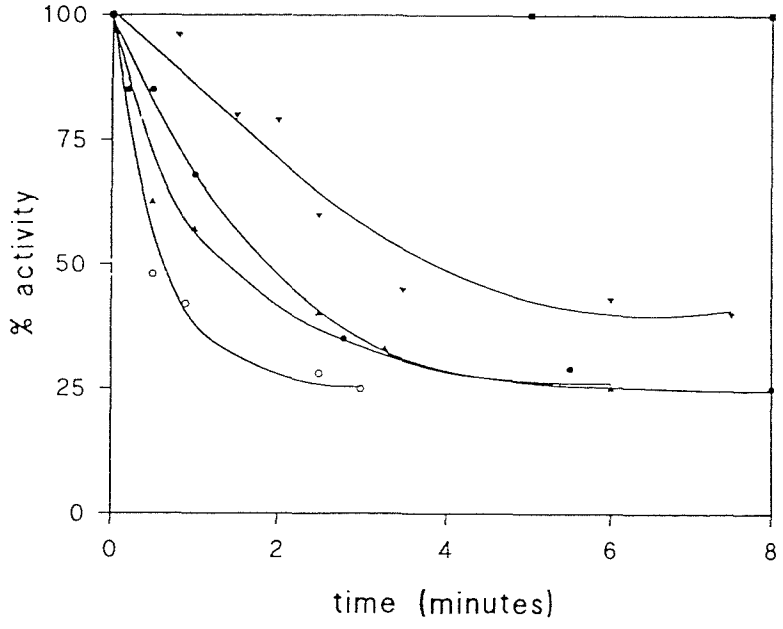


Figure 3.6.2b

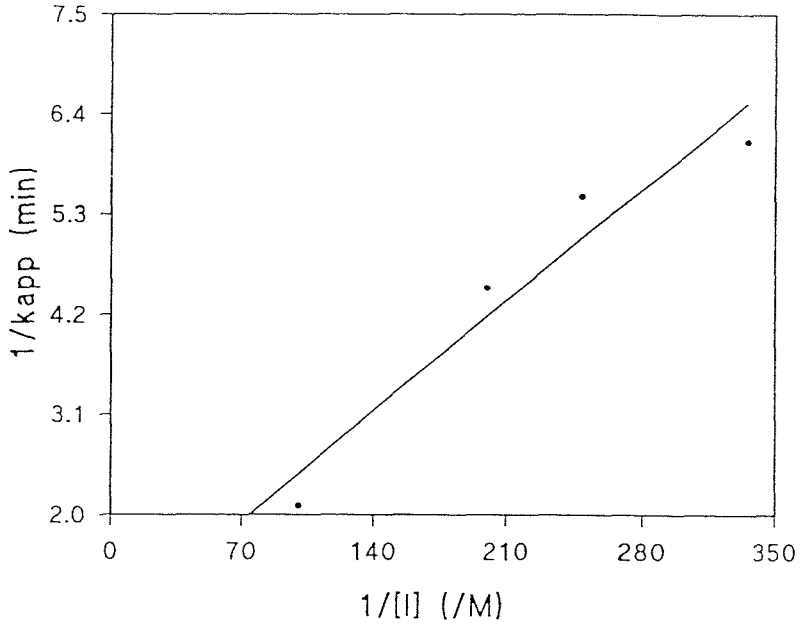


**Figure 3.6.2c:** Kinetics of inactivation of 16$\mu$M inositol monophosphatase (Mr 30,055) in 50mM Tris.HCl, pH 8.0, at 25°C, by increasing concentrations of Woodward's reagent K (prepared as a 1M stock in 50mM Tris.HCl, pH 8.0). The inactivation caused by modification by Woodward's reagent K was followed by periodically removing 50$\mu$l aliquots and assaying by the fluorescence assay of Gore *et al.*, (1992), and the rates of inactivation determined. The first order rate constant of inhibition (at saturation), $k_2$, calculated from the y-axis intercept, is $0.71 min^{-1}$, and the steady state constant (an apparent binding constant), $K_{I,app}$, calculated from the slope, is 0.012minM.

$min^{-1}$.

The kinetics of inactivation of inositol monophosphatase by Woodward's reagent K can be examined by measuring the loss of activity with time at different concentrations of Woodward's reagent K [figure 3.6.2c]. A reaction of the type A + B $\rightarrow$ products, (where, in this case, A is an acidic amino acid side chain and B Woodward's reagent K), is often second order overall, with a rate law $-d[A]/dt = k[A][B]$. However, the chemical modification of amino acid side chains is a reaction in which the concentration of the amino acid side chains ([A]) is much lower than that of Woodward's reagent K ([B]), hence, during the reaction [B] remains essentially constant, and the rate law now becomes $-d[A]/dt = k_{app}[A]$. The pseudo first order rate constants of inhibition, $K_{app}$, calculated from the slopes of log (% activity) versus time (Petra, 1971) are 0.456 $min^{-1}$ with 10mM reagent, 0.223 $min^{-1}$ with 5mM reagent, 0.179 $min^{-1}$ with 4mM reagent and 0.161 $min^{-1}$ with 3mM reagent.

Evidence for the existence of a rate limiting step in the irreversible inhibition of certain enzymes has been demonstrated. For example, the chemical modification of carboxypeptidase by Woodward's reagent K involves the formation of a reversible complex between inhibitor and enzyme prior to covalent bond formation. The model is shown below, where E.I is the reversible complex, E-I the inactive enzyme, $K_I$ the steady state constant of inactivation and $k_2$ the first order rate constant:

$$E + I \underset{k_{-1}}{\overset{k_1}{\rightleftharpoons}} E.I \xrightarrow{k_2} E\text{-}I$$

The irreversibility of the second step in the above equation was proven by the inability of the modified enzyme to regain activity after more than 12 hours.
Saturation kinetics resulting from the formation of an enzyme.reagent reversible complex were demonstrated by plotting data according to $K_{I.app} = K_I/k_2[I] + 1/k_2$ (Kitz *et al.*, 1962), [figure 3.6.2c]. The first order rate constant of inhibition (at

# CHAPTER 4

# INOSITOL MONOPHOSPHATASE AND DIVALENT CATIONS

substrate Ins(4)P, suggesting that $Mg^{2+}$ cooperativity is dependent upon the structure of the substrate (Leech *et al.*, 1993).

### 4.1.3 Previous studies involving divalent cations: Implications with respect to the mechanism of inositol monophosphatase

Studies using pyrene-maleimide labelled enzyme have shown that $Mg^{2+}$ is required to support $P_i$ binding and that $Li^+$ interacts with a post-catalytic complex (Greasley *et al.*, 1994). Rapid equilibrium dialysis studies have demonstrated that one $P_i$ is bound per subunit and only in the presence of $Mg^{2+}$ (Greasley *et al.*, 1993), supporting similar conclusions made in experiments which studied the protection of the enzyme from proteolytic degradation and chemical modification. Equilibrium dialysis studies also demonstrated that $Li^+$ does not support $P_i$ binding (Greasley *et al.*, 1993).

At high concentrations (> 10mM with Ins(1)P as the substrate), $Mg^{2+}$ is an uncompetitive inhibitor relative to substrate (Hallcher *et al.*, 1980). The inhibitory effects of $Mg^{2+}$ and $Li^+$ are mutually exclusive (Ganzhorn *et al.*, 1990), suggesting they probably bind the same site, or overlapping sites in the enzyme. The $K_m$ and $K_i$ values for $Mg^{2+}$ and $Li^+$ are strongly dependent on the nature of the substrate (Attwood *et al.*, 1988, and Leech *et al.*, 1993). The dependence of the apparent $K_i$ for $Li^+$ on the nature of the substrate is not unexpected, since uncompetitive inhibitors do not combine with free enzyme. In the presence of $Li^+$, the enzyme was able to release inositol from Ins(1)P in a burst, suggesting that $Li^+$ binds after P-O cleavage has occurred (Leech *et al.*, 1993).

Inositol does not inhibit the enzyme (at concentrations up to 50mM), suggesting that inositol release is essentially irreversible (Gee *et al.*, 1988). $P_i$, the second product released, inhibits the enzyme, competitively with respect to substrate ($K_i$ = 0.52mM), (Gee *et al.*, 1988).

### 4.1.4 Mechanism of inositol monophosphatase, as proposed by Leech *et al.*, (1993)

The mechanism of inositol monophosphatase, as proposed by Leech *et al.*, (1993), is shown in figure 4.1.4a. The mechanism indicates the binding of $Mg^{2+}$ and Ins(1)P is ordered, with Ins(1)P binding before $Mg^{2+}$. At this stage, it was postulated that only a single $Mg^{2+}$ was needed for activity. Leech *et al.*, (1993), proposes that $Mg^{2+}$ is released after Ins(1)P hydrolysis, before the first product, inositol, is released, followed by $P_i$. $Li^+$ binds to the enzyme/product complex only and not to the free enzyme.

The mechanistic implications of the near-UV CD ligand binding data, discussed in chapter 5, together with limited proteolysis (Whiting *et al.*, 1990, and Greasley *et al.*, 1993, Gee *et al.*, 1991), X-ray crystallography (Bone *et al.*, 1994, Pollack *et al.*, 1993, Pollack *et al.*, 1994), equilibrium dialysis (Greasley *et al.*, 1993), stopped flow fluorescence and fluorescence labelling studies (Greasley *et al.*, 1994) will be discussed at the end of this chapter and a refined mechanism proposed.

## 4.2 Results and Discussion

### 4.2.1 Kinetic parameters for divalent cations

7μM inositol monophosphatase (Mr 30,055), in 50mM Tris, pH 8.0 was assayed at 37°C in the presence of 1mM 4-methylumbelliferyl phosphate, according to the assay of Gore *et al.*, (1992), and increasing concentrations of different divalent cations ($Zn^{2+}$ or $Mg^{2+}$). The assay of Gore *et al.*, (1992), measures the rate of appearance of the fluorescent product, 4-methylumbelliferone. Since the fluorescence of this product is highly temperature dependent, the product fluorescence has to be calibrated at pH 8.0 and 37°C. This was done by measuring the fluorescence yield (at the wavelength used in the assay, excitation at 388nm and emission at 450nm) of increasing concentrations of the product in 50mM Tris.HCl, pH 8.0, at 37°C. By this means a value of 81,250 was calculated from the slope of a graph of

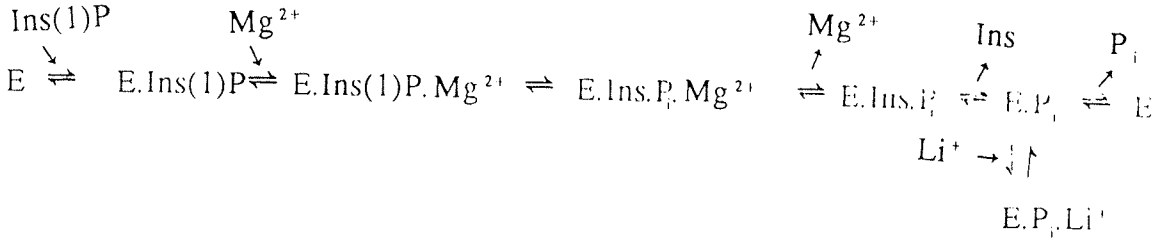


Figure 4.1.4a: Mechanism of inositol monophosphatase, as proposed by Leech *et al.*, (1993).

fluorescence against μmole of product using one particular setting of the sensitivity on the fluorimeter.

$Zn^{2+}$ inhibits the enzyme [figure 4.2.1a], with an $IC_{50}$ of 6.3 ± 3.2 mM (n=2) and, similarly to Gore *et al.*, (1992), $Mg^{2+}$ is found not to inhibit the enzyme when 4-methylumbelliferyl phosphate is the substrate [figure 4.2.1b]. The $K_m$app for $Zn^{2+}$, with 4-methylumbelliferyl phosphate as the substrate, is 0.37 ± 0.19 mM (n = 2) [figure 4.2.1a] and the $V_{max}$ for $Zn^{2+}$, with 4-methylumbelliferyl phosphate as substrate, is 0.336μmolmin$^{-1}$mg$^{-1}$ [figure 4.3.1a].

Since the enzyme exhibited divalent cation cooperativity, only values greater than 25% of the $V_{max}$ were used in the Lineweaver-Burke plots (Smith et al., 1993), as determined from activity versus concentration plots [figure 4.2.1b], to give values of 13.8 ± 4.7 mM for the $K_m$ and 0.318 ± 0.06 μM for $V_{max}$ (n = 3) [figure 4.2.1c].

### 4.2.2 Divalent cation cooperativity

The activity of inositol monophosphatase with the divalent cations, $Mg^{2+}$ and $Zn^{2+}$, exhibits positive cooperativity [figure 4.2.2a]. When there is no inhibition at higher concentrations of substrate (in this case the divalent cation), cooperativity can be assessed from the Hill plot ($\log(v/V_{max} - v)$ versus log[S]), (Hill, 1913). In the cases where the substrate inhibits at higher concentrations, as seen in the case of $Zn^{2+}$, the plot used is $\log(v/V_{max} - v\ (1 + [S]/K_i)$ versus log[S], (Ganzhorn *et al.*, 1990). The Hill coefficients, calculated from the slope of the Hill plot are 1.42 ± 0.1 for $Mg^{2+}$ and 1.26 ± 0.18 for $Zn^{2+}$ [figure 4.2.2a].

Leech *et al.*, (1993), have developed a kinetic model to explain how cooperativity effects might be observed for divalent cation binding with some substrates (2'AMP and Ins(1)P), but not for others. The model indicated that positive cooperativity would occur when the catalytic step is slow enough to ensure that both active sites of the homodimer contain $Mg^{2+}$ and are converting substrate to product. Cooperativity is not observed with the substrate, Ins(4)P. It is postulated that, in the

**Figure 4.2.1a** : Determination of the kinetic constants of inositol monophosphatase. 7$\mu$M inositol monophosphatase (Mr 30,055), in 50mM Tris.HCl, pH 8.0, was assayed using the fluorescence assay of Gore *et al.*, (1992), using 1mM 4-methylumbelliferyl phosphate in the presence of increasing concentrations of $Zn^{2+}$: $K_{mapp}$ = 0.37 $\pm$ 0.19 mM and $IC_{50}$ = 6.3 $\pm$ 3.2 mM (n = 2).

**Figure 4.2.1b**: 7$\mu$M inositol monophosphatase (Mr 30,055), in 50mM Tris.HCl, pH 8.0, was assayed using the flyorescence assay of Gore *et al.*, (1992), using 1mM 4-methylumbelliferyl phosphate in the presence of increasing concentrations of $Mg^{2+}$.

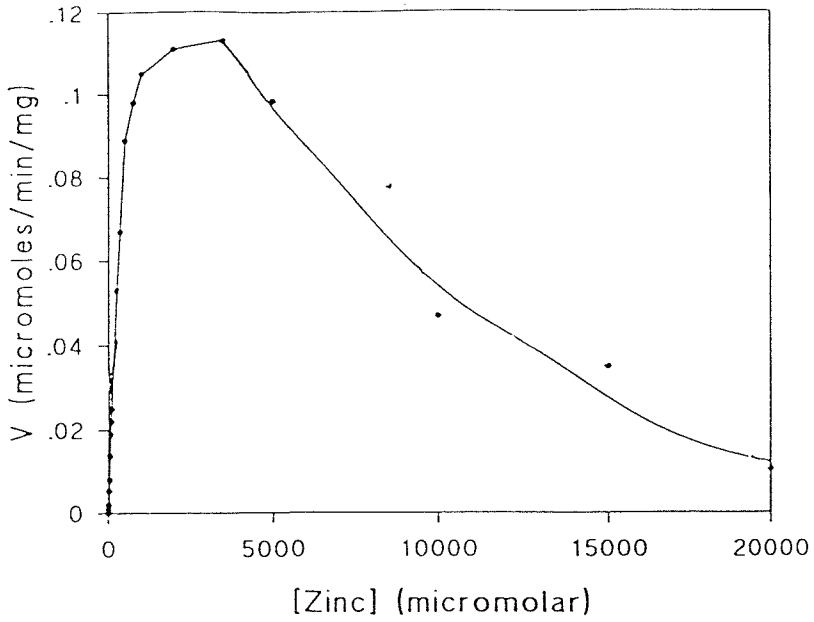


Figure4.2.1a

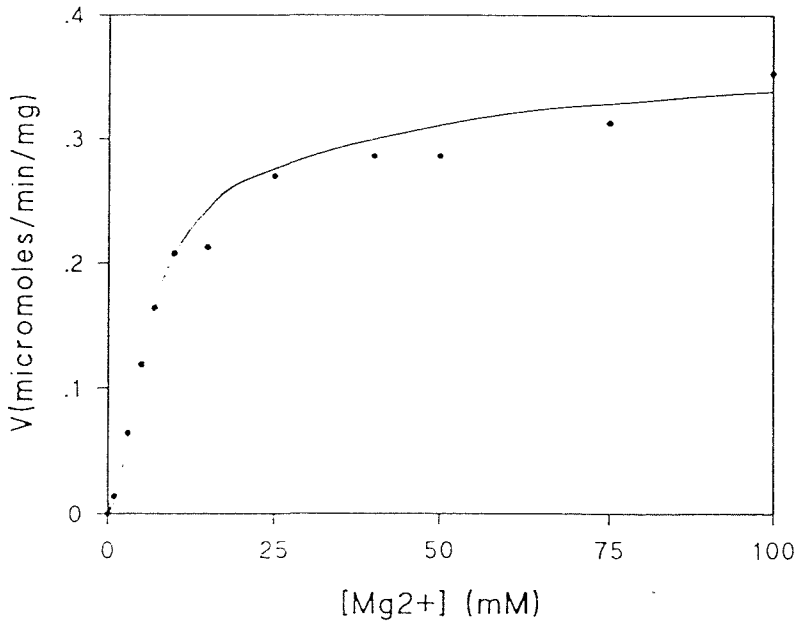


Figure4.2.1b

**Figure 4.2.1c:** 7$\mu$M inositol monophosphatase (Mr 30,055), in 50mM Tris.HCl, pH 8.0, was assayed using the fluorescence assay of Gore *et al.*, (1992), using 1mM 4-methylumbelliferyl phosphate in the presence of increasing concentrations of $Mg^{2+}$. Since the activity of $Mg^{2+}$ displays positive cooperativity, the kinetic constants are determined using only values of $V > 25$ % of $V_{max}$, as determined from figure 4.2.1b. ($K_m$ = 13.8 $\pm$ 4.7 mM and $V_{max}$ = 0.318 $\mu$mol/min/mg).

**Figure 4.2.2a:** Hill plot for the determination of cooperativity (Hill, 1913) for $Mg^{2+}$ and $Zn^{2+}$ activity. LogX, in the case of $Mg^{2+}$, stands for $\log(v/V_{max} - v)$ and in the case of $Zn^{2+}$, which inhibits at higher concentrations, $\log(v/V_{max} - v(1 + [S]/K_i)$. The Hill coefficient for $Mg^{2+}$ (■) catalysis is 1.42 $\pm$ 0.1 and for $Zn^{2+}$ (●) 1.26 $\pm$ 0.21.

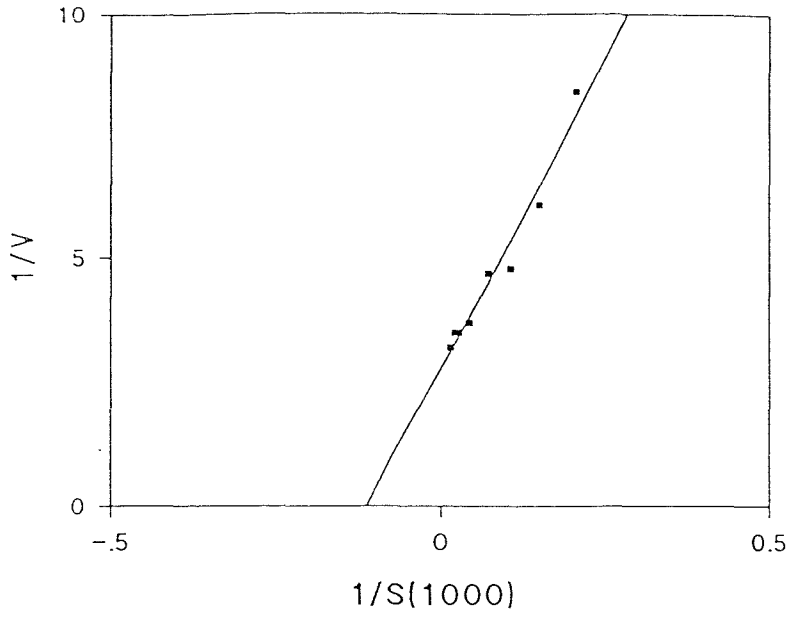


Figure4.2.1c

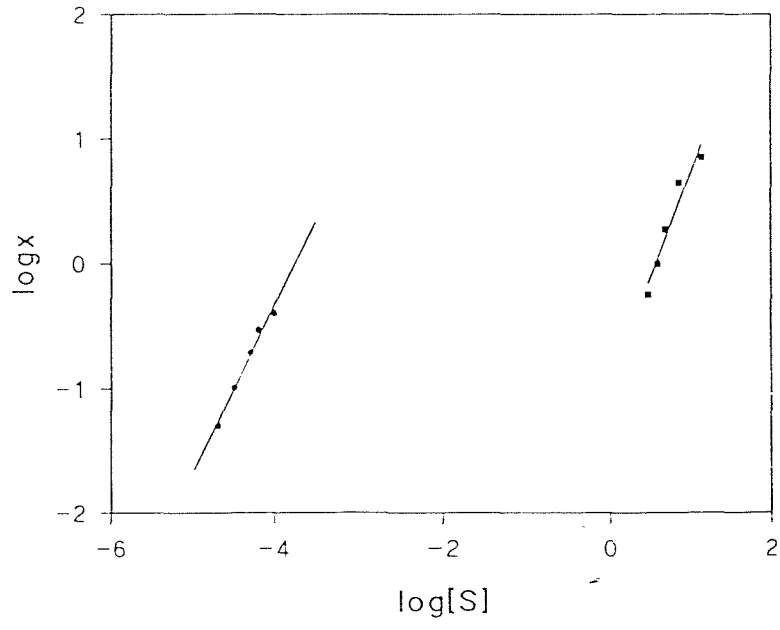


Figure4.2.2a

case of Ins(4)P, where the phosphate ester hydrolysis step is fast compared to $P_i$ release, two $Mg^{2+}$ ions will not be bound by the enzyme simultaneously and cooperativity effects should not be observed (Leech *et al.*, 1993).

### 4.3 Conclusions: Mechanism of inositol monophosphatase

Inositol monophosphatase exhibits positive cooperativity with divalent cations; that is, the binding of the first $Mg^{2+}$ ion may induce a structural change that results in an increased affinity of $Mg^{2+}$ for the second site. This sigmoidal response may act, in-vivo, to provide a much more sensitive control of the reaction rate by variations in the concentration of $Mg^{2+}$. Cooperativity is substrate dependent; with Ins(4)P no cooperativity is observed (Leech *et al.*, 1993). For substrate dependent cooperativity, the substrate must bind before the second $Mg^{2+}$.

The proposed mechanism for inositol monophosphatase, detailed in figure 4.3a, has several differences to the mechanism of Leech *et al.*, (1993), detailed in figure 4.1.4a. The CD data, presented in chapter 5, suggests that $Mg^{2+}$ binding induces a conformational change of the enzyme, which is also supported by stopped flow fluorescence studies (Mark Thorne, personal communication) and X-ray data (Bone *et al.*, 1994).

Figure 4.3a proposes that two $Mg^{2+}$ ions are necessary for catalysis (Greasley *et al.*, 1993) and that binding of the first $Mg^{2+}$, and consequent conformational change (the two different conformations of the enzyme are represented as E and $E^*$), is followed by ordered binding of the second $Mg^{2+}$ ion and substrate, Ins(1)P, with Ins(1)P binding first. The Ins(1)P is hydrolysed and inositol is the first product released. The second $Mg^{2+}$ ion must dissociate next to allow the subsequent release of the second product, $P_i$ (Leech *et al.*, 1993). Equilibrium dialysis studies demonstrate that $P_i$ will only bind enzyme in the presence of $Mg^{2+}$ (Greasley *et al.*, 1993), implying that the $P_i$ is released next leaving the species $E^*.Mg^{2+}$, followed by the $Mg^{2+}$. CD and stopped flow fluorescence (Mark Thorne, personal communication) suggest that dissociation of this last $Mg^{2+}$ is followed by a conformational change of the enzyme

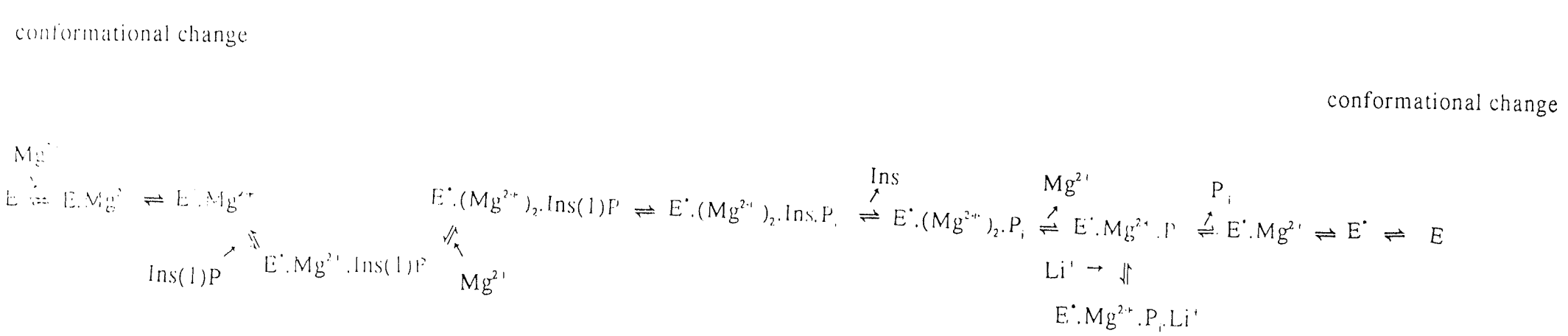


**Figure 4.3a** : Proposed mechanism of inositol monophosphatase.

case of Ins(4)P, where the phosphate ester hydrolysis step is fast compared to $P_i$ release, two $Mg^{2+}$ ions will not be bound by the enzyme simultaneously and cooperativity effects should not be observed (Leech *et al.*, 1993).

### 4.3 Conclusions: Mechanism of inositol monophosphatase

Inositol monophosphatase exhibits positive cooperativity with divalent cations; that is, the binding of the first $Mg^{2+}$ ion may induce a structural change that results in an increased affinity of $Mg^{2+}$ for the second site. This sigmoidal response may act, in-vivo, to provide a much more sensitive control of the reaction rate by variations in the concentration of $Mg^{2+}$. Cooperativity is substrate dependent; with Ins(4)P no cooperativity is observed (Leech *et al.*, 1993). For substrate dependent cooperativity, the substrate must bind before the second $Mg^{2+}$.

The proposed mechanism for inositol monophosphatase, detailed in figure 4.3a, has several differences to the mechanism of Leech *et al.*, (1993), detailed in figure 4.1.4a. The CD data, presented in chapter 5, suggests that $Mg^{2+}$ binding induces a conformational change of the enzyme, which is also supported by stopped flow fluorescence studies (Mark Thorne, personal communication) and X-ray data (Bone *et al.*, 1994).

Figure 4.3a proposes that two $Mg^{2+}$ ions are necessary for catalysis (Greasley *et al.*, 1993) and that binding of the first $Mg^{2+}$, and consequent conformational change (the two different conformations of the enzyme are represented as E and $E^*$), is followed by ordered binding of the second $Mg^{2+}$ ion and substrate, Ins(1)P, with Ins(1)P binding first. The Ins(1)P is hydrolysed and inositol is the first product released. The second $Mg^{2+}$ ion must dissociate next to allow the subsequent release of the second product, $P_i$ (Leech *et al.*, 1993). Equilibrium dialysis studies demonstrate that $P_i$ will only bind enzyme in the presence of $Mg^{2+}$ (Greasley *et al.*, 1993), implying that the $P_i$ is released next leaving the species $E^*.Mg^{2+}$, followed by the $Mg^{2+}$. CD and stopped flow fluorescence (Mark Thorne, personal communication) suggest that dissociation of this last $Mg^{2+}$ is followed by a conformational change of the enzyme

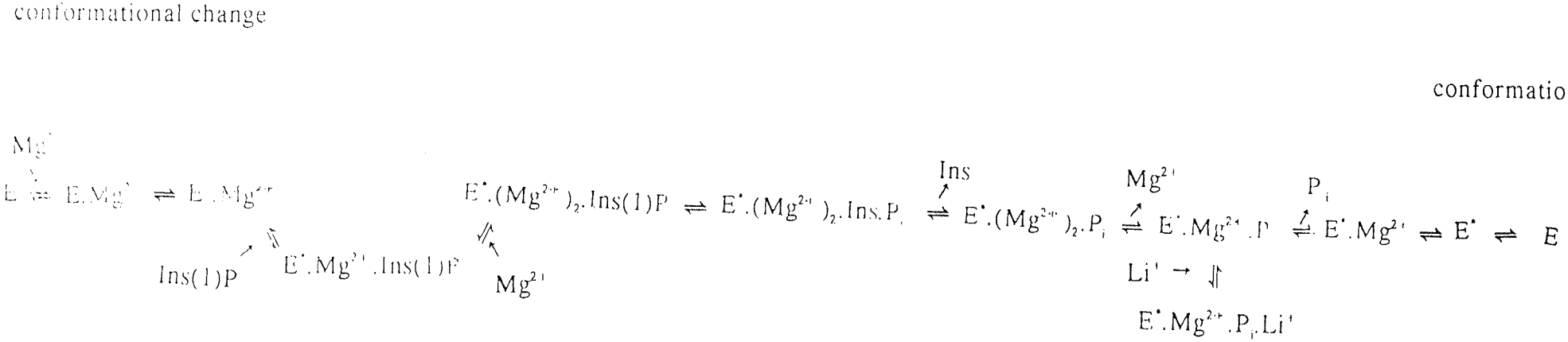


**Figure 4.3a** : Proposed mechanism of inositol monophosphatase.

which may be the reversal of the enzyme structure to its ground state.

A final point to note in the mechanism is the form of the $Li^+$ inhibition complex. Equilibrium dialysis show that $P_i$ will not bind in the absence of $Mg^{2+}$ and that $Li^+$ does not support $P_i$ binding (Greasley *et al.*, 1993). Therefore, the $Li^+$-trapped intermediate cannot be $E^*.Li^+.P_i$. At high concentrations, it is postulated that this second $Mg^{2+}$ remains bound to the enzyme trapping the $P_i$ in an $E^*.(Mg^{2+})_2.P_i$ complex and that the second $Mg^{2+}$ ion may be substituted by a $Li^+$ ion. Hence, the $Li^+$ inhibited complex would be $E^*.Mg^{2+}.Li^+.P_i$.

# CHAPTER 5

# NEAR-UV CD

# Chapter 5

## Near-UV circular dichroism

### 5.1. Introduction

Inositol monophosphatase is a homodimer, with each subunit having a molecular weight of 30055 (Gee *et al.*, 1988). The X-ray structure of human inositol monophosphatase has been elucidated (Bone *et al.*, 1993) and using this information the various elements of secondary structure of the enzyme can be visualised using a modelled ribbon structure of the enzyme [figure 5.1a].

Figure 5.1a shows just a single subunit of the enzyme; the other subunit being identical. The structure is comprised of three α-helices (shown in red) separated by ß-sheets (shown in green). The remainder of the structure is composed of regions of irregular structure, of particular importance, with respect to enzyme activity, is the N-terminal loop, shown in blue (Whiting *et al.*, 1990, and Greasley *et al.*, 1993). This model is of the enzyme in the absence of substrate. In the presence of substrate, Ins(1)P, and $Mg^{2+}$, it is postulated that the N-terminal loop (shown in blue) moves upwards to constrict the entrance to the active site. There is ordering of several protein segments, residues 30-40 and 70-75, in the presence of divalent cations (Bone et al., 1994).

Evidence for a conformational change at the N-terminus came from limited proteolysis studies (Whiting *et al.*, 1990, and Greasley *et al.*, 1993). In the studies of Greasley *et al.*, (1993), bovine inositol monophosphatase was incubated with trypsin under conditions such that only limited proteolysis occurred; a single bond, Lys36-Ser37, in the N-terminal loop, was cleaved. The result of cleavage was a decrease in molecular weight of the enzyme by approximately 2kDa and a concurrent inactivation of the enzyme. When the limited proteolysis was attempted in the presence of the substrate, Ins(1)P, and $Mg^{2+}$ (required for activity), no cleavage occurs (Gee *et al.*, 1991), suggesting that the Lys36-Ser37 bond in the N-terminal

Figure 5.1a : The structure of inositol monophosphatase determined by X-ray crystallography (Bone *et al.*, 1992).

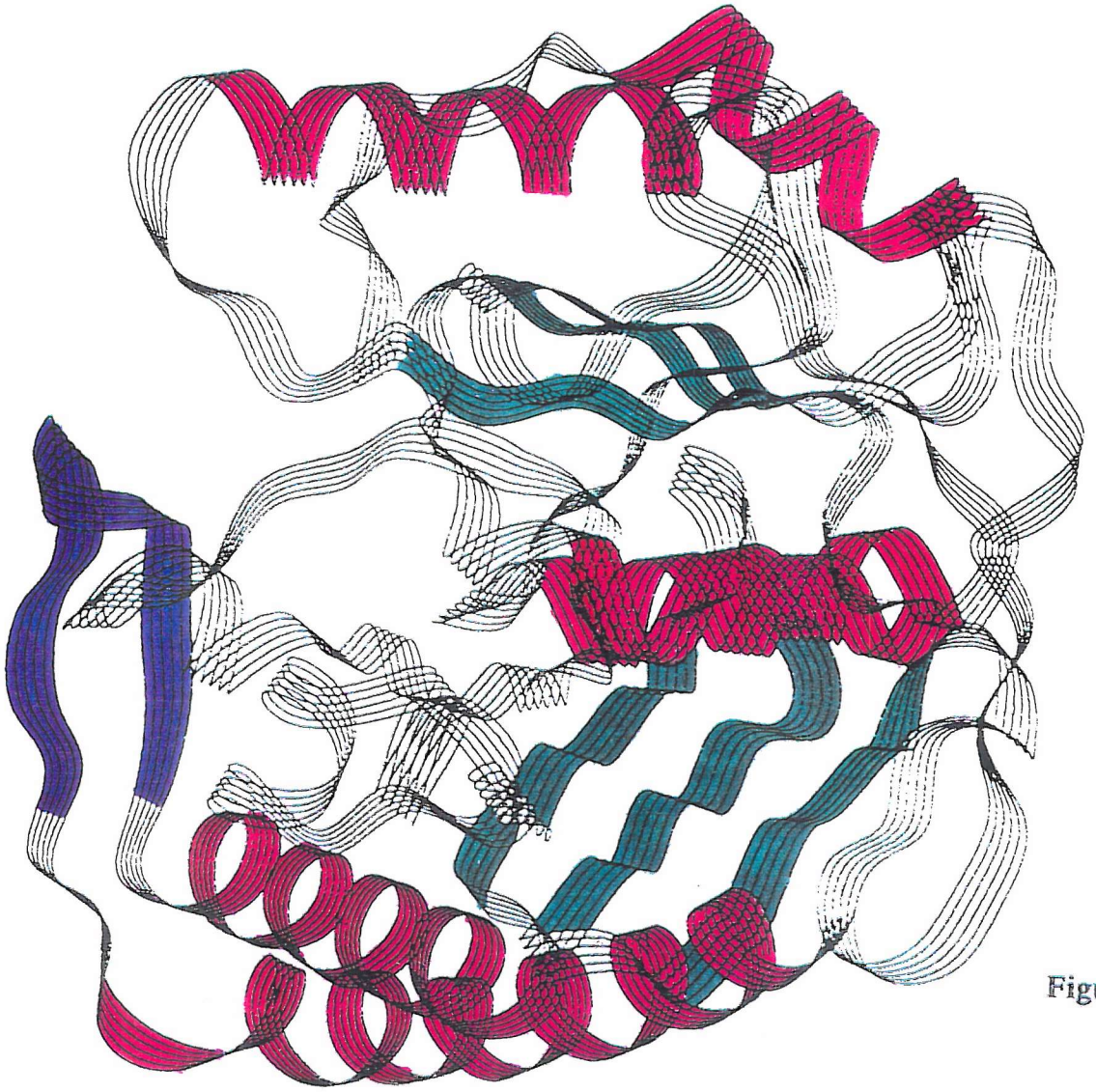

Figure 5.1a

loop is no longer accessible to trypsin. The inaccessibility of this bond in the presence of substrates could arise if the N-terminal loop moved to make the site of proteolysis inaccessible to the protease.

Limited proteolysis has, therefore, demonstrated that the N-terminus is important for activity (Greasley *et al.*, 1993) and has suggested that the N-terminus is important for activity because it undergoes a conformational change after substrate, Ins(1)P, and or $Mg^{2+}$ binding and that this conformational change is necessary for enzyme activity. This possible conformational change was, therefore, investigated by a combination of near-UV circular dichroism and limited proteolysis as described in this chapter.

A further finding from the limited proteolysis work (Gee *et al.*, 1991) is that protection against proteolysis is given by $P_i$ (the second product of the enzyme reaction and also a competitive inhibitor) and $Mg^{2+}$, or by the substrate analogue, 1S-phosphoryloxy-2R,4S-dihydroxycyclohexane, in the presence of $Mg^{2+}$.

### 5.1.1 Circular dichroism

Circular dichroism (CD) gives information about the differential absorption of left and right circularly polarised light (Drake, 1994). CD bands occur in the same region of the spectrum as absorption bands, provided the chromophore is located within an asymmetric environment. There are two regions of spectral importance for proteins. CD bands in the far-UV region, 170-250nm, are due primarily to amide bonds and, therefore, this region of the spectrum gives information about the peptide backbone structure (Drake, 1994). CD bands in the near-UV region are due to aromatic amino acids and disulphide bonds located in asymmetric environments. If the asymmetry around the absorbing species changes, a corresponding change in the CD spectrum in the near-UV region will occur.

Since CD is a phenomenon often very poorly explained in standard biochemistry text books, a brief description is given here from elementary physics and chemistry texts

(Drake, 1994, Whelan and Hodgson, 1978, and Von Hans-Joachim Galla, 1988). Unpolarised light is rendered both monochromatic and plane (linearly) polarised by the monochromator. Circularly polarised light is produced when two plane polarised light beams, in phase but perpendicular to each other, pass through a crystal at a certain orientation with respect to the plane polarised light beams. The effect of the crystal is to slow one of the beams one quarter of a phase with respect to the other. The result of this phase shift is circularly polarised light. The orientation of the crystal is then shifted through 90° and as a result the alternative $90^0$ phase shift of one beam with respect to the other occurs. In one crystal orientation, the resultant beam is right-circularly polarised and in the other orientation, left-circularly polarised. In the CD spectrometer the crystal, the polarisation modulator, moves between the two orientations to produce a cycle of left- and right-circularly polarised light. Hence, the optically active sample is illuminated by alternating left- and right-circularly polarised light. The resulting CD spectrum arises from the differential absorption of left- and right-circularly polarised light at each wavelength.

### 5.1.2 Previous ligand binding studies with inositol monophosphatase

Equilibrium dialysis studies demonstrate that there are two $Mg^{2+}$ binding sites important for activity (Greasley *et al.*, 1994) and X-ray crystallographic data indicates that $Mg^{2+}$ binding leads to a tightening of the enzyme structure around the $Mg^{2+}$ binding sites in the region of residues 30-40 and 70-75 (Bone *et al.*, 1994). Equilibrium dialysis studies have also demonstrated that the presence of $Mg^{2+}$ is essential for $P_i$ binding and that $Li^+$ does not support $P_i$ binding (Greasley *et al.*, 1993).

### 5.1.3 Mechanism of inositol monophosphatase

The mechanistic implications of the near-UV CD ligand binding data discussed in this chapter, together with limited proteolysis (Whiting *et al.*, 1990, Greasley *et al.*,1993, Gee *et al.*, 1991), X-ray data (Bone *et al.*, 1994, Pollack *et al.*, 1993, Pollack *et al.*, 1994), equilibrium dialysis (Greasley *et al.*, 1993), stopped flow

| LIGAND | % INCREASE IN MOLAR RESIDUE ELLIPTICITY AT 272nm |
|---|---|
| 10mM $Mg^{2+}$ | 30.2 ± 5.4 (n = 10) |
| 0.2mM $Ca^{2+}$ | 16.0 ± 2.8 (n = 2) |
| 0.02mM $Zn^{2+}$ | 0 (n = 2) |
| 1mM Ins(1)P | 0 (n = 6) |
| 10mM $Li^{+}$ | 0 (n = 6) |
| 5mM $P_i$ | 0 (n = 7) |
| 0.1mM 1s-phosphoryloxy-2R,4S-dihydroxycyclohexane | 0 (n = 5) |

**Table 5.2.1a** : The use of near-UV CD spectroscopy to study ligand binding to inositol monophosphatase. The studies were performed using inositol monophosphatase (0.45mg/ml) in 50mM Trizma.HCl, pH 8.0 (prepared in analaR water). The CD spectra were recorded using enzyme prepared in the absence of metal initially. Spectra were recorded using a 1cm path length cell and are an accumulation of three runs at 20nm/min at a slit width of 500$\mu$m, band width of 1nm and response of 0.125sec. The CD spectra were converted to molar residue ellipticity (obtained by dividing the enzyme concentration in g/l by 110, the average molecular weight of an amino acid).

Figure 5.2.1a: The use of near-UV CD spectroscopy to study $Mg^{2+}$ binding to inositol monophosphatase. The studies were performed using inositol monophosphatase (0.45mg/ml) in 50mM Trizma.HCl, pH 8.0 (prepared in analaR water). The CD spectra were recorded using enzyme prepared in the absence of metal initially. The spectra were recorded using a 1cm path length cell and are an accumulation of three runs at 5nm/min at a slit width of 500$\mu$m, band width of 1nm and response of 0.125sec. The CD spectra recorded were converted to molar residue ellipticity (with the units deg $cm^2$ /dmol) by dividing the enzyme concentration in g/l by 110, the average molecular weight of an amino acid. The CD spectra were recorded at many concentrations of $Mg^{2+}$, only a selection of recorded spectra are shown above. However, the molar residue ellipticity at 280nm of all recorded spectra are used in the determination of $K_d$ (see figure 5.2.3a).

Figure 5.2.1a

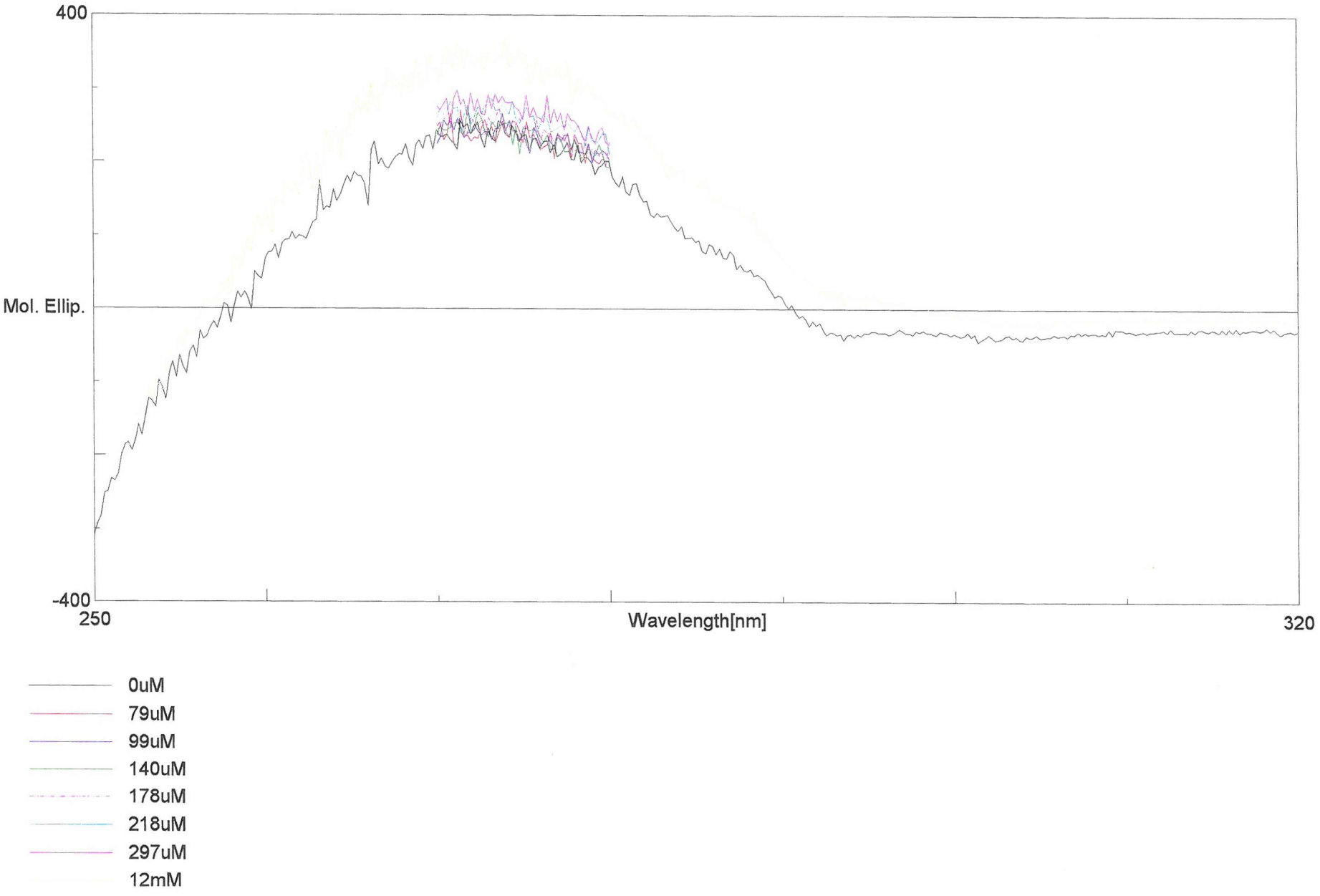
400
Mol. Ellip.
-400
250
Wavelength[nm]
320
0uM
79uM
99uM
140uM
178uM
218uM
297uM
12mM

ellipticity at 272nm [table 5.2.1a]. Subsequent addition of Ins(1)P causes no change in the CD spectrum. Only the subsequent addition of $Mg^{2+}$ leads to an increase in the signal in the near-UV CD spectrum.

The signal increase upon $Mg^{2+}$ binding can be abolished by the addition of the metal chelator EDTA; the signal reverts to that seen for the enzyme in the absence of $Mg^{2+}$. Figure 5.2.1b shows that addition of EDTA to the enzyme causes no change in the CD spectrum of the enzyme and that subsequent addition of $Mg^{2+}$ has no effect; all the $Mg^{2+}$ is chelated by the EDTA.

Hence, near-UV CD ligand binding studies show that upon $Mg^{2+}$ binding and dissociation there is a change in the environment of the aromatic amino acids of inositol monophosphatase, possibly a conformational change.

Equilibrium dialysis studies suggest that $Mg^{2+}$ must be present for $P_i$ (the second product and also a competitive inhibitor) to bind (Greasley *et al.*, 1993). This interaction was also investigated by near-UV CD spectral studies. The increase in the mean residue ellipticity at 272nm upon addition of $Mg^{2+}$ does not alter upon the subsequent addition of $P_i$. In the absence of $Mg^{2+}$, the addition of $P_i$ causes no change in the mean residue ellipticity at 272nm compared to the enzyme in the absence of any ligands [table 5.2.1a]. Subsequent addition of $Mg^{2+}$ leads to an increase in the mean residue ellipticity.

The divalent cations $Zn^{2+}$ and $Ca^{2+}$ are competitive inhibitors of $Mg^{2+}$ binding (Gee *et al.*, 1988, Hallcher *et al.*, 1980). In the absence of $Mg^{2+}$, $Zn^{2+}$ can also support activity (Gee *et al.*, 1988). The binding of these divalent cations was investigated by near-UV CD studies. Addition of $Ca^{2+}$ to inositol monophosphatase leads to a small increase in the mean residue ellipticity at 272nm (16.0 ± 2.8 % (n = 2)), [table 5.2.1a]. Addition of $Zn^{2+}$ to the enzyme causes no change in the mean residue ellipticity at 272nm [table 5.2.1a]. These CD data suggest that there may be a smaller change in the environment of the aromatic residues as a result of $Zn^{2+}$ or $Ca^{2+}$ binding.

**Figure 5.2.1b:** Near-UV CD spectral studies on inositol monophosphatase. The studies were performed using 0.45mg/ml enzyme in 50mM Trizma.HCl, pH 8.0 (prepared in analaR water, in the absence of metal initially). Spectra were recorded using a 1cm path length cell and are an accumulation of three runs at 20nm/min and response of 0.125sec. The CD spectra were converted to molar residue ellipticity (with the units deg $cm^2$ /dmol) by dividing the enzyme concentration in g/l by 110, the average molecular weight of an amino acid. The spectrum of inositol monophosphatase was initially recorded in the absence of any ligands and then after the successive addition of first 1mM EDTA and then 0.5mM $Mg^{2+}$.

Figure 5.2.1b

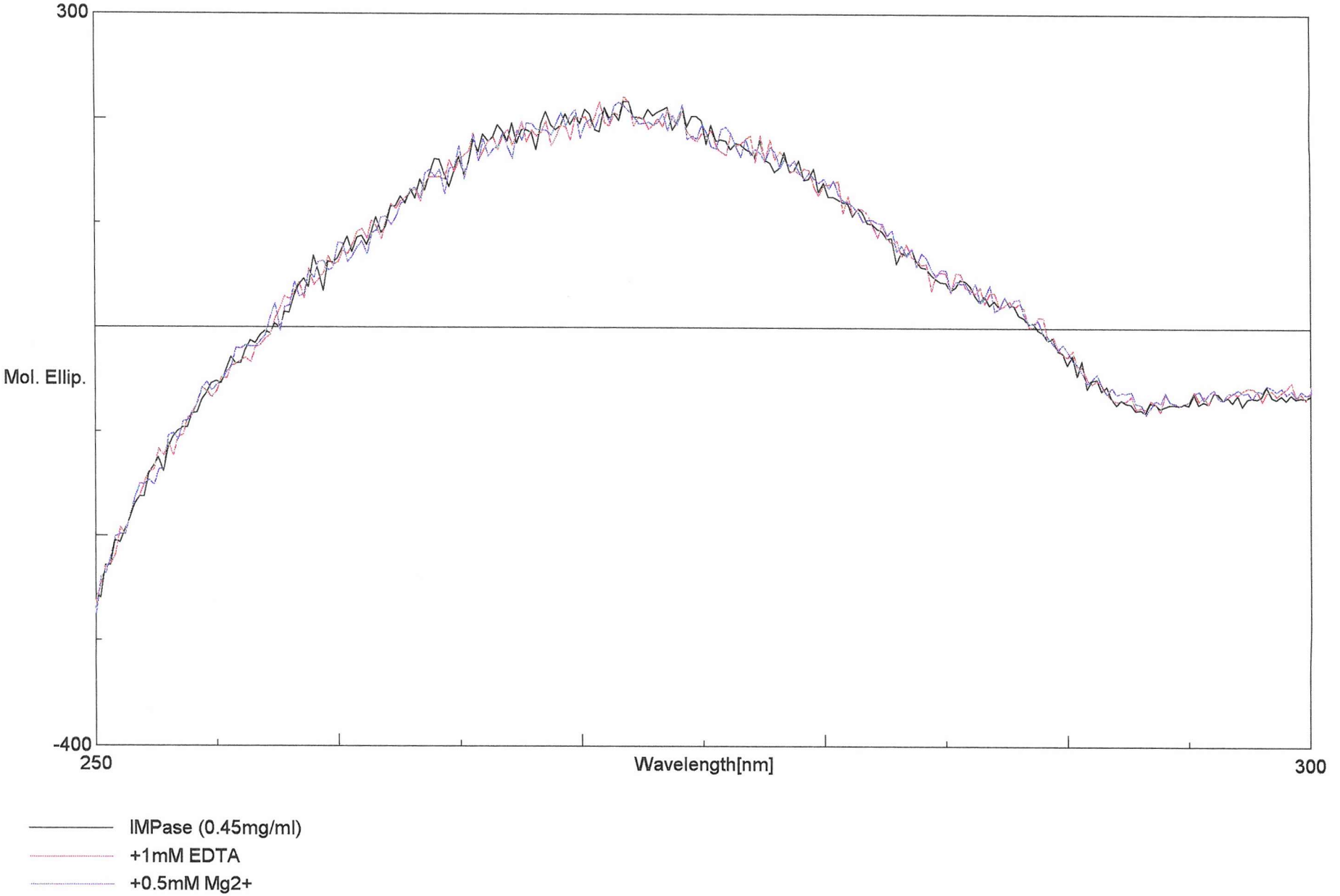
300
Mol. Ellip.
-400
250
Wavelength[nm]
300
IMPase (0.45mg/ml)
+1mM EDTA
+0.5mM Mg2+

### 5.2.2 The use of near-UV CD and limited proteolysis to study $Mg^{2+}$ binding

Near-UV CD ligand binding studies demonstrate a change in the environment of aromatic residues of inositol monophosphatase upon $Mg^{2+}$ binding (5.2.1) and limited proteolysis studies show that the N-terminus is important for activity (Greasley *et al.*, 1993, and Whiting et al., 1990). A combination of limited proteolysis and near-UV CD was employed to investigate the hypothesis that $Mg^{2+}$ binding leads to a conformational change at the N-terminus which is essential for activity.

Enzyme was incubated with trypsin under conditions such that only limited proteolysis occurred at a single bond, Lys36-Ser37, in the N-terminal loop. The procedure for proteolysis was slightly different to that of Greasley *et al.*, (1993), in that it had to be carried out the absence of $CaCl_2$. The degree of proteolysis was followed by measuring the decrease in activity with time. When the activity fell no further an aliquot was removed and run on a SDS denaturing gel [figure 5.2.2a], and the remainder retained for near-UV CD spectral studies in the presence and absence of $Mg^{2+}$. The CD spectra for proteolysed [figure 5.2.2b] and unproteolysed [figure 5.2.1a] enzyme in the presence and absence of 10mM $Mg^{2+}$ show that there is no CD signal change upon addition of $Mg^{2+}$ to the proteolysed enzyme, suggesting that either the $Mg^{2+}$ does not bind to the proteolysed enzyme or binds but does not cause a spectral/conformational change.

### 5.2.3 Determination of $K_d$ for $Mg^{2+}$ binding from near-UV CD studies

There are two $Mg^{2+}$ binding sites important for activity in inositol monophosphatase (Bone *et al.*, 1994, Greasley *et al.*, 1993, Greasley *et al.*, 1994). One of these sites has a high affinity for $Mg^{2+}$ ($K_d$ = 300μM) (Greasley *et al.*, 1994) and is important for $P_i$ binding (Greasley *et al.*, 1993). The second $Mg^{2+}$ binding site is of low affinity and binds the catalytic $Mg^{2+}$ ion. The $Mg^{2+}$ binding site involved in the CD signal

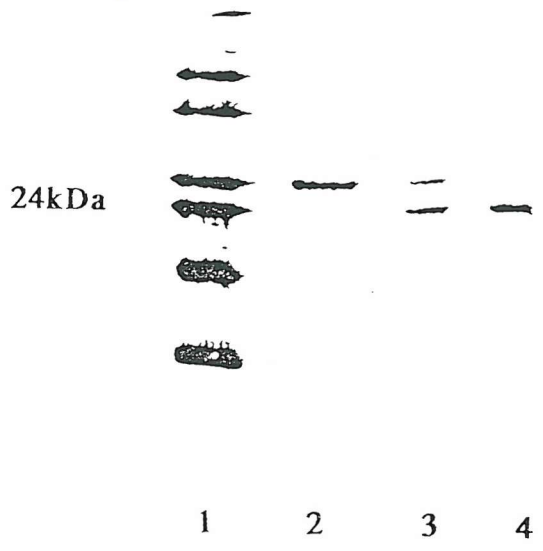


**Figure 5.2.2a**: Limited proteolysis studies on bovine inositol monophosphatase. The above photograph of a 12% SDS polyacrylamide gel shows, from left to right: (1) molecular weight markers, (2) native inositol monophosphatase (Mr 30,055), (3) proteolysed inositol monophosphatase (60% activity and 0.05% w/w trypsin), (4) proteolysed inositol monophosphatase (0% activity and 0.5% w/w trypsin). Limited proteolysis was carried out at 25°C and the concentration of trypsin (0.05% w/w and 0.5% w/w) was such that proteolysis occurred at a single site only (Lys36-Ser37). The extent of proteolysis was monitored by measuring the fall in activity with time using the fluorescence assay of Gore *et al.*, (1992).

**Figure 5.2.2b :** Near-UV CD spectral studies of proteolysed inositol monophosphatase in the presence and absence of 10mM $Mg^{2+}$. The studies were performed using inositol monophosphatase (0.45mg/ml) in 50mM Trizma.HCl, pH 8.0 (prepared in analaR water). The CD spectra were recorded using enzyme prepared in the absence of metal initially. Spectra were recorded using a 1cm path length cell and are an accumulation of three runs at 500$\mu$m, band width of 1nm and response of 0.125sec. The CD spectra were converted to molar residue ellipticity (with the units deg $cm^2$ /dmol) by dividing the enzyme concentration in g/l by 110, the average molecular weight of an amino acid.

Figure 5.2.2b

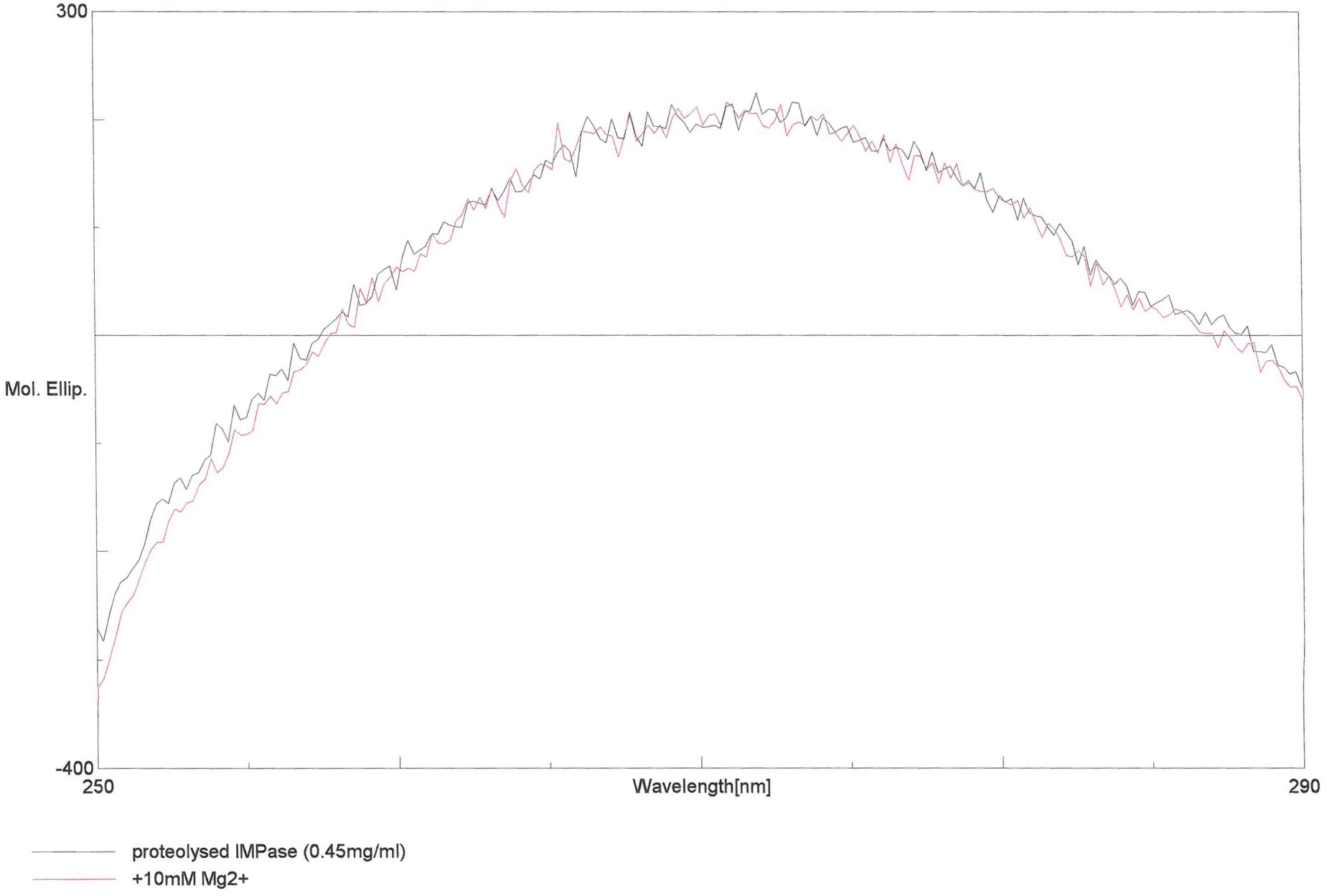
300
Mol. Ellip.
-400
250
Wavelength[nm]
290
proteolysed IMPase (0.45mg/ml)
+10mM Mg2+

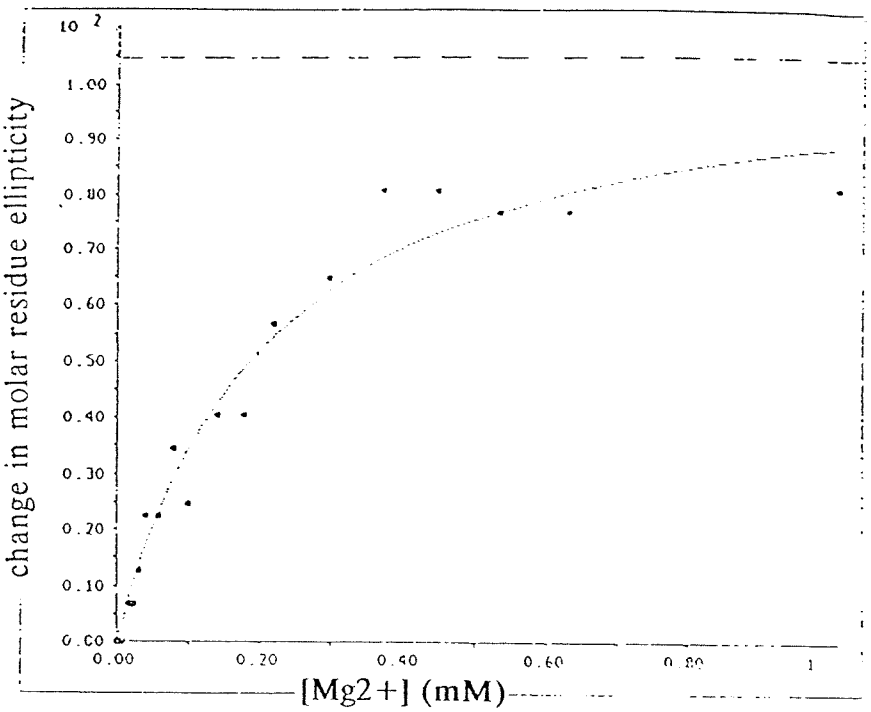


**Figure 5.2.3a:** Determination of the dissociation constant for $Mg^{2+}$ binding to inositol monophosphatase by measuring the increase in the CD signal in the near-UV region with increasing concentrations of $Mg^{2+}$. The figure shows the change in molar residue ellipticity at 280nm versus concentration of $Mg^{2+}$. The dissociation constant ($K_d$) was calculated using ENZFIT and averaged for four repeat titrations ($K_d$ = 275 ± 71 nM).

change was elucidated by the determination of the $K_d$ for $Mg^{2+}$ binding. The CD signal in the near UV region was measured in the presence of increasing concentrations of $Mg^{2+}$ (a selection of recorded spectra are shown in figure 5.2.1a) and by plotting the change in molar residue ellipticity at 280nm for all recorded spectra against $Mg^{2+}$ concentration [figure 5.2.3a] a value for $K_d$ of 275 (± 71) μM is averaged from four titration experiments. This value for $K_d$ is comparable to that obtained for the high affinity site by pyrene maleimide labelling studies (Greasley *et al.*, 1994). Hence, the signal change in the near UV region seen in the presence of $Mg^{2+}$ is due to $Mg^{2+}$ binding at the high affinity site, that is the site important for $P_i$ binding.

## 5.3 Conclusions

The CD data has important implications with respect to the mechanism of the enzyme. The proposed mechanism for inositol monophosphatase detailed in figure 4.3a has several differences to the mechanism of Leech *et al.*, (1993), detailed in figure 4.1.4a. Stopped flow fluorescence studies (Mark Thorne, personal communication) suggest that binding of $Mg^{2+}$ causes a conformational change of the enzyme; E and $E^*$ represent the two conformations of the enzyme [figure 4.3a]. X-ray studies suggest that this conformational change involves a tightening of the structure on $Mg^{2+}$ binding (residues 30-40 and 70-74), (Bone *et al.*, 1994). This suggests that the near-UV CD changes may be due to this conformational change. Parallel studies by Mark Thorne, using the pyrene-maleimide labelled enzyme, show that the change in fluorescence occurs after the initial binding of $Mg^{2+}$. The rate of change of fluorescence is independent of the concentration of $Mg^{2+}$, suggesting a conformational change. Therefore, stopped flow CD at different concentrations of $Mg^{2+}$ would most probably confirm this is a conformational change.

# CHAPTER 6

# INOSITOL MONOPHOSPHATASE : STRUCTURAL AND STABILITY STUDIES

# Chapter 6

## Inositol monophosphatase : Structural and stability studies

### 6.1 Introduction

#### 6.1.1 Protein structure and stability

The stability of proteins, especially enzymes, has long been a practical concern (O'Sullivan, 1890), because this is a factor that most limits their usefulness. There are two very different aspects of protein stability (Creighton, 1990). One is the chemical stability of the covalent structure, changes in which involves covalent changes and are usually irreversible. The other is the conformational stability of the folded state, in the absence of covalent changes (Kauzmann, 1959, Tanford, 1968 and 1970, Pace, 1974, Privalov, 1979, Pfeil, 1981, Creighton, 1978, and Schellman, 1987). The folded conformation of proteins is marginally stable relative to the unfolded conformation (approximately 10-20kJmol$^{-1}$) (Lowenthal *et al.*, 1992). The stabilisation energy of the folded state is mainly a result of non-covalent interactions between constituent amino acids. Whether or not a protein folds depends on a small balance between two large energy terms, the sum of the non-covalent energies in the folded state minus those in the unfolded state, (Serano *et al.*, 1992). Included in those energies is a major term resulting from conformational entropy that greatly favours unfolding. The dominant terms favouring folding are believed to be the hydrophobic effects, with smaller contributions from specific interactions, such as ion pairs and hydrogen bonds (Matthews *et al.*, 1987, Alber, 1989, Dill, 1990). Weak electrostatic interactions, however, can be crucial in determining the final folded structure, since unpaired charges are highly destabilising when their partners are missing (Ferhst, 1987).

A recent study of protein crystal structures has revealed that the frequency of aromatic amino acids in close proximity to histidine is statistically higher than random (Lowenthal *et al.*, 1992). Histidine residues are present in the active site of

enzymes, and have been implicated in binding and catalysis. Aromatic amino acids are also common in active sites. A histidine-phenylalanine pair in a model peptide has been shown to stabilise an α-helix (Rico *et al.*, 1986, and Shoemaker *et al.*, 1990), and histidine-indole pairs have been found to form charge transfer complexes in model compounds (Shinitzky *et al.*, 1967). The interaction between a histidine residue (His18) and tryptophan residue (Trp94) in barnase has been studied by Lowenthal *et al.*, (1992). The aromatic-histidine interaction stabilises the protonated form of histidine relative to the unprotonated form and, thereby, increase its $pK_a$ value (Lowenthal, 1992).

Measuring the conformational stability of a protein requires determination of the equilibrium constant and free energy change for the unfolding process. Techniques most often used to follow unfolding are UV-spectroscopy, fluorescence, electrophoresis, circular dichroism, and biological activity measurements.

Following experimental evidence that the conformation of a globular protein is determined by its amino acid sequence (Anfinsen *et al.*, 1961), there have been many attempts to predict protein secondary structure from the amino acid sequence alone (Robson *et al.*, 1976, Garnier, 1979, and Lim, 1974). There are several methods of structure prediction from the amino acid sequence (Busetta *et al.*, 1982). The method of Garnier *et al.*, (1978), takes into account the influence of the residues before and after the conformation of the given residue, the number of amino acids in the "window" is variable but usually about eight residues either side of the current position are used.

The experimental determination of the structure of proteins, derived from X-ray crystallographic studies, has greatly advanced the understanding in structural terms of the properties of these macromolecules. Frequently, however, it becomes necessary to establish structural features of these molecules in solution and, in particular, to monitor changes in structure that may occur as a result of changes in the environment. At present, the evidence seems to suggest that the structures of most proteins in solution are not significantly different from that in the crystal state

(Rupley, 1969).

The studies described in this chapter were performed to address several aspects, (a) to examine the stability of the enzyme (b) to determine whether the tryptophan residues report local unfolding before global unfolding (comparison of unfolding measurements made by far-UV CD and protein fluorescence) (c) does unfolding approximate to a two state system (that is folded ⇌ unfolded, which gives straight line secondary plots).

### 6.1.2 Fluorescence

Fluorescence spectra of a number of native and denatured proteins have been analyzed using spectral band width, spectral maximal position, fluorescence quenching by external ionic quenchers, lifetime and quantum yield and its changes analyzed upon denaturation (Burstein *et al.*,1973). It can be assumed that protein ultra-violet fluorescence is completely due to the constituent amino acids, tryptophan and tyrosine (Konev, 1973). Tryptophan residues in native proteins are not found in identical locations nor are they equally influenced by the environment. The microenvironment of every residue is characterised by a particular set of physico-chemical conditions (polarizability, microviscosity, availability of charged groups, possible specific interactions) that influence chromophore fluorescence (Bakhshiev, 1960). As a result, the protein fluorescence is conditioned by the sum of fluorescence contributions of individual tryptophan residues, which vary over a wide range (Burstein *et al.*, 1973). If all fluorescence measurements are performed above 290nm, only tryptophanyl fluorescence is measured (Burstein *et al.*, 1973).

### 6.1.3 Circular dichroism

Considerable information concerning the structure of proteins in solution can be obtained from the measurement of their optical activity. The great asymmetry of protein molecules is responsible for the large signals that they display in CD (Drake, *et al.*, 1994). "It is the conformation of the protein, that is the asymmetric and

periodic arrangement of peptide units in space, which gives rise to their characteristic spectra" [figures 6.1.3a and 6.1.3b], (Drake, 1994). Circular dichroism is a technique which lacks the capacity for the exact structural determination possible with X-ray crystallography, but has the advantage that one can readily approximate the percentages of conformations present in dilute solutions of proteins. CD is a very sensitive tool and is of use in studying any reactions involving changes in optical activity. Hence, CD is an excellent tool for measuring protein denaturation.

### 6.1.4 Previous structural and stability studies with bovine inositol monophosphatase

The incubation of bovine inositol monophosphatase with concentrations of urea above 4M leads to a progressive loss of activity (Gee *et al.*, 1988). However, if the enzyme was pretreated with urea and then either dialysed or diluted, a substantial return of activity is found (Gee *et al.*, 1988) suggesting that denaturation by urea is reversible, Kwon *et al.*, (1993) demonstrated that in the case of the pig enzyme urea first causes subunit dissociation without protein denaturation. Ganzhorn *et al.*, (1993), estimate an α-helical content of bovine inositol monophosphatase of 38% from the far-UV CD spectrum which is in agreement with figure of 40% found in the studies reported here and in Greasley *et al.*, (1992). Raman spectroscopic experiments (Ganzhorn *et al.*, 1993) suggest that the three tryptophan residues in bovine inositol monophosphatase are not exposed to solvent and that the enzyme is approximately 33% α-helix, as estimated from the amide I and III regions of the Raman spectrum (Ganzhorn *et al.*, 1993).

### 6.1.5 Typical energy profile for the unfolding reaction

The reaction profile for the unfolding of a protein is shown in figure 6.1.5a and indicates that there are two energy terms to be considered in the unfolding process; the activation energy ($E_a$) is energy that has to be put into the system to form the transition state, a necessary intermediate along the reaction pathway, and $\Delta G$, the small difference in energy between the folded and unfolded state. For the unfolding

| Conformation | Molecular Shape | CD Spectrum |
|---|---|---|
| α-helix<br>(H-bonded) |  | 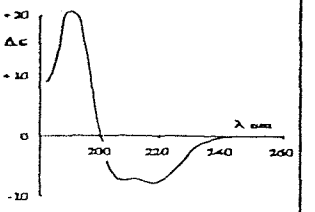 |
| β-sheet<br>(parallel and anti-parallel)<br>(H-bonded) | 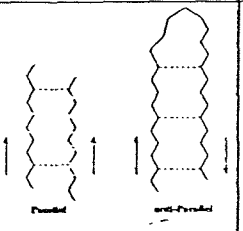 | 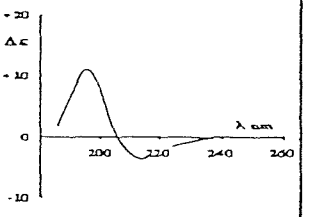 |
| β-turn<br>(Type I,II,III,...)<br>(Some turns not H-bonded in proteins)<br>γ-turn<br>(H-bonded) | 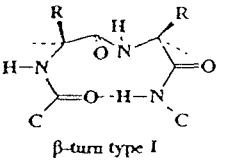 | 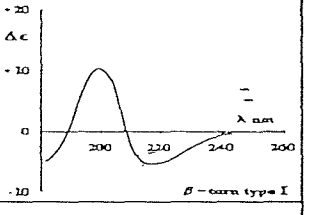 |
| 3$_1$-helix<br>(Left handed extended)<br>(polyproline II)<br>(not H-bonded) | 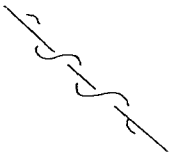 | 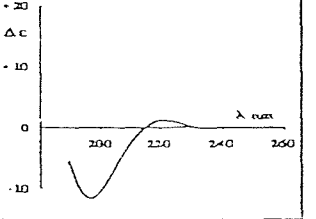 |
| Irregular Structure<br>(not H-bonded) |  | 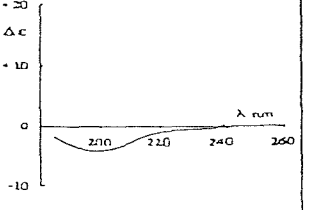 |

Figure 6.1.3a: Protein conformation and CD spectra (Drake, 1994).

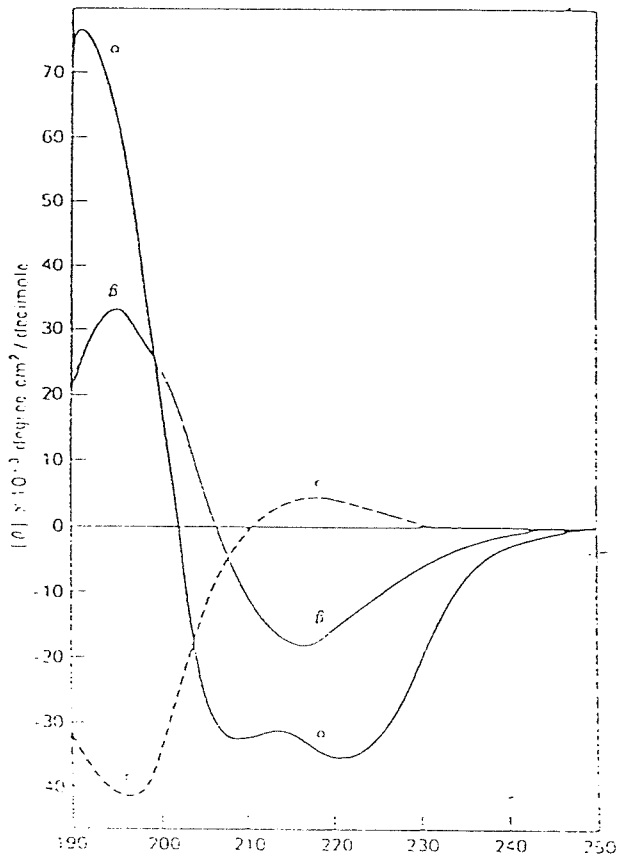


**Figure 6.1.3b:** CD spectra obtained for peptides 100% $^{\alpha}$-helical ($^{\alpha}$), ß-sheet (ß), or random coil (r), (Drake, 1994).

of a protein, energy has to be into the system overall since the unfolded protein has a higher conformational energy than the folded enzyme. When investigating the stability of the folded protein both the $E_a$ and the $\Delta G$ have to be considered. A typical value of $\Delta G$ for globular proteins is quite small at about 10-15kJmol$^{-1}$ (Price *et al.*, 1986) and a high value for $E_a$ is considered to be any value greater than 50kJmol$^{-1}$. A value for $E_a$ can be calculated from an Arrhenius plot (a plot of lnk versus 1/T, where k is the first order rate constant of unfolding). The resulting plot is a straight line whose slope gives the $E_a$.

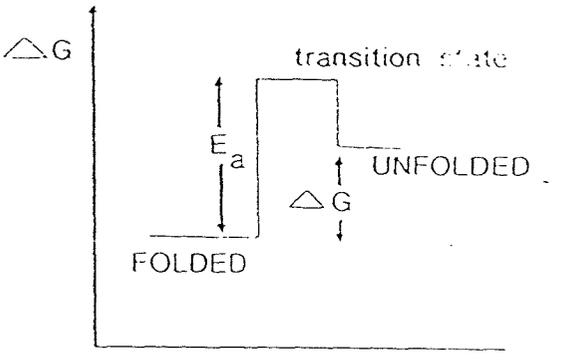


**Figure 6.1.5a** : Typical reaction profile for the unfolding of a protein.

## 6.2 Results and Discussion

### 6.2.1 Structure of bovine inositol monophosphatase

The helical content of inositol monophosphatase can be estimated from its circular dichroism spectrum in the far UV region [figure 6.2.2a]. The spectrum of the enzyme in 0M GuHCl has two minima (210nm and 220nm), and a maximum at 190nm [figure 5.2.2a] and is typical of an αß protein. Analysis of the data by the methods of Fasman, (1974), and Provencher *et al.*, (1981), suggest an α-helical content of 40% and 34%, respectively. The structural prediction algorithm of Garnier *et al.*, (1978), which calculates the helical content of a protein without consideration of tertiary or quaternary structural interactions, calculates a value of 47% for the α-helical content of bovine inositol monophosphatase (Greasley *et al.*, 1993).

### 6.2.2 Conformational energy difference between folded and unfolded bovine inositol monophosphatase : Changes in secondary structure, and polarity.

Next to biological function (that is, enzyme activity), the most powerful methods applied in folding studies make use of the specific spectral properties of proteins (Creighton, 1990). The spectral changes observed upon unfolding depend on different features of protein structure; for example, fluorescence measurements (at 335nm upon excitation at 292nm) are influenced by the dielectric constant of the microenvironment of tryptophan residues (the location of the tryptophan residues (at positions 5, 87 and 219) in the inositol monophosphatase can be visualised in the X-ray structure [figure 6.2.2o]), while CD measurements below 250nm depend mainly on changes in the secondary structure of a protein (Creighton, 1990).

A large number of reagents affect protein stability when added to the aqueous solvent. Those reagents that decrease protein stability are known as denaturants, the best known of which are urea and GuHCl, and these are used in the denaturation studies involving bovine inositol monophosphatase described here.

The CD spectrum of bovine inositol monophosphatase is determined in the far UV region at different concentrations of the denaturant guanidium hydrochloride [figure 6.2.2a]. The CD bands in the far UV region are primarily due to amide bonds, although some contribution is made from spectral transitions from aromatic amino acid side chains (Drake *et al.*, 1994) and this region of the CD spectrum gives information about the protein secondary structure (Drake *et al.*, 1994). Figure 6.2.3a shows that as the concentration of GuHCl increases the structure changes from a predominantly α-helical structure to that of a random coil.

An unfolding curve can be plotted: unfolding curves can be conveniently divided into three regions: the pretransition region, the transition region and the post-transition region. The pre-transition region shows how a physical parameter (y) for the folded protein depends on the denaturant. The transition region shows how y

Figure 6 .2.2a: Denaturation of bovine inositol monophosphatase (Mr 30,055), in 50mM Tris.HCl, pH 8.0, by GuHCl (0 to 5.8M) at pH 8.0, 25°C. The extent of denaturation is determined by measuring the CD signal in the far-UV region (where information about the protein secondary structure can be obtained). The curves shown ( with details from left to right: concentration of GuHCl, protein concentration (expressed as OD at 280nm) and cell path length are:

1: ——— BIMP, 0M GuHcl, OD (280) =0.69, 1cm
2: ——— BIMP, 1.7M GuHcl, OD (280) =0.69, 0.5mm
3: ——— BIMP, 2.5M GuHcl, OD (280) =0.69, 0.5mm
4: ——— BIMP, 3.3M GuHcl, OD (280) =0.69, 0.5mm
5: ——— BIMP, 4.2M GuHcl, OD (280) =0.69, 0.5mm
6: ——— BIMP, 5.0M GuHcl, OD (280) =0.69, 0.5mm
7: — — — — BIMP, 5.8M GuHcl, OD (280) =0.69, 0.5mm

Figure 6.2.2a

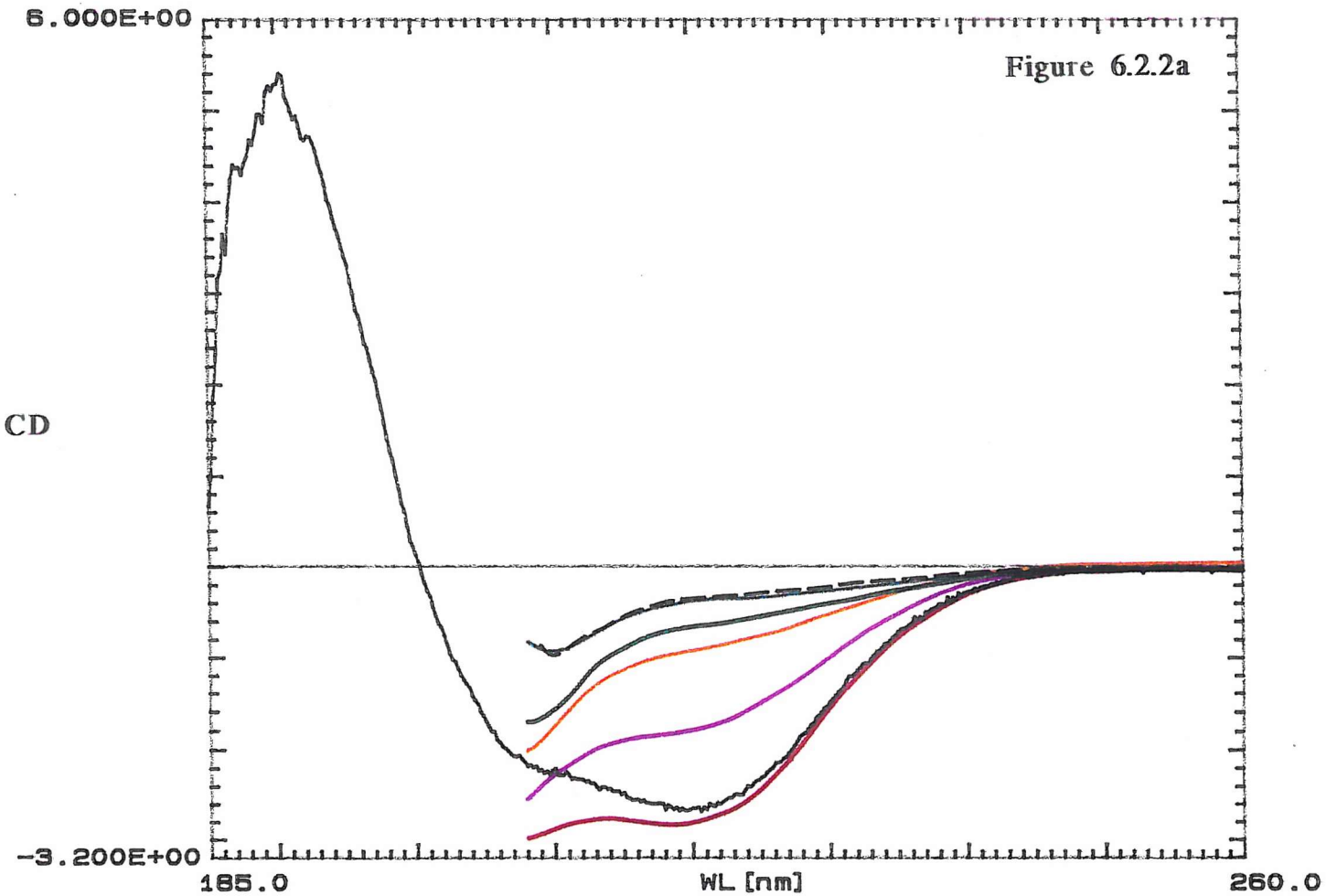
6.000E+00
CD
-3.200E+00
185.0
WL [nm]
260.0
1: BIMP, 0M GuHcl, OD (280) =0.69, 1cm
2: BIMP, 1.7M GuHcl, OD (280) =0.69, 0.5mm
3: BIMP, 2.5M GuHcl, OD (280) =0.69, 0.5mm
4: BIMP, 3.3M GuHcl, OD (280) =0.69, 0.5mm
5: BIMP, 4.2M GuHcl, OD (280) =0.69, 0.5mm
6: BIMP, 5.0M GuHcl, OD (280) =0.69, 0.5mm
7: BIMP, 5.8M GuHcl, OD (280) =0.69, 0.5mm

**Figure** 6.2.2o: X-ray crystallographic structure of inositol monophosphatase. The two subunits are shown in different colours and the tryptophan residues (at positions 5, 87 and 219) in white.

**Figure** 6.2.5b: X-ray crystallographic structure of inositol monophosphatase. The two subunits are shown in different colours and the tryptophan and histidine residues (at positions 5, 87 and 219 for tryptophan and 65, 100, 150, 188 and 217 for histidine) in white.

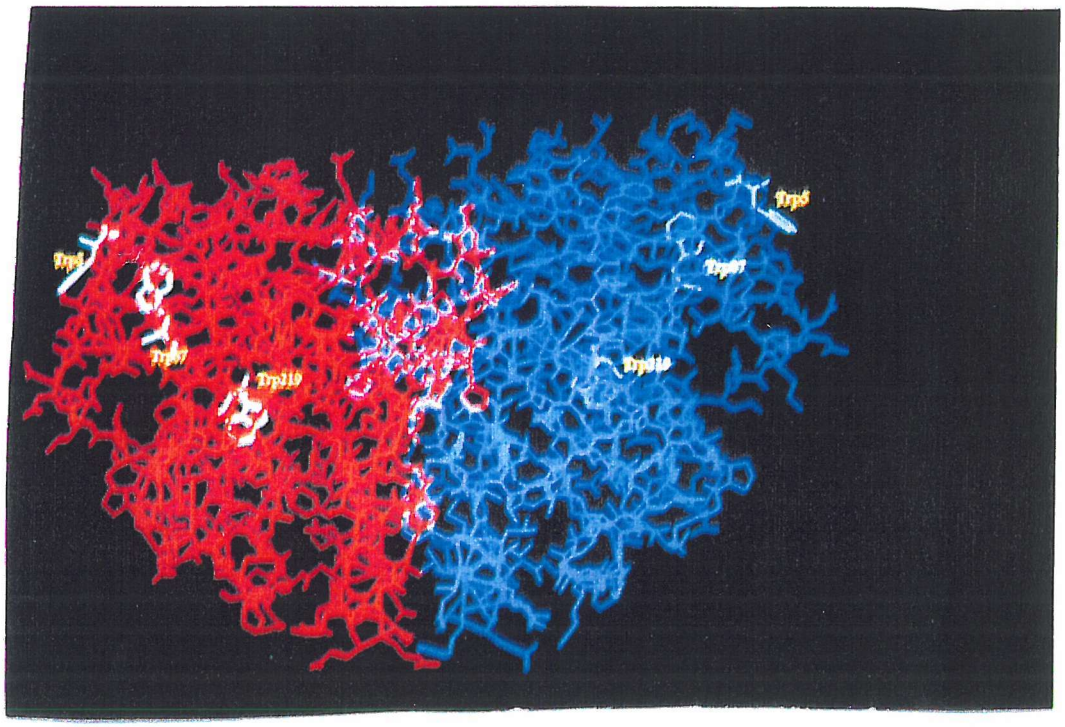

Figure 6 .2.2o

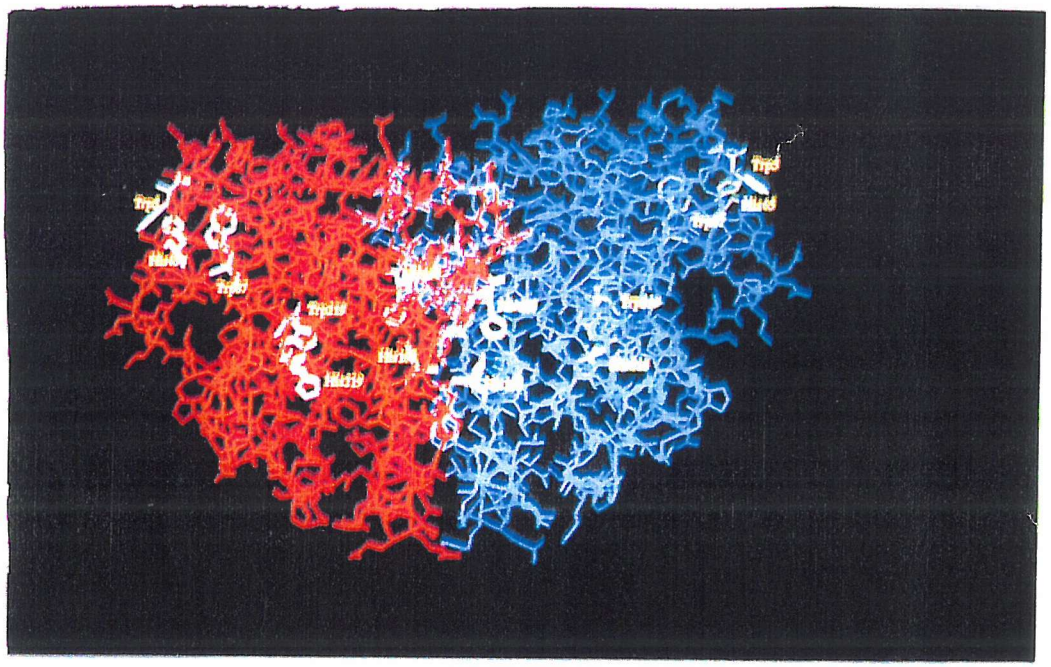

Figure 6.2.5b

varies as unfolding occurs. The post-transition region shows how y for the unfolded protein varies with denaturant. From a plot of CD signal at 220nm versus concentration of GuHCl (an unfolding curve) [figure 6.2.2b] the conformational energy difference between native and denatured enzyme at different concentrations of GuHCl can be determined. Hence the conformational energy difference at 0M GuHCl between native and denatured enzyme can be determined as 14.6 ± 0.8 $kJmol^{-1}$ [figure 6.2.2c].

Measurement of protein fluorescence at 25°C (excitation at 292nm and emission recorded at 335nm) in the presence of increasing concentrations of GuHCl [figure 6.2.2d] gives an indication of polarity changes of the microenvironment around the tryptophan residues of inositol monophosphatase as the protein unfolds. By measuring the change in fluorescence at 335nm, and hence polarity changes of the medium, a conformational energy difference of 14.2 ± 0.5 $kJmol^{-1}$ is calculated [figure 6.2.2e]. CD studies in the far-UV region and protein fluorescence studies, give a comparable estimate for the conformational energy difference between folded and unfolded protein suggesting that the changes in secondary structure and polarity of tryptophan residues occur to a similar extent.

The cooperativity of protein folding / unfolding is confirmed by the two state nature of the unfolding transition [figures 6.2.2 b and d]. Partially folded conformations are unstable relative to the fully folded and unfolded conformations. Therefore, weakening of one or a few interactions by partial unfolding weakens the other interactions so that their contributions to stability are decreased. The unfolding transition is much more abrupt than would be expected from the disruption of a single interaction (Creighton, 1993).

There are many reasons for the cooperativity of protein folding transitions. One is that unfavourable interactions may occur in the partially folded states that do not occur in either the fully folded or fully unfolded states, which would place a conformational strain on partially folded structures and hence contribute to the cooperativity of folding / unfolding.

**Figure** 6.2.2b: Denaturation of bovine inositol monophosphatase by GuHCl at 25°C, pH 8.0 (data was taken from figure 6.2.2a). A value for the conformational energy difference ($\Delta G$) between folded and unfolded enzyme at several different concentrations of GuHCl can be obtained by first determining the ratio of denatured to native enzyme (k) in the region of the curve between 2 and 4M GuHCl and then using the equation $\Delta G = -RT \ln_e k$ (where R = the gas constant ($8.31 kJmol^{-1}$) and T is the absolute temperature (298K)).

**Figure** 6.2.2c: Determination of the conformational energy difference between folded and unfolded bovine inositol monophosphatase by the use of GuHCl denaturation followed by measuring the far-UV CD signal changes. The CD spectrum in the near-UV region is due to the amide bonds and gives information about the protein backbone structure. A value of $\Delta G$ obtained from the y-axis intercept of this curve gives information about changes in the protein secondary structure during the unfolding process. The value of $\Delta G$ obtained is an average from three such experiments and is calculated as $14.6 \pm 0.8 kJmol^{-1}$.

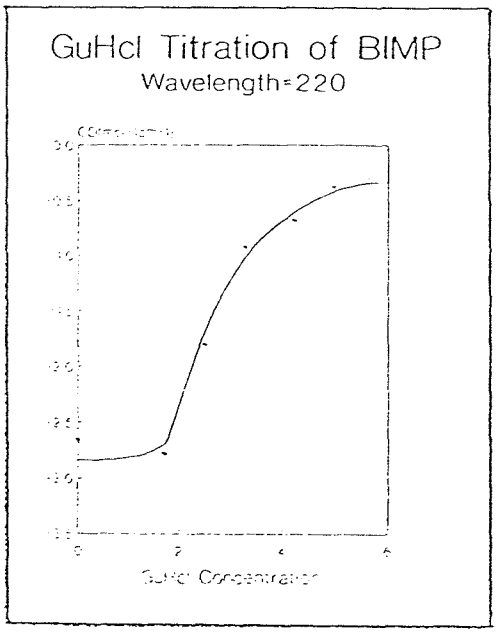


Figure 6.2.2b

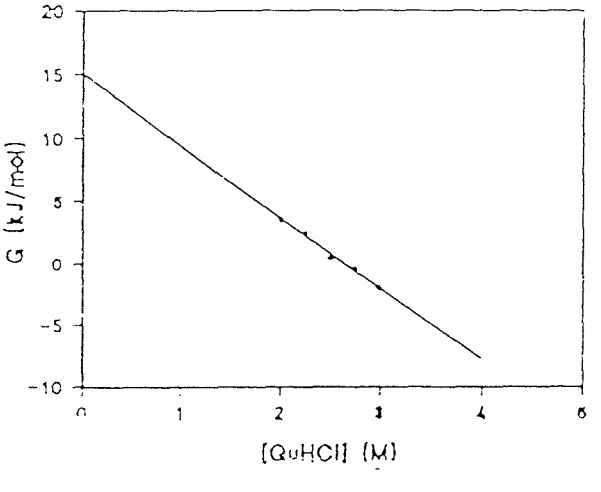


Figure 6.2.2c

**Figure** 6.2.2d: Denaturation of 10$\mu$M bovine inositol monophosphatase (Mr 30,055) in 50mM Tris.HCl, pH 8.0, at 25°C by GuHCl. The degree of denaturation is determined by measuring the protein fluorescence at 335nm upon excitation at 292nm.

**Figure** 6.2.2e: Determination of the $\Delta G$ at 0M GuHCl for the unfolding of bovine inositol monophosphatase by determining the ratio of folded to unfolded enzyme (k), (see figure 6.2.2d), and hence, $\Delta G$ (from the equation $\Delta G = -RT\ln_e k$ (where R, the gas constant, is 8.31kJmol$^{-1}$, and T, the absolute temperature, 298K) at different concentrations of GuHCl and plotting this against the concentration of GuHCl: a value of 14.2 $\pm$ 0.5 kJmol$^{-1}$ is obtained as the average from three such experiments.

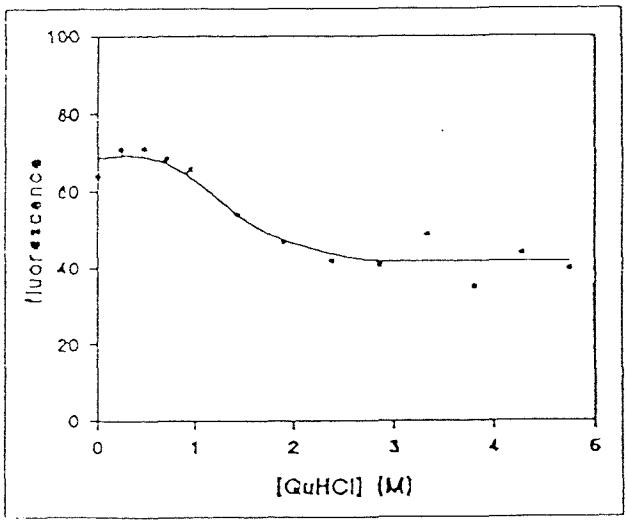


Figure 6.2.2d

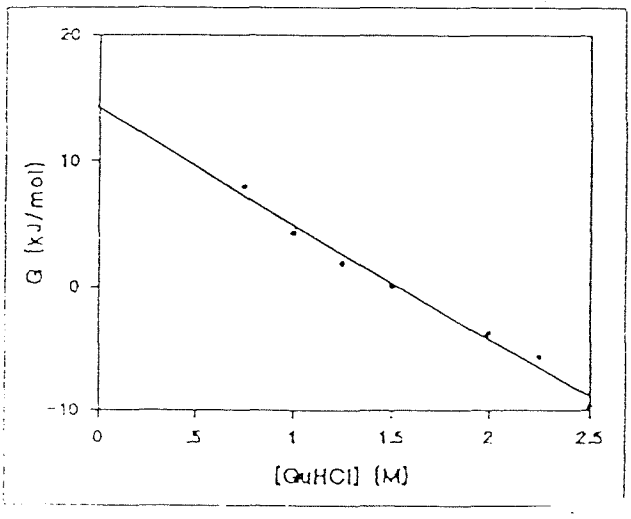


Figure 6.2.2e

Denaturation of bovine inositol monophosphatase with urea is reversible (Gee *et al.*, 1988) and this fact forms the basis of denaturation/renaturation studies in section 6.2.4. However, the extent to which the native structure is perturbed by denaturants can differ widely. For globular proteins in the presence of maximum concentrations of denaturant the following order of denaturing capacity holds: GuHCl> urea, which are both greater than SDS or high temperature (Creighton, 1990). Hence, the $\Delta G$ for the unfolding processes should be determined and compared to check that GuHCl and urea denaturation processes both go to completion. It can be assumed that high concentrations of GuHCl will fully denature a protein, if urea denaturation gives a similar value for $\Delta G$, then it also fully denatures the protein. The conformational energy difference at 0M urea between native and denatured enzyme is not significantly different from that observed for GuHCl denaturation, suggesting that urea and GuHCl alter the secondary structure equally. The CD spectra for bovine inositol monophosphatase at increasing concentrations of urea are drawn in figure 6.2.2f (there is no appreciable change in the CD spectra at 1, 2 and 3M urea). The conformational energy difference between folded and unfolded enzyme can then be determined as described for GuHCl denaturation above [figures 6.2.2g and h]. The values of $\Delta G$ determined by various means are detailed in table 6.2.2a.

The CD spectrum of bovine inositol monophosphatase can also be determined in the near UV region at different concentrations of the denaturant guanidium hydrochloride [figure 6.2.2l]. The CD bands in the near UV region are due to the side chains of aromatic amino acids and disulphide bonds located within an asymmetric environment, and this region of the spectrum is extremely sensitive to changes in the environment of these residues. The aromatic residues in denatured proteins give no appreciable signal in this region (Drake *et al.*, 1994).
These initial near-UV CD studies suggest a general loosening of the structure without destruction of the secondary structure gives increased mobility to the side chains and thus permits them to rotate more freely (a molten globule state).

A number of proteins have been observed to exist, under certain conditions, in

**Figure 6.2.2f:** Denaturation of bovine inositol monophosphatase (Mr 30,055) in 50mM Tris.HCl by urea at 25°C, pH 8.0. The reaction is followed by measuring the CD spectrum in the far-UV region. There was no appreciable difference in the CD spectrum for 0. 1, 2 and 3M urea. The curves shown are detailed below (from left to right: protein concentration, concentration of urea and pH, and cell path length).

1: ———— BIMP, 0.3mg/ml, 0M Urea, Tris, pH-8.0, 0.5mm
2: ———— BIMP, 0.3mg/ml, 4M Urea, Tris, pH-8.0, 0.2mm
3: ———— BIMP, 0.3mg/ml 4.5M Urea, Tris, pH-8.0, 0.2mm
4: ———— BIMP, 0.3mg/ml, 5M Urea, Tris, pH-8.0, 0.2mm
5: ———— BIMP, 0.3mg/ml, 6M Urea, Tris, pH-8.0, 0.2mm
6: ———— BIMP, 0.3mg/ml, 7M Urea, Tris, pH-8.0, 0.2mm
7: ———— BIMP, 0.3mg/ml, 8M Urea, Tris, pH-8.0, 0.2mm

Figure 6.2.2f

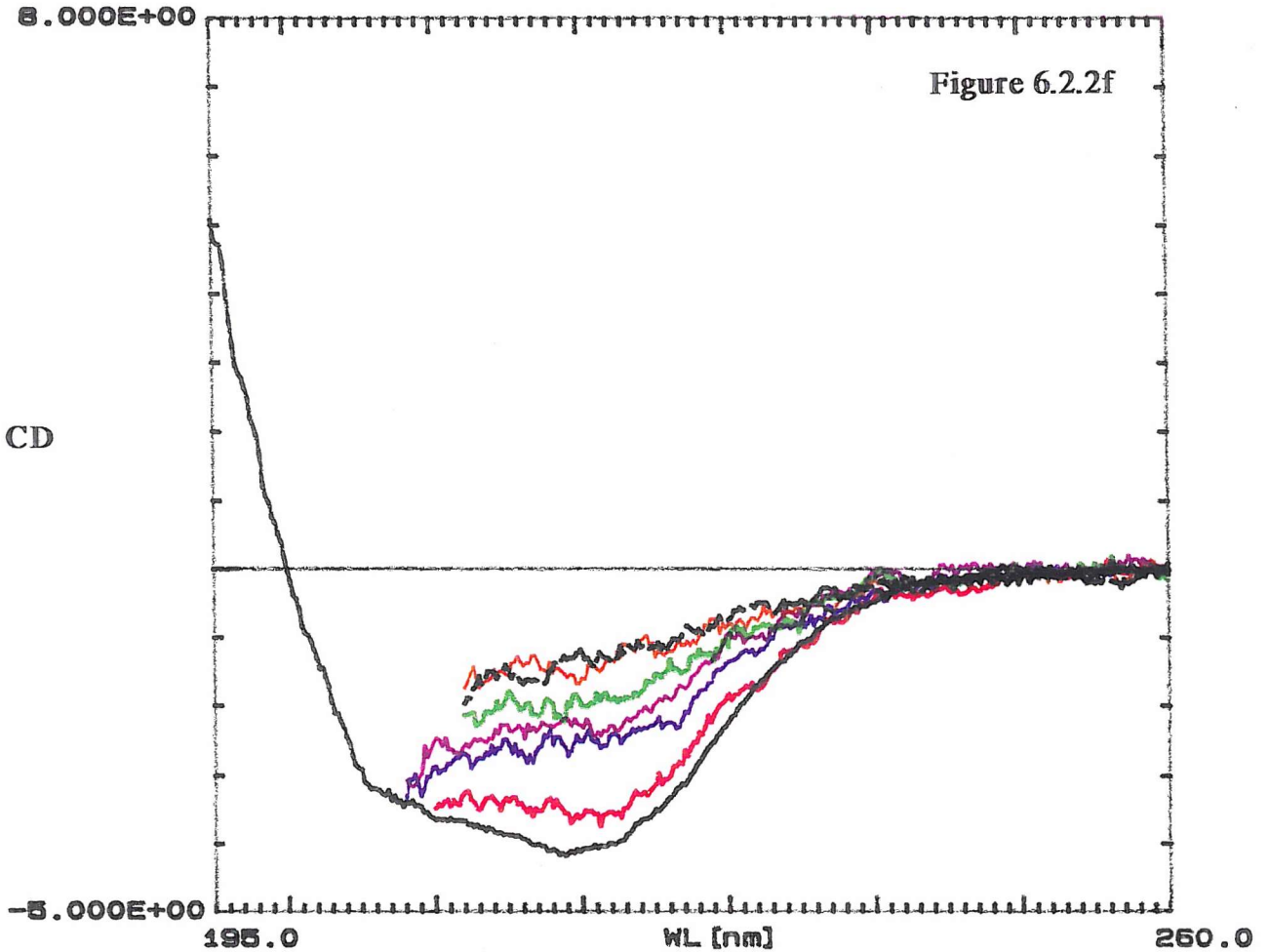
8.000E+00
CD
-5.000E+00
195.0
WL [nm]
260.0
1: BIMP, 0.3mg/ml, 0M Urea, Tris, pH=8.0, 0.5mm
2: BIMP, 0.3mg/ml, 4M Urea, Tris, pH=8.0, 0.2mm
3: BIMP, 4.5M Urea, Tris, pH=8.0, 0.2mm
4: BIMP, 0.3mg/ml, 5M Urea, Tris, pH=8.0, 0.2mm
5: BIMP, 0.3mg/ml, 6M Urea, Tris, pH=8.0, 0.2mm
6: BIMP, 0.3mg/ml, 7M Urea, Tris, pH=8.0, 0.2mm
7: BIMP, 0.3mg/ml, 8M Urea, Tris, pH=8.0, 0.2mm

**Figure** 6.2.2g: Denaturation of bovine inositol monophosphatase by urea. The CD signal at 222nm (as determined from figure 6.2.2f) is plotted against the concentration of urea. A value for the $\Delta G$ (conformational energy difference) between folded and unfolded enzyme at different concentrations of urea can be determined by calculating the ratio of folded to unfolded enzyme (k) between 2 and 6M urea and the using the equation $\Delta G = -RT \ln_e k$ (where R, the ideal gas constant, is $8.31 kJmol^{-1}$ and T, the absolute temperature, 298K).

**Figure** 6.2.2h: Determination of the conformational energy difference ($\Delta G$) between native and denatured bovine inositol monophosphatase as determined by urea denaturation. The values of $\Delta G$ at different concentrations of urea, as determined from figure 6.2.2g, are plotted against the concentration of urea to obtain a value of $\Delta G$ in 0M urea from the slope of the curve of $12.9 \pm 1.1$ $kJmol^{-1}$ (averaged from three such experiments). The CD spectrum in the near-UV region is due to the amide bonds and gives information about the protein backbone structure. A value of $\Delta G$, obtained from the y-axis intercept of this curve, gives information about changes in the protein secondary structure during the unfolding process.

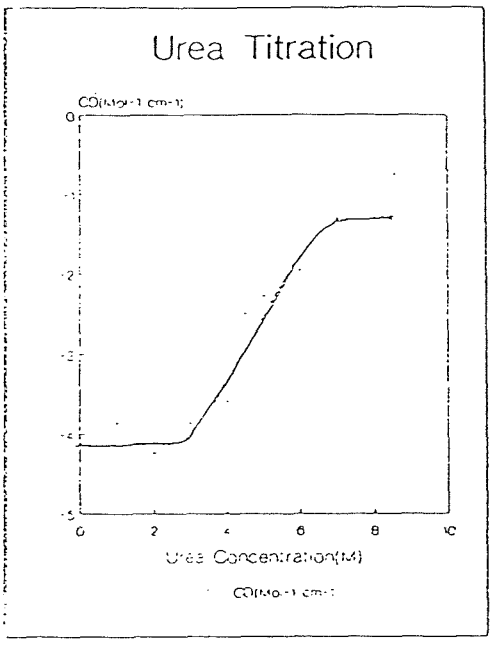


**Figure 6.2.2g**

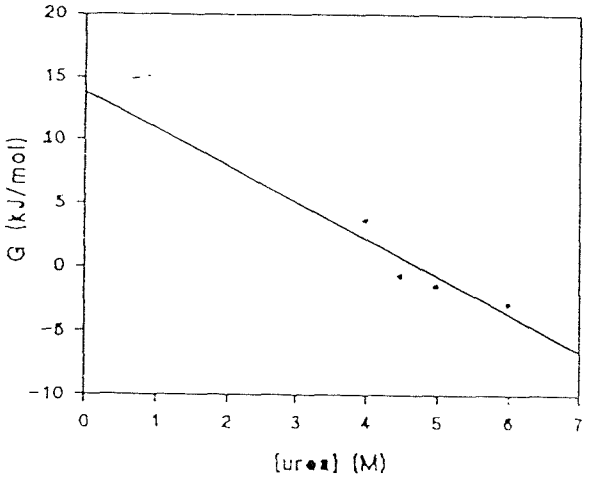


**Figure 6.2.2h**

| $\Delta G$ ($kJmol^{-1}$) | METHOD | FIGURES |
|---|---|---|
| 14.6 ± 0.8 | CD at 220nm with increasing concentrations of GuHCl | 6.2.2a-c |
| 14.2 ± 0.5 | protein fluorescence with increasing concentrations of GuHCl | 6.2.2d-e |
| 12.9 ± 1.1 | CD at 220nm with increasing concentrations of urea | 6.2.2f-i |
| 10.0 ± 2.8 | protein fluorescence with increasing concentrations of urea | |
| 15 | thermal denaturation at 60°C | |

**Table 6.2.2a :** Table summarising the conformational energy difference ($\Delta G$) between folded and unfolded bovine inositol monophosphatase, calculated by various experimental procedures.

Figure 6.2.21: Denaturation of 10$\mu$M bovine inositol monophosphatase (Mr 30,055), in 50mM Tris.HCl, pH 8.0, at 25°C by GuHCl. The denaturation is followed by recording the CD spectrum in the near-UV region.

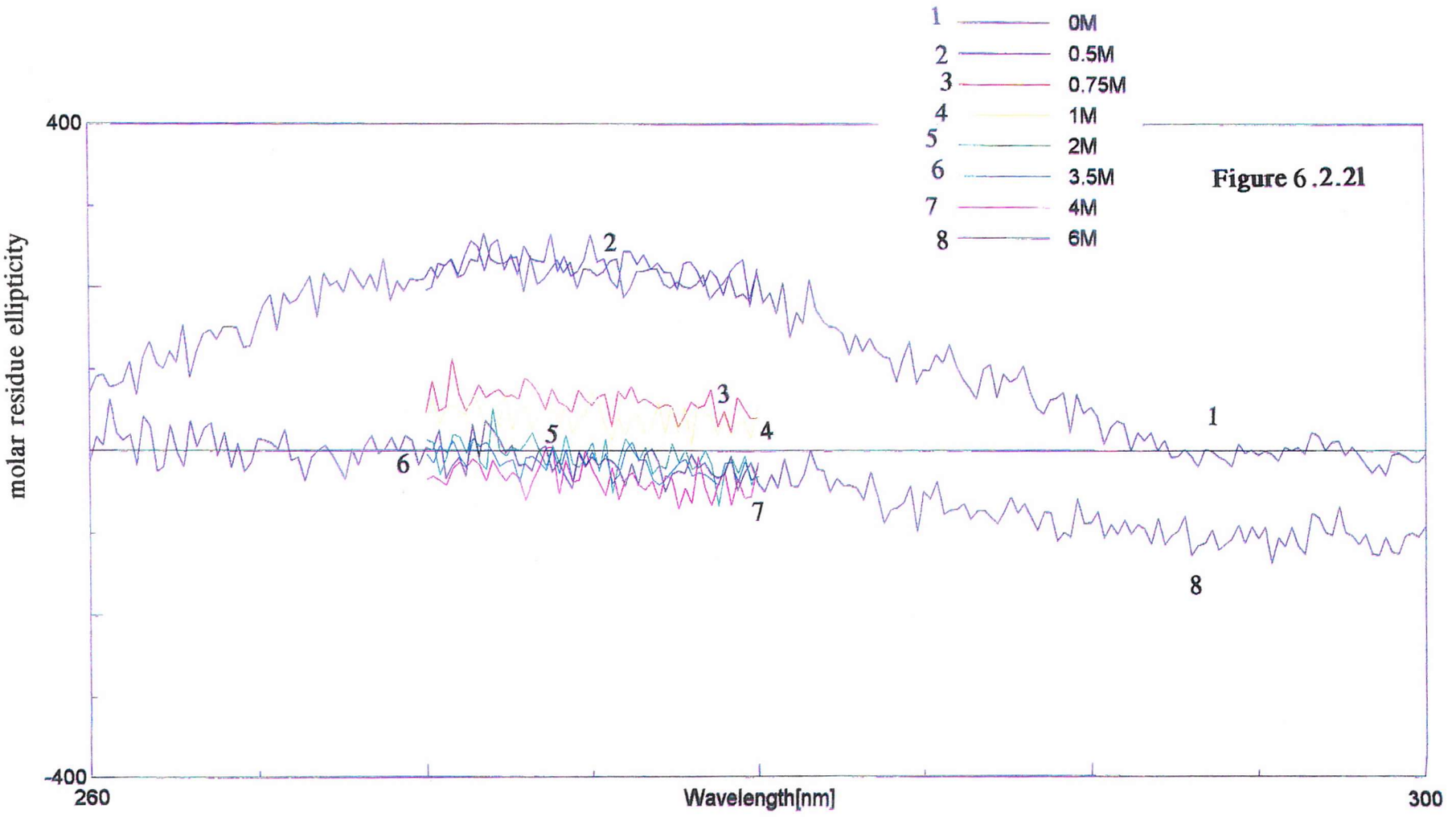
1 0M
2 0.5M
3 0.75M
4 1M
5 2M
6 3.5M
7 4M
8 6M
400
-400
260
300
Wavelength[nm]
molar residue ellipticity
1
2
3
4
5
6
7
8

Figure 6.2.21

conformations that are neither fully folded nor fully unfolded; this state is referred to as the "molten-globule state". The most common properties of this state are briefly discussed here (Creighton *et al.*, 1993), however, it should be noted that the precise structural features of this molten-globule conformational state are not yet known. Whilst the overall dimensions of the polypeptide chain are much less than those of a random coil they are only marginally greater than those of the fully folded state. The average content of secondary structure (as measured by far-UV CD spectroscopy) is similar in the fully folded and the molten globule state. The side chains are in homogeneous surroundings in contrast to the asymmetric environments they have in the interior of the fully folded state (as deduced from near-UV CD and NMR data). Certain experimental findings are observed when a molten globule state exists, for example, many of the amide groups exchange hydrogen atoms with the solvent much more rapidly than they do in the folded state, but more slowly than in the fully unfolded state. The enthalpy of the molten globule state is very nearly the same as that of the fully unfolded state but different from that of the folded state. Finally, interconversions of the molten globule state with the fully unfolded state are reported to be rapid and noncooperative, whereas those with the fully folded state are slow and cooperative.

### 6.2.3 Activation energy for the unfolding of bovine inositol monophosphatase

The increase in reaction rate with temperature is due to an increase in collision frequency (the kinetic energy and hence velocity, since the mass of a given particle remains constant, is proportional to temperature). However, the speed at which the reaction rate increases with temperature cannot be explained by the collision theory. The Arrhenius equation ($k = Ae^{-Ea/RT}$) describes how the reaction rate varies with temperature and A (the Arrhenius constant) can be regarded as a collision frequency and orientation factor in the reaction rate, whilst $e^{-Ea/RT}$ represents an activation state factor, where $E_a$ is the activation energy which all reactants must reach and RT is the thermal energy available (R is the gas constant and T the absolute temperature). Thus, A is determined by the total number of collisions per unit time and the

orientation of molecules when they collide, whereas $e^{-Ea/RT}$ is determined by the fraction of sufficient molecules to react.

The activation energy for the unfolding of bovine inositol monophosphatase can be estimated by determining the rate of inactivation of enzyme in, for example, urea at several different temperatures. The fall in activity at 31°C for several concentrations of urea is shown in figure 6.2.3a (similar figures were obtained at 25°C and 39°C). The rate of inactivation (k) is determined from a plot of ln (% activity) versus time and from an Arrhenius plot (logk versus 1/T) [figure 6.2.3b], the activation energy ($E_a$) for the unfolding process at each concentration of urea can be determined [table 6.2.3a]. The $E_a$ for unfolding in the absence of denaturant can be calculated by plotting the $E_a$ at different urea concentrations and extrapolating to the intercept on the y-axis [figure 6.2.3c], ($E_a$ = 65.0 $kJmol^{-1}$). The unfolding of bovine inositol monophosphatase by denaturants is, therefore, very sensitive to temperature, and has an $E_a$ greater than $51kJmol^{-1}$, the average value for proteins (Price *et al.*, 1986).

Similarly, a value of $E_a$ for unfolding can also be obtained by following the denaturation of bovine inositol monophosphatase in 7M urea at different temperatures by monitoring the decrease in fluorescence at 335nm upon excitation at 292nm [figure 5.2.3d and e]; the activation energy is 38.5 ± 8.6 $kJmol^{-1}$.

The Arrhenius plots are all linear with no definite changes in slope, suggesting that the same step is rate limiting at all temperatures.

The high value for $E_a$ obtained from chemical denaturation could explain the high thermostability of bovine inositol monophosphatase; since the $\Delta G$ value at approximately $15kJmol^{-1}$ is only average and cannot be responsible for the high thermostability of bovine inositol monophosphatase.

**Figure 6.2.3a**: Inactivation of 10$\mu$M bovine inositol monophosphatase (Mr 30,055) in 50mM Tris.HCl, pH 8.0, when denatured by urea. The activity is measured by periodically removing 100$\mu$l aliquots and assaying by the fluorescence assay of Gore *et al.*, (1992). The curves drawn are the loss of activity with time at 31°C at several concentrations of urea: 8M (●), 7M (○), 6M (▲), 5M (■) and 4M (▼). Similiar curves were obtained for the inactivation of bovine inositol monophosphatase by urea at 25°C and 39°C. The rate of inactivation is obtained from the slope (X 2.303) of a plot of log(% activity) against time.

**Figure 6.2.3b**: Arrhenius plot for the determination of $E_a$ (the activation energy for the folding/unfolding reaction at different concentrations of urea). The curves drawn are 8M (○), 7M (●), 6M (■), 5M (▲) and 4M (△).

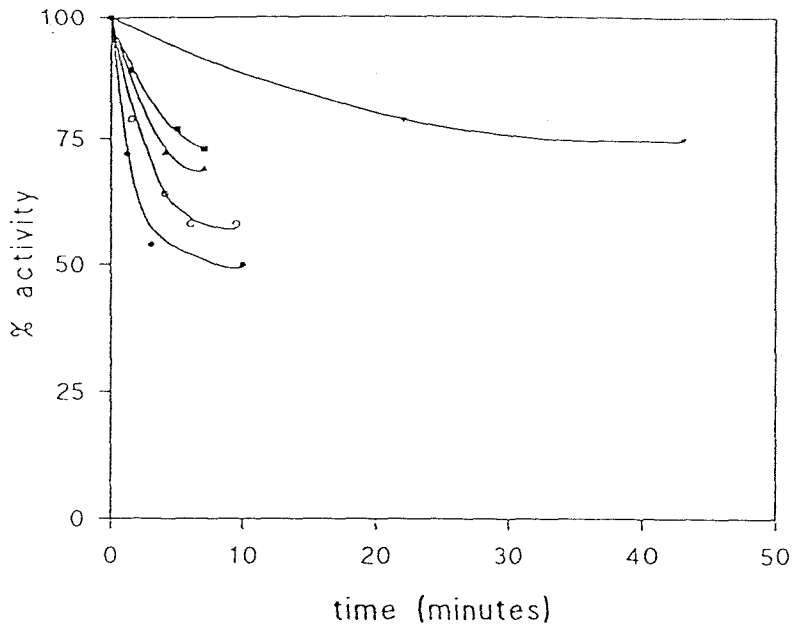


Figure 6.2.3a

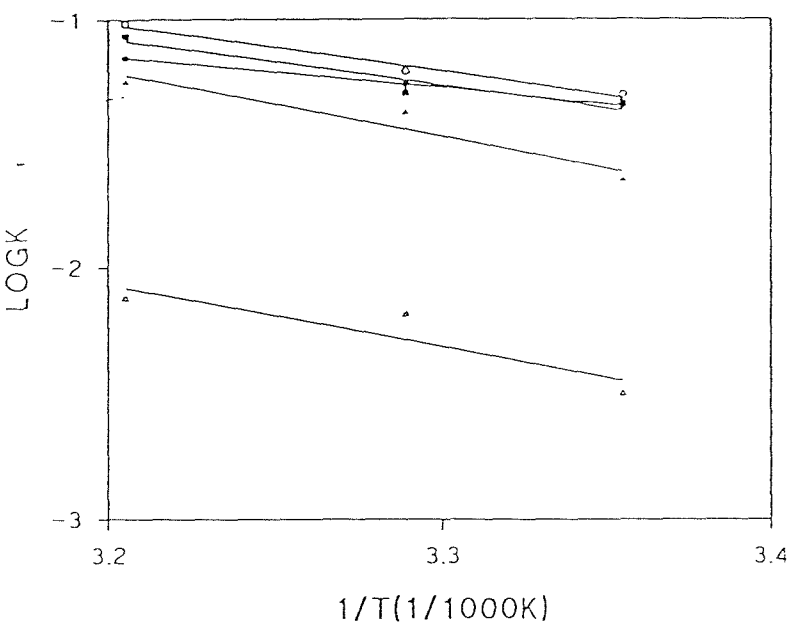


Figure 6.2.3b

| [UREA] (M) | k: 39°C ($min^{-1}$) | k: 31°C ($min^{-1}$) | k: 25°C ($min^{-1}$) | $E_a$ ($kJmol^{-1}$) |
|---|---|---|---|---|
| 4 | 0.007 | 0.006 | 0.001 | 46.7 |
| 5 | 0.055 | 0.042 | 0.022 | 48.5 |
| 6 | 0.085 | 0.050 | 0.019 | 35.5 |
| 7 | 0.069 | 0.054 | 0.019 | 24.1 |
| 8 | 0.095 | 0.061 | 0.049 | 36.6 |

Table 6.2.3a: Inactivation of 10$\mu$M bovine inositol monophosphatase (Mr 30,055), in 50mM Tris.HCl, pH 8.0, by urea. The table shows the pseudo first order rate constants (k) for the inactivation of enzyme by urea at 4-8M urea at different temperatures (25°C, 31°C and 39°C), which were calculated from the slope of plots of log(%activity) versus time, and the $E_a$ for the unfolding reaction at 4-8M urea.

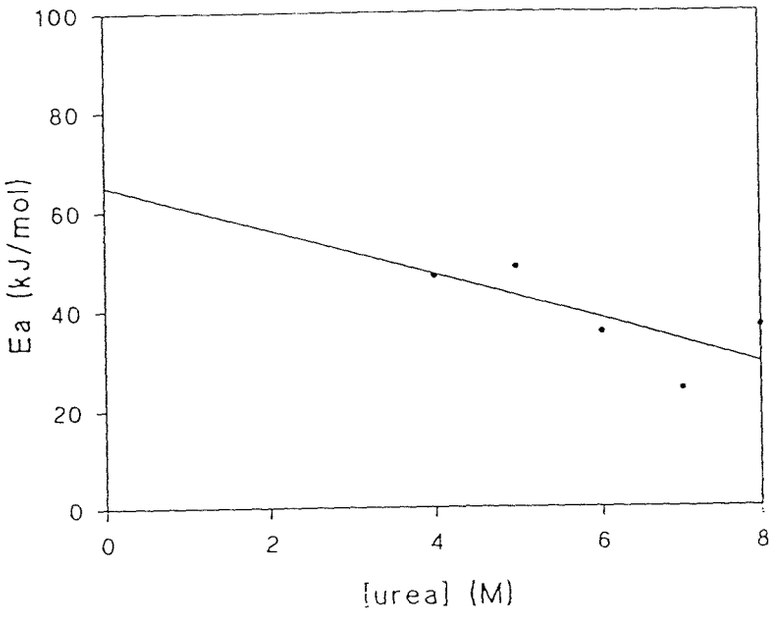


**Figure 6.2.3c**: Denaturation of bovine inositol monophosphatase by urea at different temperatures. Extrapolation of the curve to the y-axis gives a value of 65kJmol$^{-1}$ for the $E_a$ at 0M denaturant.

**Figure 6.2.3d**: Denaturation of 10$\mu$M bovine inositol monophosphatase (Mr 30,055), in 50mM Tris.HCl, pH 8.0, by 7M urea. The curves drawn are % fluorescence at several different temperatures: 22°C (▲), 26.5°C (□), 51.5°C (○) and 56°C (●). The rate of inactivation is obtained from the slope (X 2.303) of a plot of log(% fluorescence) against time.

**Figure 6.2.3e** : Arrhenius plot for the denaturation of 10$\mu$M inositol monophosphatase (Mr 30,055) by urea. From plots of $\ln_e$(% fluorescence) versus time, the pseudo first order rate constants (k) can be calculated from the slope. The $E_a$ for the denaturation of inositol monophosphatase in 7M urea is calculated from the Arrhenius plot ($E_a$ = 38.5 $\pm$ 8.6 kJmol$^{-1}$, averaged from three experiments).

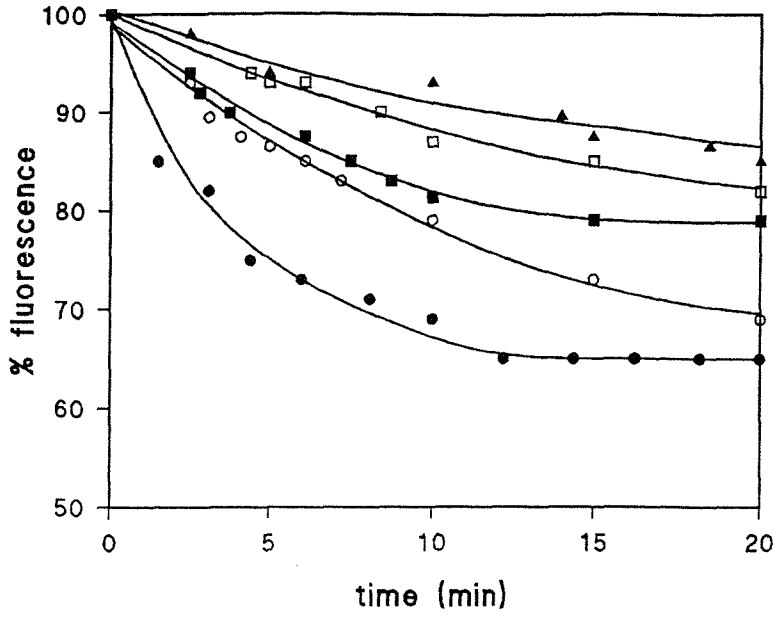


Figure 6.2.3d

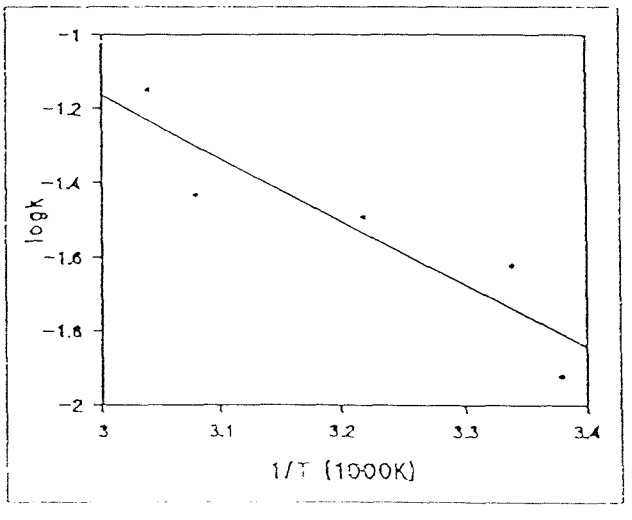


Figure 6.2.3c

### 6.2.4 Bovine inositol monophosphatase : Denaturation and renaturation studies

Generally, biological activity requires the three-dimensional structure of a given protein to be in its native state (Creighton, 1990). In the case of enzymes, this means that measurement of the enzyme activity is the method of choice if one is looking for a fast, sensitive and highly specific test to examine protein folding and unfolding (Creighton,1990).

The activity of bovine inositol monophosphatase [figure 6.2.4a] falls with increasing concentrations of urea and bovine inositol monophosphatase is reversibly denatured by urea, as shown by return of activity upon ten fold dilution of the urea and incubation overnight at 4°C [figure 6.2.4a]. A major problem in unfolding/folding is the kinetic competition of folding and aggregation. Attempts to refold proteins by lowering the concentration of protein (by dilution into buffer) usually increase the yield of renaturation (Creighton, 1990).

The fact that bovine inositol monophosphatase can refold in-vitro, suggests that this protein is not formed as a precursor in-vivo (Creighton, 1993). Proteins that do not refold in-vitro may have undergone some sort of covalent modification, lost some cofactor required for the folded state, or precipitated (Creighton, 1993). Some proteins, however, require biological factors in-vivo to prevent aggregation. Bovine and pig (Kwon *et al.*, 1993) inositol monophosphatase can be refolded in-vitro. However, human inositol monophosphatase is irreversibly denatured suggesting that there are factors absent in-vitro which are found in-vivo and are required for protein folding. Refolding of human inositol monophosphatase, as demonstrated by the return of enzyme activity, has been achieved in-vitro in the presence of ß-mercaptoethanol, suggesting that inappropriate disulphide bond formation prevents refolding in-vitro; intracellular reducing agents would prevent this in-vivo (Creighton, 1993).

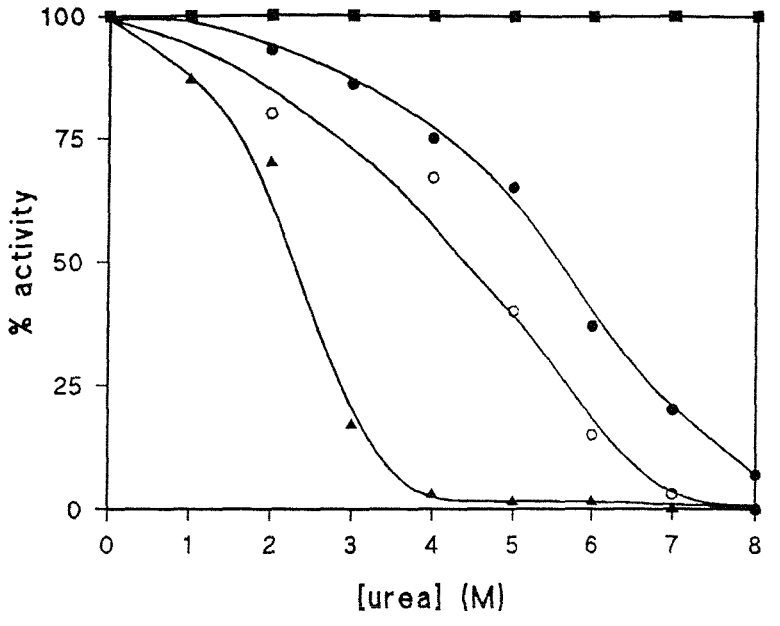


Figure 6.2.4a : The denaturation and renaturation of bovine inositol monophosphatase, in 50mM Tris.HCl, by urea at 25°C and pH 8.0. The extent of denaturation and renaturation are assessed by the measurement of enzyme activity. The curves drawn are after increasing times of incubation with denaturant: 60 minutes (●), 270 minutes (○) and overnight (▲). The enzyme is renatured by ten fold dilution with 50mM Tris.HCl, pH 8.0, and incubation overnight, at 4°C. 940$\mu$l of the renaturation mix was assayed, $Mg^{2+}$ was added to 7mM and substrate to 1mM, to give a total volume of 1ml.

### 6.2.5 Denaturation studies with double tryptophan mutants of bovine inositol monophosphatase : Indole-imidazole interactions

Bovine inositol monophosphatase contains three tryptophan residues at positions 5, 87 and 219. Mutants were prepared by Dr. P. Greasley in which only one tryptophan was present.

Wild type bovine inositol monophosphatase is thermostable and use is made of this in the enzyme preparation where the extract is heated at 60°C for one hour to remove some contaminating proteins. From a plot of $\ln_e$(%activity) versus time of incubation at 60°C, a pseudo-first order constant (k) of $0.0045min^{-1}$ was calculated for wild type bovine inositol monophosphatase. By substituting the value of k into the equation $\Delta G = -RT\ln_e k$, a value of $15kJmol^{-1}$ is calculated; this value for the conformational energy difference between folded and unfolded enzyme ($\Delta G$) is comparable to that obtained by the use of chemical denaturants to unfold inositol monophosphatase. The tryptophan mutants were not thermostable at 60°C and precipitated within five minutes. The pseudo-first order rate constant (k) for the thermal denaturation of the double tryptophan mutants at 60°C was$<0.5min^{-1}$ and the value for $\Delta G < 4.5kJmol^{-1}$ for the folding/unfolding reaction.

The double tryptophan mutants of bovine inositol monophosphatase have negligible activity [table 6.2.5a] and the fluorescence properties of the double tryptophan mutants differ from the wild type enzyme [table 6.2.5a]. The mutant enzymes have both a longer wavelength of maximal fluorescence, suggesting a more solvent exposed environment, and also a greater intensity of fluorescence at this wavelength. The latter could be a result of quenching of the three tryptophan residues in the wild type enzyme due to loss of excitation energy during resonance energy transfer processes which may readily occur due to their close proximity.

The secondary structure of the mutant and wild type enzymes can be compared by examination of their circular dichroic spectra. The wild type enzyme has the characteristic double troughed spectrum of an αß protein with minima at 220nm and

| ENZYME | % ACTIVITY RELATIVE TO WILD TYPE ENZYME | % FLUORESCENCE INTENSITY RELATIVE TO WILD TYPE ENZYME | POSITION OF MAXIMAL FLUORESCENCE (nm) |
|---|---|---|---|
| wild type | 100 | 100 | 338 |
| W5/87F | 7 | 238 | 344 |
| W5/219F | 2 | 202 | 344 |
| W87/219F | 1 | 300 | 344 |

Table 6.2.5a: Properties of the double tryptophan mutants of bovine inositol monophosphatase. The table shows the % activity and % fluorescence of the mutant enzymes, relative to the wild type enzyme, and the position of maximal fluorescence of wild type and mutant enzymes.

210nm and a maximum at 190nm. The tryptophan mutants have less pronounced troughs. The spectra of the mutant proteins compared to the wild type enzyme is very similar to those seen when the wild type enzyme is incubated in moderately high (3-4M) concentrations of urea or guanidium hydrochloride. This may, therefore, suggest that they are not folded completely, a conclusion which would be supported by their low catalytic activity.

In an attempt to ascertain whether the double tryptophan mutants are completely folded, denaturation studies with GuHCl were performed. The fall in fluorescence with increasing concentrations of GuHCl suggests that the protein has some degree of order in the absence of denaturation, but that this is small. In all cases the concentration at which the protein is 50% denatured is about half that calculated for the wild type enzyme.

Wild type bovine inositol monophosphatase may exhibit similar contributions as barnase from close charge-aromatic interactions between tryptophan and histidine residues. Tryptophan-histidine interactions in barnase are predicted to make contributions to protein stability (Vuilleumier *et al.*, 1993). By using double mutant enzyme structures, the interaction energy between His18 and Trp94 was shown to contribute as much as $6kJmol^{-1}$ to barnase protein stability at pH 5.8 (Lowenthal, 1992). There are two such close charge-aromatic interactions in bovine inositol monophosphatase that could make considerable contributions to protein stability; these are His65 and Trp5, and His217 and Trp219 [figure 6.2.5b]; the absence of these tryptophan-histidine interactions in bovine inositol monophosphatase could result in a stability $12kJmol^{-1}$ lower.

## 6.3 Summary and conclusions

Bovine inositol monophosphatase is reversibly denatured by chemical denaturants. Changes in the secondary structure of the enzyme and also the polarity of the medium around the tryptophan residues occur to the same extent. The conformational energy difference between folded and unfolded enzyme is only

average but the activation energy for unfolding is high, suggesting that the high energy for the transition state in the unfolding process accounts for the high thermal stability of bovine inositol monophosphatase.

# CHAPTER 7

# SUMMARY AND GENERAL DISCUSSION

# Chapter 7

## Summary and general discussion

Inositol monophosphatase is the putative target of $Li^+$ therapy for manic depression and occupies a pivotal role in the recycling of inositol within the phosphatidylinositol second messenger signalling pathway. $Li^+$ therapy is specific for manic depression for two reasons. Firstly, inhibition of inositol monophosphatase by $Li^+$ is uncompetitive; that is, $Li^+$ will only bind the enzyme-substrate or enzyme-intermediate complex, not the free enzyme. Hence, the overactive neurones of manic depression will be preferentially inhibited over the normal neurones. The second reason for $Li^+$ specificity for manic depression, arises from the fact that inositol crosses the blood-brain barrier only very poorly, hence, $Li^+$ inhibition of inositol monophosphatase in the brain effectively prevents inositol recycling for the resynthesis of the phosphatidylinositol phospholipids. Unfortunately, $Li^+$ therapy does have drawbacks, and these are particularly associated with the chronic use of $Li^+$, for example, liver and kidney damage. Hence, characterisation of the putative target of $Li^+$ therapy, inositol monophosphatase, is essential if an alternative treatment for manic depression is to be found. To meet this end, my post-graduate research has focused on structural and functional studies of inositol monophosphatase.

Bovine inositol monophosphatase is reversibly denatured by chemical denaturation. Changes in the secondary structure of the enzyme and also the local environment of the tryptophan residues occur at the same rate. The conformational energy difference between the folded and unfolded enzyme is only average, but the activation energy for the unfolding process is high and probably accounts for the high thermostability of inositol monophosphatase. It is possible that two charge-aromatic interactions, between His65-Trp5 and His217-Trp219, may contribute considerably to the stability of bovine inositol monophosphatase. Lowenthal, (1992), has shown that His-Trp interactions contribute considerably to protein stability, for example the interaction energy between His18 and Trp94 (approximately $6kJmol^{-1)}$ in barnase is an important contribution to protein stability; the stabilisation of the folded state is mainly a result

of non-covalent interactions between constituent amino acids, and is only marginally stable relative to the unfolded state (approximately 15kJmol$^{-1}$), Loewenthal *et al.*, 1992).

Limited proteolysis studies in the presence and absence of the substrate, Ins(1)P, and $Mg^{2+}$ (required for activity) have shown that the N-terminus of the enzyme is important for activity and it was postulated that the N-terminus of the enzyme undergoes a conformational change after Ins(1)P and, or, $Mg^{2+}$ binding (Greasley *et al.*, 1993). Near-UV CD and limited proteolysis studies performed to investigate this, demonstrate a change in the environment of the aromatic amino acids when $Mg^{2+}$ binds, possibly signalling a conformational change at the N-terminus of the enzyme upon $Mg^{2+}$ binding or dissociation.

$Mg^{2+}$ binding to the enzyme can be cooperative depending on the substrate used (Leech *et al.*, 1993); cooperativity is not observed for Ins(4)P, which is turned over quickly ($V_{max}$ relative to Ins(1)P is 150%), but is observed for substrates turned over more slowly (Ins(1)P and 4-methylumbelliferyl phosphate). Other divalent cations, $Zn^{2+}$ and $Mn^{2+}$, will support enzyme activity in the absence of $Mg^{2+}$.

A combination of site directed mutagenesis and chemical modification with diethylpyrocarbonate demonstrate that His217 is located near the active site. Diethylpyrocarbonate inactivates the enzyme and modifies three residues (one slowly and two quickly). The rate of inactivation occurs at the same rate as the modification of the slow reacting residue. In the presence of Ins(1)P, $Li^{+}$ and $Mg^{2+}$, only two sites per subunit are modified and the enzyme is not inactivated, suggesting that there is a residue reactive to diethylpyrocarbonate in inositol monophosphatase located at or near the active site. The inactivation by diethylpyrocarbonate is reversed by hydroxylamine, suggesting that the residue important for activity is a histidine residue. Steps were taken to identify this histidine residue by consideration of species sequence homology: His150 is unlikely to be important for activity since it is not conserved in the human enzyme. His65 reacts with the cysteine modification reagent iodoacetic acid, suggesting that it is both accessible and reactive and could be one

of the fast reacting residues with diethylpyrocarbonate. His217 has an abnormally high $pK_a$ value (Greasley *et al.*, 1993) and so could be the histidine residue important for activity in bovine inositol monophosphatase. A mutant, H217Q, is not inactivated upon incubation with diethylpyrocarbonate and only two sites are modified per subunit, at the fast rate, suggesting that His217 is the residue located at or near the active site. Kinetic analysis of H217Q shows that His217 is not important for catalysis, and that diethylpyrocarbonate modification of His217 inhibits the enzyme due to steric effects.

Research involving the mammalian enzyme, inositol monophosphatase, is an on-going project at the University of Southampton. Future work will include the use of stopped flow CD to determine the rate of the CD signal change that occurs in the near-UV region when $Mg^{2+}$ binds and hence ascertain the mechanism step involved [figure 4.3a]. If the rate of this signal change is shown to be dependent on the concentration of $Mg^{2+}$, then the CD signal change discussed in chapter 5 is signalling $Mg^{2+}$ binding, that is the following step in the mechanism proposed in chapter 4 [figure 4.3a]:

$$E + Mg^{2+} \leftrightarrow E.\ Mg^{2+}$$

If, however, the rate of change of the CD signal is shown to be independent of the concentration of $Mg^{2+}$, then the CD signal change discussed in chapter 5 is signalling a conformational change of the enzyme which occurs after $Mg^{2+}$ binding, that is, the following step in the reaction mechanism [figure 4.3a]:

$$E.\ Mg^{2+} \leftrightarrow E^{*}.\ Mg^{2+}$$

Enzyme stability studies, have formed a major part of my research at Southampton and future work in this research area will involve the completion of construction of a hybrid enzyme of the human and bovine inositol monophosphatase, in which the first ninety or so residues of the cloned bovine enzyme are replaced by the human sequence using molecular biology. Bovine inositol monophosphatase is reversibly

denatured by chemical denaturants, whereas the human enzyme requires the presence of reducing agents for reversible denaturation, suggesting that inappropriate disulphide bond formation is responsible for the irreversible denaturation of the human enzyme in the absence of reducing agents. The human and bovine enzymes contain seven and six cysteine residues, respectively, per subunit. The extra cysteine, located in the N-terminal α-helix at position 24, in the human enzyme may play a role in disulphide formation during denaturation/renaturation in the absence of reducing agents; an hypothesis that can be examined by denaturation / renaturation studies of the human-bovine enzyme hybrid construct.

# REFERENCES

**References**


Alber, A., (1989), *Ann. Rev. Biochem.*, **58**, 765-798.

Anfinsen, C.B., Haber, E., Sela, M., White, F.H., (1961), *Proc. Natl. Acad. Sci USA*, **47**, 1307-1314.

Attwood, P.V., Ducep, J.B., Chanal, M.C., (1988), *Biochem. J.*, **253**, 387-394.

Baker, R., Kulagowski, J.J., Billington, D.C., Leeson, P.D., Lennon, I.C., Liverton, N., (1989), *J. Chem. Soc. Commun.*, 1383-1385.

Benesch, R., Benesch, R.F., Boyer, P.D., Klotz, I.M., Middlebrook, W.R., Szent-Gyolgyi, A.G., Schwarz, D.R., Eds., (1959), *Sulfur in Proteins Proc. Symp. Falmouth, mass.*

Berger, S.L., (1975), *Anal. Biochem.*, **67**, 428.

Berridge, M.J., Downes, C.P., Hanley, M.R., (1982), *Biochem. J.*, **206**, 587-595.

Berridge, M.J., Downes, C.P., Hanley, M.R., (1989), *Cell*, **59**, 411-419.

Bone, R., Springer, J.P., Atack, J.R., (1992), *Proc. Natl. Acad. Sci. USA*, **89**, pp10031-10035.

Bone, R., Frank, L., Springer, J.P., Atack, J.R., (1994), *Biochemistry*, in press.

Bradford, M., (1976), *Anal. Biochem.*, **72**, 248-254.

Boyer, P.D., (1959), *Enzymes*, **1**, 511.

Burstein, E.A., Vedenkina, N.S., Ivkova, M.N., (1973), *Photochem. and Photobiol.*, **18**, 261-279.

Busetta, B., Hospital, M., (1982), *Biochimica et Biophysica Acta.*, **701**, 111-118.

Cecil, R., (1963), *Proteins*, **379.**

Cheung, S.T., Fonda, M.L., (1979), *Biochem. Biophys. Res. Commun.*, **90**, 940-949.

Cohen, S.N., Chang, A.C.Y., Hsu, L., (1972), *Proc. Natl. Acad. Sci. USA*, **69**, 2110-2114.

Connelly, M.L., (1983), J. Appl. Crystallogr., **16**, 548-558.

Creighton, T.E., (1978), *Progr. Biophys. Mol. Biol.*, **33**, 231.

Creighton, T.E., (1990), *Protein Structure: a Practical Approach*, IRL Press.

Creighton, T.E., (1993), *Proteins: Structures and molecular properties, second edition*, W.H. Freeman and Company, New York.

Diehl, R.E., Whiting, P., Potter, J., Gee, N., Ragan, C.I.,
Linemeyer, D., Schoepfer, R., Bennet, C., Dixon, R.A.F., (1990), *J. Biol. Chem.*, **265**, 5946-5949.

Dill, A.K., (1990), *Biochem.*, **29**, 7142-7155.

Dolgikh, D.A., Kolomiets, A.P., Bolotina, I.A., Ptitsyn, O.B., (1984), *FEBS Letts.*, **165**, 88.

Dominici, P., Tancini, B., Voltattorni, C.B., (1985), *J. Biol. Chem.*, **260**, 10583-10589.

Downes, C.P., MacPhee, C.H., (1990), *Eur. J. Biochem.*, **193**, 1-18.

Drake, A.F., *"Microscopy, Optical Spectroscopy, and Macroscopic Techniques"*, ed.

Jones, C., Mulloy, B., Thomas, A.H., **vol.22**, (1994), pp151-173.

Edman, P., (1956), *Acta. Chem. Scand.*, **10**, 761.

Edsall, J.T., Wyman, (1958), *Biophysical Chemistry*, Ch.8, Academic Press.

Ellman, G.L., (1959), *Arch. Biochem. Biophys.*, **82,** 70-77.

Fabiny, J.M., Jayakumar, A., Chinault, A.C., Barnes, E.M., Jr., (1991), *J. Gen. Microbiol.*, **137**, 983-989.

Fasman, G.D., (1974), *PAABS Rev. 2*, 587-591.

Feldman, F., Butler, L.G., (1969), *Biochem. Biophys. Res. Commun.*, **36**, 119-125.

Fersht, A.R, (1985), *Enzyme Structure and Mechanism*, W.H Freeman and Co., New York.

Fehrst, A.R., (1987), *Trends Biochem. Sci.*, **12**, 301-304.

Fields, R., (1971), *Biochem. J.*,**124**, 581.

Fonda, M.L., Anderson, B.M., (1969), *J. Mol. Biol.*, **244**, 666.

Freedman, R.B., Radda, G.K., (1968), *Biochem. J.*, **108**, 383.

Galla, Von Hans-Joachim unter Muller, Mitarbeit Von Hans-Jurgen, (1988), *Spektroskopische Methoden in der Biochemie*, ed. Georg Thieme Verlag Stuttgart, New York, pp1-143.

Ganzhorn, A.J., Chanal, M.C., (1990), *Biochemistry*, **29**, 6065-6071.

Ganzhorn, A.J., Vincendon, P., Pelton, J.T., (1993), *Biochem. Biophys. Acta*, **1161**,

303-310.

Garnier, J., Osguthorpe, D.J., Robson, B., (1978), *J. Mol. Biol.*, **120**, 97-120.

Gee, N.S., Ragan, C.I., Watling, K.J., Aspley, S., Jackson, R.G., Reid, G.G., Gani, D., Shute, J.K., (1988), *Biochem. J.*, **249**, 883-889.

Gee, N.S., Howell, S., Ryan, G., Ragan, C.I., (1989), *Biochem. J.*, **264,** 793-798.

Gee, N.S., Knowles, M.R., McAllister, G., Ragan, C.I., (1991), *FEBS*, **284**, 95-97.

Geever, R.F., Huiet, L. Baum, J.A., Tyler, B.M., Patel, V.B., Rutledge, B.J., Case, M.E., Giles, N.H., (1989), *J. Mol. Biol.*, **207**, 15-34.

Giles, N.H., Greever, R.F., Asch, D.K., Avalos, J., Case, M.E., (1991), J. Hered., **82**, 1-7.

Goldfarb, A.R., (1966), *Biochem. J.*, **5**, 2574.

Gore, M.G., Greasley, P.J., Ragan, C.I., (1992), *J. Biochem. Biophys. Method*, **25**, 55-60.

Greasley, P.J., Gore, M.G., Rees-Milton, K.J., Ragan, C.I., (1993), **319**, *FEBS*, 49-53.

Greasley, P.J., Gore, M.G., (1993), *FEBS*, **331**, no.1,2, 114-118.

Greasley, P.J., Hunt, L.G., Gore, M.G., (1994), *Eur. J. Biochem.*, **798**, 1-8.

Gurd, F.R.N, *Methods Enzymol.*, (1967), **11**, 532.

Habeeb, A.F.S., Hiramoto, R., (1968), *Arch. Biochem.*, **126**, 16, 68.

Hallcher, L.M., Sherman, W.R., (1980), *J. Biol. Chem.*, **255**, 10896-10901.

Hanahan, D.J., (1983). *J. Mol. Biol.*, 7, 471.

Hawkins, A.R., Lamb, H.K., Smith, M., Keyte, J.W., Roberts, C.F., (1988), *Mol. Gen. Genet.*, **214**, 224-231.

Hill, A.J., (1913), *Biochem. J.*, 7, 471.

Jackson, R.G., Gee, N.S., Ragan, C.I., (1989), *Biochem. J.*, **264**, 419-422.

Janin, J., (1979), *Nature*, **277**, 491-492.

Kauzman, W., (1959). *Adv. Protein Chem.*, **14**, 1.

Ke, H., Liang, J., Zhang, Y., Lipscomb, W.N., (1991), *Biochem.*, **30**, 4412-4420.

Knowles, M.R., Gee, N., McAllister, G., Ragan, C.I., Greasley, P.J., Gore, M.G., (1992), *Biochem. J.*, **285,** 461-468.

Kunkel, T.A., Roberts, J.D., Zalour, R.A., (1987), *Methods Enzymol.*, **154**, 367-382.

Kuwajima, K., (1989), *Proteins*, **6**, 87.

Kwon, O-S, Lo, S.C.L., Kwok, F., Churchich, J.E., (1993), *J.Biol.Chem.*, **268**, 11, 7912-7916.

Laemmli, U.K., (1970). *Nature*. **277**, 680-684.

Leech, A.P., Baker, G.R., Shute, J.K., Cohen, M.A., Gani, D., (1993), *Eur. J. Biochem.*, **212**, 693-704.

Lim, V.I., (1974), *J. Mol. Biol.*, **88**, 873-894.

Loewenthal, R. Sancho, J., Fehrst, A.R., (1992) *J. Mol. Biol.*, **224**, 759-770.

Lundblad, R.L., Noyes, C.M., Chemical Reagents for Protein Modification, CRC Press. vol.1, (1970).

Majerus, P.W., Connolly, T.M., Bansal, V.S., Inhorn, R.C., Ross, T.S., Lips, D.L., (1988), *J. Biol. Chem.*, **263**, 3031-3054.

Maniatis, T., Fritsch, E.F., Sambrook, J., (1982), *Molecular Cloning: A Laboratory Manual*, C.S.H.N.Y.

Matthews, B.W., (1987), *Biochem.*, **26**, 6885-6888.

McAllister, G., Whiting, P.J., Hammond, E.A., Knowles, M.R., Atack, J.R., Bailey, F.J., Maiggetler, R., Ragan, C.I., (1992), *Biochem. J.*, **284**, 749-754.

Means, G.E., Feeney, R.E., (1971), Chemical Modification of Proteins, Holden-Day Inc., San Francisco.

Melchior, W.B. Jr., Fahrney, D., (1970), *Biochemistry*, **251**,

Miles, E.W., (1977), *Methods Enzymol.*, **47**, 431-442.

Mitaku, S., Ishido, S., Hirano, Y., Itoh, H., Kataoka, R., Saito, N., (1991), *Biophys. Chem.*, **40**, 217-222.

Moore, S., Stein, W.H., (1954), *J. Biol. Chem.*, **211**, 907.

Nahorski, S.R., Ragan, C.I., Challis, R.A.J., (1991), *Trends Pharmacol. Sci.*, **12**, 297-303.

Neuwald, A.F., York, J.D., Majerus, P.W., (1991), *FEBS Letts.*, **294**, 16-17.

Ohgushi, M., Wada, A., (1983), *FEBS Letts.*, **164**, 21.

Okuyama, T., Satake, K., (1960), *J. Biochem. (Tokyo)*, **47**, 454.

O'Sullivan,C., Tompson,F.W., (1890), *J. Chem. Soc.*, **57**, 834.

Ovádi, S., Libor, Elodi, P., (1967), *Biochem. Biophys. Acta*, **2**, 19.

Pace, C.N., (1974), *Crit. Rev. Biochem.*, **3**,1.

Patthy, L., Thesz, J., (1980), *Eur. J. Biochem.*, **105**, 387-393.

Pearson, R.G., (1963), *J. Amer. Chem. Soc.*, **85**, 3533.

Pelton, P.D., Ganzhorn, A.J., (1992), *J. Biol. Chem.*, **267**, 9, 5916-5920.

Perham, R.N., Richards, F.M., (1967), *J. Mol. Biol.*, **33**, 795.

Petra, P.H., (1971), *Biochem.*, **10**, 3163-3170.

Pfeil, W., (1981), *Mol. Cell Biochem.*, **40**, 3.

Polgar, L., (1975), *Eur. J. Biochem.*, **51**, 1, 63-71.

Pollack, S.J., Knowles, N.R., Atack, J.R., Broughton, H.B., Ragan, C.I., Osborne, S.A., McAllister, G., (1993), *Eur. J. Biochem.*, **217**, 281-287.

Pollack, S.J., Atack, J.R., Knowles, N.R., McAllister, G., Ragan, C.I., Baker, R., Fletcher, S.R., Iverson, L.L., Broughton, H.B., (1994), *Proc. Natl. Acad. Sci. USA*, **91**, 5766-5770.

Price, N.C., Dwek, R.A., (1986), *Principles and Problems in Physical Chemistry for Biochemists*, second edition.

Privalov, P.L., (1979), *Adv. Protein Chem.*, **33**, 167.

Provencher, S.W., Glockner, J., (1981), *Biochemistry*, **20**, 33-40.

Rico, M., Santora, J., Bermejo, F.J., Herranz, J., Nieto, J.L., Gallego, E., Jimenez, M.A., (1986), *Biopolymers*, **25**, 1031-1053.

Riordan, J.F., McElvany, K.D., Borders, C.L., Jr., (1977), *Science*, **195**, 884-886.

Robson, B., Suzuki, E., (1976), *J. Mol. Biol.*, **107**, 327-356.

Roosemont, J.L., (1978), *Anal. Biochem.*, **88**, 314-320.

Rose, Z.B., (1970), *Arch. Biochem. Biophys.*, **140**, 508-513.

Rosen, C.G., (1966), *Biochem. Biophys. Acta*, 1966, **130**, 401.

Roth, S.C., Harkness, D.R., Issacks, R.E., (1981), *Arch. Biochem. Biophys.*, **210**, 465-473.

Satake, K., Okuyama, T., Ohasi, M., Shinoda, T., (1960), *J. Biochem. (Tokyo)*, **50**, 6.

Saito, Y., Wada, A., (1983), Biopolymer, **22**, 2105.

Schneider, F., (1978), *Angew. Chem. Int. Ed. Engl.*, **17**, 583-592.

Schellman, J.A., (1987), *Ann. Rev. Biophys. Chem.*, **16**115.

Segel, I.H., (1975), *Biochemical Calculations*, second edition, Wiley.

Serrano, L., Kellis Jr., J.T., Cann, P., Matouschek, A.,
Fehrst, A.R., (1992), *J. Mol. Biol.*, **224**, 783-804.

Tejwani, G.A., (1983), *Adv. Enzymol.*, **54**, 121-194.

Van Etten, R.L., Hickey, M.E., (1977), *Arch. Biochem. Biophys.*, **183**, 250-259.

Vuilleumier, S., Sancho, J., Lowenthal, R., Fersht, A.R., (1993), *Biochem.*, **32**, 10303-10313.

Whelan, P.M., Hodgson, M.J., (1978), *Essential Principles of Physics*, John Murray Ltd.

Whiting, P., Gee, N.S., Potter, J., Howell, S., Ragan, C.I., (1990), *Biochem. J.*, **272**, 465-468.

Yano, R., Nagai, H., Shiba, K., Yura, T., (1990), *J. Bacteriol.*, **172**, 2124-2130.

York, E.J., Stewart, J.M., Baldwin, R.L., (1990), *Biopolymers*, **29**, 1-11.

Zhang, Y., Liang, J-Y., Lipscomb, W.N., (1993), *Biochem. Biophys. Res. Commun.*, **3**, 1080-1083.

Zoller, M.J., (1991), *Curr. Opin. Struct. Biol.*, **1**, 605-610.

Volume 319, number 1,2, 49–53 FEBS 12196 March 1993


# Bovine inositol monophosphatase: proteolysis and structural studies

P.J. Greasley[a], M.G. Gore[a], K.J. Rees-Milton[a] and C.I. Ragan[b]

[a]*Dept. of Biochemistry, Centre of Molecular Recognition, School of Biological Sciences, University of Southampton, Bassett Crescent East, Southampton, SO9 3TU, UK* and [b]*Neurosciences Research Centre, Merck Sharp and Dohme, Terlings Park, Eastwick Road, Harlow, Essex, CM20 2QR, UK*

Received 12 January 1993

Bovine brain inositol monophosphatase is inactivated when trypsin catalyses the cleavage of a single peptide bond between Lys-36 and Ser-37. This proteolysis is closely followed by cleavage at two other sites in the protein between Lys-78 and Ser-79 and between Lys-156 and Ser-157 suggesting that all of these sites are exposed in the native conformation of the protein. All of these residues are predicted to lie at the ends of α helices. The most susceptible bond (Lys-36–Ser-37) is predicted to lie in a highly flexible region of the protein. Circular dichroism studies suggest that approximately 40% of the secondary structure of this protein is helical which is similar to that predicted by the algorithm of Garnier et al. [(1978) J. Mol. Biol. 120, 97–120].

Inositol monophosphatase; Proteolysis; Protein structure; Circular dichroism

## 1. INTRODUCTION

Inositol monophosphatase dephosphorylase Ins(1)P, Ins(3)P and Ins(4)P as well as a number of non-inositol-containing compounds [2]. The enzyme has a subunit molecular weight of 30 kDa and exists as a homodimer. Catalysis is a $Mg^{2+}$-dependent process although high concentrations of this metal causes inhibition of the enzyme [3]. The enzyme is also inhibited in an uncompetitive manner by $Li^{+}$ [3], a feature which may underlie the anti-manic and anti-depressive actions of this ion [4]. The cDNA cloning and sequencing of the bovine [5], rat and human [6] genes has demonstrated a high level of sequence homology between these species (79%) and therefore fails to highlight any one particular area of the protein as being significant in the catalytic process of the enzyme. The production of a monoclonal antibody against the enzyme has led to the N-terminal region of the protein being implicated in the catalytic process [7]. The epitope of the antibody is centred around Cys-8 [8] and binding gives rise to inhibition of the enzyme [9]. Further studies which utilised the enzyme endoprotease Lys-C have demonstrated that in inositol monophosphatase there is a bond located between Lys-36 and Ser-37 highly susceptible to proteolysis [9]. The susceptibility of this bond to cleavage is decreased by the presence of substrate and other ligands known to bind at the active site of this enzyme [9]. Hydrolysis of this bond by endoprotease Lys-C leads to concurrent loss of enzyme activity suggesting that this region of the protein is important in the functioning of the enzyme. Prolonged exposure to very high concentrations of endoprotease Lys-C was shown to cleave the protein at one additional site (not identified) producing a fragment of $M_r$ 23,000. Here we report observations made using limited proteolysis by an alternative protease, trypsin, which has enabled the identification of three other peptide regions of the enzyme with exposed target residues. These sites of cleavage are correlated with secondary structural predictions which place the target residues at ends of α-helices.

*Correspondence address:* M.G. Gore, Dept. of Biochemistry, Centre of Molecular Recognition, School of Biological Sciences, University of Southampton, Bassett Crescent East, Southampton, SO9 3TU, UK.

## 2. MATERIALS AND METHODS

### 2.1. *Materials*

The growth of bacterial cultures and subsequent extraction and purification of inositol monophosphatase is described elsewhere [5]. All reagents were purchased from Sigma Chemical Co., Poole, UK.

### 2.2. *Enzyme activity*

Inositol monophosphatase activity was determined either by the discontinuous assay of Lanzetta et al. [10] or the fluorescent assay described by Gore et al. [11].

### 2.3. *Protein concentration*

The concentration of inositol monophosphatase was determined by the method of Smith et al. [12].

### 2.4. *Proteolysis of inositol monophosphatase*

To 1 ml of inositol monophosphatase (1 mg/ml) was added 20 μl of 0.005% trypsin in 10 mM Tris-HCl buffer (pH 8.0) and 10 mM $CaCl_2$ at 21°C. Samples were withdrawn at various times and run on a 12% SDS-PAGE gel [13].

2.5. *Electroblotting of peptides from SDS-PAGE*

Inositol monophosphatase was treated with 0.01% trypsin as described above for 30 min and the various proteolytic products separated by 12% SDS-PAGE. The gel was electroblotted onto Problott (ABI) by the method of Matsudaira [14]. The blot was then stained for 30 s using Coomassie blue and the visualised protein bands excised and identified by N-terminal sequencing.

2.6. *Protein sequencing*

The amino-terminus of each peptide was determined using an Applied Biosystems 477A sequencer with on line 120A HPLC for identification of the PTH-amino acids released at each cycle.

2.7. *Gel filtration*

A column of Sephadex G-75 (2.2 × 30 cm) was prepared and equilibrated in 100 mM Tris-HCl buffer (pH 8.0) with a flow rate of 1.4 ml/min. The column was calibrated using solutions of Dextran blue, pyridoxal phosphate, cytochrome *c*, trypsin inhibitor, DNase I, ovalbumin, glyceralderhyde 3-phosphate dehydrogenase, alcohol dehydrogenase and alkaline phosphatase. Inositol monophosphatase was digested with 0.005% trypsin for 10 min at 21°C followed by the addition of trypsin inhibitor to prevent further hydrolysis. This was then applied to the column for estimation of the molecular weight of the proteolysed inositol monophosphatase.

2.8. *Gel scanning*

The $M_r$ of each peptide fragment was estimated by SDS-PAGE and the intensity of each band was estimated by integration using a Joyce Loebl Chromoscan 3 gel scanner.

2.9. *Circular dichroism studies*

The far CD spectrum of the bovine inositol monophosphatase was determined using a Jasco J600 CD spectrometer with a 0.2 mm light path. The protein concentration used was 1 mg/ml in 50 mM Tris-HCl (pH 8.0).

## 3. RESULTS AND DISCUSSION

Approximately 85% of the activity of inositol monophosphatase is lost in 10 min when the enzyme is incubated with 0.005% w/w trypsin at 21°C and pH 8.0. The loss in enzyme activity is accompanied by a decrease in $M_r$ from 30,000 to 26,500 (Fig. 1). Ligand protection studies (data not shown) demonstrated that the cleavage by trypsin is prevented by the inclusion of the substrate Ins(1)P (0.6 mM) and the inhibitor LiCl (10 mM). The latter forms a stable complex with the enzyme and the phosphate group released after the hydrolytic step of the reaction [15]. Control experiments demonstrated that these ligands have no effect on the action of trypsin. These results are consistent with those of Gee et al. [9] who demonstrated the loss of enzyme activity as a result of proteolysis by endoprotease Lys-C.

The structural nature of the major proteolytic product of this first period of incubation was investigated by gel filtration chromatography. Native inositol monophosphatase was found to have a molecular weight of 48 kDa when chromatographed on a Sephadex G-75 column. This value is low when compared to the molecular weight deduced from the gene sequence but is consistent with the findings of other workers [8,16]. When proteolysed enzyme was applied to the same column, the apparent molecular weight was reduced to 44.7

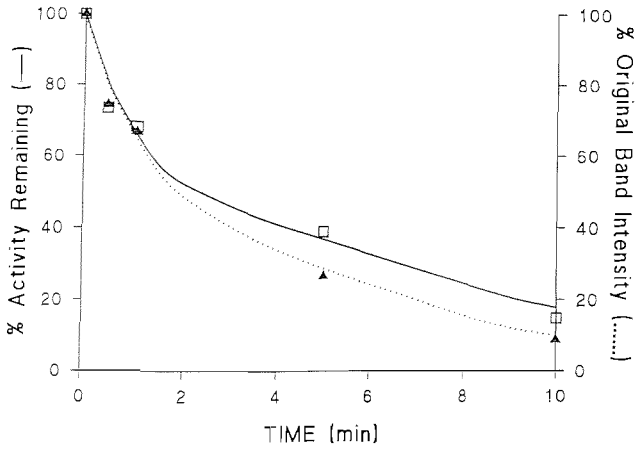


Fig. 1. The correlation of the time course of inactivation of inositol monophosphatase by trypsin with the time course of loss of the N-terminal fragment from the enzyme. 1 mg of enzyme in 1 ml of 50 mM Tris-HCl, pH 8.0 was incubated for various times with 0.005% w/w trypsin at 21°C. Aliquots were removed and assayed for activity (see section 2) and subjected to SDS-PAGE.

kDa. Both of these figures are low compared to the expected $M_r$ of 60,000 deduced from the gene sequence [5] but are in broad agreement with the data of Meek et al. [16]. However, Whiting et al. [8] showed that the molecular weight of proteolysed enzyme appeared to increase from 48 kDa (native) to 51 kDa. The latter could be due to conformational relaxation following proteolytic cleavage, thus giving rise to a larger Stokes radius. It is also possible that the low molecular weight of the protein determined by gel filtration chromatography may indicate that hydrophobic interactions between the protein and the matrix delays the elution of the enzyme resulting in an erroneously low estimate of the molecular weight. In order to test this, native and proteolysed enzyme was applied to a Gilson HPLC system equipped with a 250 × 7.5 mm TOSOH-TSK G3000SW gel permeation column in high (50 mM Tris-HCl, 200 mM NaCl, pH 8.0) or low (50 mM Tris-HCl, pH 8.0) salt conditions. Using the high salt conditions of Whiting et al. [8] the native protein eluted after 17.25 ml and the proteolysed enzyme eluted after 16.35 ml consistent with an apparent increase in size. However, under the low salt conditions the reverse situation occurred. The native protein eluted after 12.9 ml whereas the cleaved protein eluted after 13.8 ml consistent with an apparent decrease in size. These data show that both the native and the proteolysed samples interact with this matrix since both eluted earlier when in low salt conditions. The observation that the cleaved protein in particular is retained longer by the column matrix under high salt conditions may suggest that the loss of the N-terminal 36 residues of the protein exposed an additional hydrophobic surface. Both groups identify a change in molecular weight of about 3 kDa although the possible interactions with the gel matrices used make this value

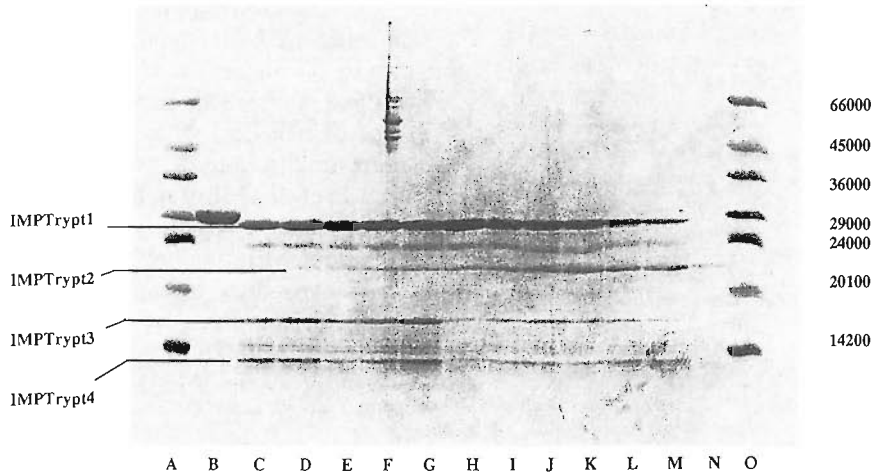


Fig. 2. Proteolytic digestion of inositol monophosphatase with trypsin produced four main peptide intermediates labelled as IMPTrypt 1–4. The band of $M_r$ 24,000 corresponds to trypsin inhibitor which was used to terminate the reaction. Lanes (A) and (O) are $M_r$ markers; (B) shows undigested inositol monophosphatase; (C) 1 min; (D) 2 min; (E) 5 min; (F) 10 min; (G) 20 min; (H) 30 min; (I) 45 min; (J) 60 min; (K) 90 min; (L) 120 min; (M) 150 min and (N) 24 h incubation with 0.01% w/w trypsin.

questionable. Since SDS-PAGE experiments show that all subunits are cleaved with a loss of a peptide of $M_r$ 3,000 from each subunit the data above also suggest that the dimeric nature of the enzyme is maintained in the first proteolysed protein intermediate.

By increasing either the concentration of trypsin or by prolonging the duration of exposure to the protease, native inositol monophosphatase undergoes slow but complete digestion under non denaturing conditions unlike the situation when endoprotease Lys-C is used. This process appears to occur in a very ordered manner and several major peptide intermediates are formed under the conditions used (see section 2). These peptides appear to be produced by hydrolysis at only a few of the possible 27 tryptic sites in inositol monophosphatase. It therefore seems probable that these sites are relatively accessible to trypsin in the native tertiary structure of the protein, thus generating several major intermediates before being digested to their constituent tryptic peptides. Fig. 2 shows the time course of tryptic degradation of inositol monophosphatase. The disappearance of the 30 kDa native inositol monophosphatase band is complete within one minute under the conditions used. This initial site of cleavage is shortly followed by cleavage predominantly at three other sites. These major protein fragments produced are stable for up to 2 h, though after 24 h only a small amount of a single band remains of apparent $M_r$ 20,500. The N-terminal sequence of each of the proteolytic products was identified by electroblotting onto Problott membrane (ABI) with subsequent sequencing as described in section 2. The main product (IMPTrypt 1, see Table I) with an apparent $M_r$ 26,540 was identified as being produced by proteolysis between Lys-36 and Ser-37 as was noted from previous experiments with endoprotease Lys-C [8]. The other three peptides have N-terminal sequences as described in Table I. The peptides IMPTrypt 3 and IMPTrypt 4 appear to be products which share a common peptide bond cleavage. These two peptides are produced by tryptic action between Lys-156 and Ser-157 of the protein already truncated by cleavage between Lys-36 and Ser-37. The fourth peptide (IMPTrypt 2) is the product of proteolysis between Lys-78 and Ser-79. However, the $M_r$ of IMPTrypt 2 estimated from its electrophoretic mobility suggests that some truncation has occurred at a site near to the C-terminus. Its molecular weight would suggest that a suitable truncation site to give rise to such a peptide would be between Lys-256 and Thr-257.

When extended proteolysis is performed in the presence of Ins(1)P, $Mg^{2+}$ and $Li^+$ hydrolysis of the bond between Lys-36 and Ser-37 occurs at a much slower rate as expected for the ligand protected enzyme. However, the secondary sites of proteolysis are still hydrolysed in the protected protein. This suggests that proteolysis of these sites does not arise as a result of denaturation caused by the primary hydrolysis at the peptide bond between Lys-36 and Ser-37.

Table I

Shows the four main tryptic products of inositol monophosphatase generated upon incubation of the enzyme with 0.01% trypsin as described in section 2. The table shows the N-terminal sequence of each peptide and its estimated molecular weight

| Peptide | N-terminal sequence | $M_r$ measured | Predicted fragment | $M_r$ calculated |
|---|---|---|---|---|
| IMPTrypt1 | SSPAD | 26,540 | 37–277 | 25,976 |
| IMPTrypt2 | SILTD | 20,700 | 79–256 | 19,781 |
| IMPTrypt3 | SSPAD | 15,140 | 37–156 | 13,112 |
| IMPTrypt4 | SLLVT | 11,520 | 157–277 | 12,864 |

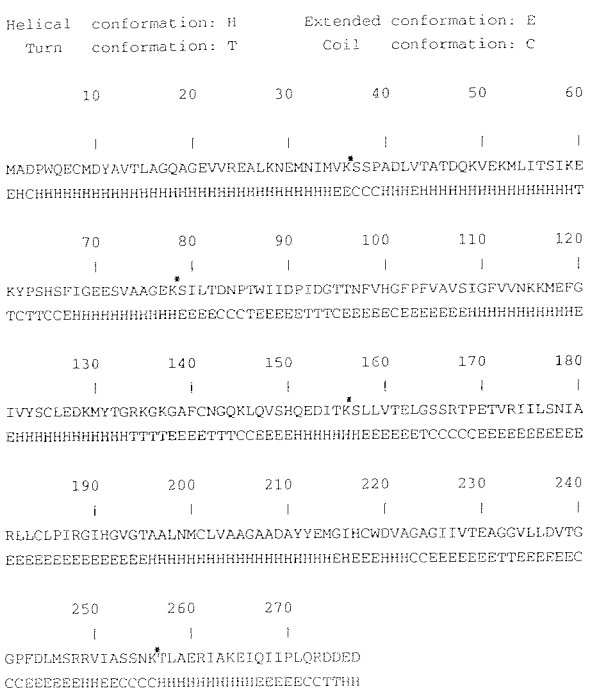


Fig. 3. The predicted secondary structure of inositol monophosphatase using the method of Garnier et al. [1].

The greater susceptibility to proteolysis of all these peptide bonds is probably due to them being more exposed in the proteins tertiary structure and therefore available to the protease. Such expectations are supported by structural predictions. Analysing the protein sequence of bovine inositol monophosphatase for potential antigenic regions by searching for regions of high flexibility [17,18] revealed that three out of the four proteolytic sites are predicted to be antigenic sites and therefore of high flexibility. Of these three sites, the region encompassing residues Val-35 to Asp-41 is most strongly predicted to be flexible. The other predicted sites are the regions between Ala-252 and Leu-258 and between His-150 and Ser-157.

It is interesting that all cleavages occur between lysine–serine bonds (i.e. Lys-36–Ser-37, Lys-78–Ser-79, Lys-156–Ser-157). Serine is a very weak helix former [1,19] and the cleavage sites identified lie at the carboxy ends of predicted α-helical motifs as shown in Fig. 3. Since the molecular weight of peptide IMPTrypt 2 suggests that it has undergone proteolysis at the carboxyl-terminal end there must be a susceptible proteolytic site available to trypsin. This site is possibly between Lys-256 and Thr-257 which is predicted to be at the amino-end of an α-helix. All of the cleavage sites available to trypsin but not endoprotease Lys-C involve a lysyl residue which is also the target residue for endoprotease Lys-C. Failure of the latter to cleave the protein at 3 of these sites may reflect a greater steric hindrance to the approach of this protease.

The amino-terminal region of inositol monophosphatase is strongly predicted to be α-helical in nature by the algorithm of Garnier et al. [1]. The sequence of this region of the protein may be represented in the form of a helical wheel, amphipathic in nature. It is interesting to note that Cys-8 resides on the hydrophobic face of this helix (an expected location for this amino acid in such a structure [20]). Such an observation is consistent with our previous findings [21] in which the cysteine residues of inositol monophosphatase where chemically modified by DTNB, *N*-ethylmaleimide and iodoacetic acid. In these studies only the cysteine residues at positions 141, 184 and 218 were available in the native conformation of the protein for modification by the above reagents. This observation also supports the gel filtration studies described above which suggest that loss of the amino-terminal peptide from the protein exposes an additional hydrophobic surface.

We have estimated the helical content of the protein from its circular dichroic spectrum in the far UV range to be between 185 and 260 nm (see Fig. 4). The spectrum shows a narrow shoulder on the negative peak of ellipticity at 205–210 nm and a wide negative elliptical band at 212–224 nm. Such a spectrum in this region is indicative of helix–helix interactions or some helical distortion (Dr. A. Drake, personal communication). Analysis of the data of Fig. 4 by the methods of Fasman [22] and Provencher and Glockner [23] suggest a helical content of 40% and 34%, respectively. These estimates are reasonably similar to that (47%) obtained using the structural prediction algorithm of Garnier et al. [1] which calculates the possible helical content of a protein without consideration of tertiary or quaternary structural interactions.

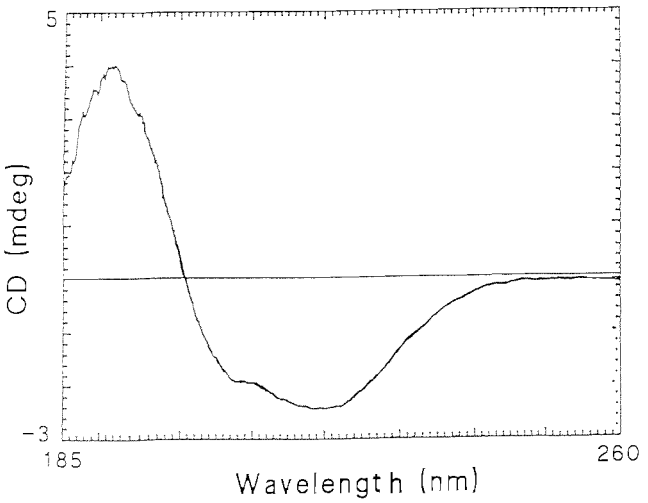


Fig. 4. The Circular Dichroic spectrum of a solution of inositol monophosphatase between 185 nm and 260 nm. The enzyme was dissolved (1 mg/ml) in 10 mM Tris-HCl buffer pH 8.0.

*Acknowledgements:* M.G.G. is indebted to the SERC Molecular Recognition Initiative for the provision of the ABI protein sequencer, to the SERC for the studentships to P.J.G. and K.R.-M. and to Dr. Alex Drake, University College, London, for his assistance with the Circular dichroism studies.

## REFERENCES

[1] Garnier, J., Osguthorpe, D.J. and Robson, B. (1978) J. Mol. Biol. 120, 97–120.
[2] Gee, N.S., Ragan, C.I., Watling, K.J., Aspley, S., Jackson, R.G., Reid, G.R., Gani, D. and Shute, J.K. (1988) Biochem. J. 249, 883–889.
[3] Hallcher, L.M. and Sherman, W.R. (1980) J. Biol. Chem. 255, 10986–10991.
[4] Nahorski, S.R., Ragan, C.I. and Challiss, R.A. (1991) Trends Pharmacol. Sci. 12, 297–303.
[5] Diehl, R.E., Whiting, P., Potter, J., Gee, N.S., Ragan, C.I., Linemeyer, D., Schoepfer, R., Bennett, C. and Dixon, R.A. (1990) J. Biol. Chem. 265, 5946–5949.
[6] McAllister, G., Whiting, P.J., Hammond, E.A., Knowles, M.R., Atack, J.R., Bailey, F.J., Maigetler, R. and Ragan, C.I. (1992) Biochem. J. 285, 461–468.
[7] Gee, N.S., Knowles, M.R., McAllister, G. and Ragan, C.I. (1991) FEBS Lett. 284, 95–97.
[8] Whiting, P., Gee, N.S., Potter, J., Howell, S. and Ragan, C.I. (1990) Biochem. J. 272, 465–468.
[9] Gee, N.S., Howell, S., Ryan, G. and Ragan, C.I. (1989) Biochem. J. 264, 793–798.
[10] Lanzetta, P.A., Alvarez, L.J., Reinach, P.S. and Candia, O.A. (1979) Anal. Biochem. 100, 95–97.
[11] Gore, M.G., Greasley, P.J. and Ragan, C.I. (1992) J. Biochem. Biophys. Methods 25, 55–60.
[12] Smith, P.K., Krohn, R.I., Hermanson, G.T., Mallia, A.K., Gartner, F.H., Provenzano, M.D., Fujimoto, E.K., Goeke, N.M., Olson, B.J. and Klent, D.C. (1985) Anal. Biochem. 150, 76–85.
[13] Laemmli, U.K. (1970) Nature 227, 680–685.
[14] Matsudaira, P. (1987) J. Biol. Chem. 262, 10035–10038.
[15] Shute, J.K., Baker, R., Billington, D.C. and Gani, D. (1988) J. Chem. Soc. Chem. Commun., 626–628.
[16] Meek, J.L., Rice, T.L. and Anton, E. (1988) Biochem. Biophys. Res. Commun. 156, 143–148.
[17] Van Rengenmortal, M.H.V. (1986) Trends Biochem. Sci. 11, 36–39.
[18] Karplus, P.A. and Schutz, G.E. (1985) Naturwissenschiften 72, 212–213.
[19] Chou, P.Y. and Fasman, G.D. (1978) Adv. Enzymol. 47, 45–148.
[20] Kyte, J. and Doolittle, R.F. (1982) J. Mol. Biol. 157, 105–132.
[21] Knowles, M.R., Gee, N.S., McAllister, G., Ragan, C.I., Greasley, P.J. and Gore, M.G. (1992) Biochem. J. 285, 461–468.
[22] Fasman, G.D. (1974) PAABS Rev. 2, 587–591.
[23] Provencher, S.W. and Glockner, J. (1981) Biochemistry 20, 33–40.

Volume 321, number 1, 37–40 FEBS 12331 April 1993


# Bovine inositol monophosphatase

## The identification of a histidine residue reactive to diethylpyrocarbonate

K.J. Rees-Milton[a], P.J. Greasley[a], C.I. Ragan[b] and M.G. Gore[a]

[a]*SERC Centre for Molecular Recognition, Department of Biochemistry, University of Southampton, Southampton, S09 3TU, UK* and [b]*Neurosciences Research Centre, Merck Sharp and Dohme, Harlow, Essex, UK*

Received 1 March 1993

The inositol monophosphatase from bovine brain is inactivated by the histidine-specific reagent diethylpyrocarbonate. Using 4 mM reagent at pH 6.5, the reaction results in the modification of 3 equivalents of histidine per polypeptide chain. The loss of activity occurs at the same rate as the slowest reacting of these residues. Site directed mutagenesis studies have been used to generate a mutated enzyme species bearing a His-217→Gln replacement and have shown that it is the modification of histidine 217 which results in the inactivation of the enzyme.

Inositol monophosphatase; Histidine; Diethylpyrocarbonate; Site-directed mutagenesis

## 1. INTRODUCTION

Bovine inositol monophosphatase is a key enzyme of the phosphatidylinositol signalling system [1,2] and has been implicated as the therapeutic target for lithium in the treatment of manic depression [3]. Agonists binding to receptors stimulate the generation of the second messengers, inositol-1,4,5-trisphosphate (Ins(1,4,5)*P*) and *sn*1,2-diacylglycerol, via the phosphatidylinositol cycle. A series of phosphatases and kinases [1] result in the recycling of inositol for subsequent re-synthesis of the phosphatidylinositols. Bovine inositol monophosphatase catalyses the final dephosphorylation step of inositol 1-phosphate (Ins(1)*P*), inositol 3-phosphate (Ins(3)*P*) and inositol 4-phosphate (Ins(4)*P*) to inositol and inorganic phosphate [1].

Since transport of dietary inositol across the blood–brain barrier is slow [4] there are just two main sources of the inositol to maintain the synthesis of phosphatidyl inositol. One is the de novo synthesis of inositol from glucose 6-phosphate via inositol monophosphatase [5] and the second is the dephosphorylation of Ins(1)*P*, Ins(3)*P*, or Ins(4)*P* again by inositol monophosphatase. Hence, this enzyme occupies a pivotal position in the recycling and supply of inositol in the brain.

Bovine inositol monophosphatase is a homodimer with subunits of $M_r$ 30,055 [6]. There is an absolute requirement for $Mg^{2+}$ for catalytic activity [7] although concentrations of this ion above 10 mM lead to uncompetitive inhibition of the enzyme [7].

To date, there is relatively little known concerning the amino acid residues important for catalysis. The modification studies of Knowles et al. [8] have demonstrated that reaction of Cys-218 with *N*-ethylmaleimide results in the loss of catalytic activity seen in this enzyme. However, use of site directed mutagenesis to replace Cys-218 by Ala showed that although substrate protected the enzyme against modification , this residue is not essential for activity suggesting that this modification inhibits the enzyme by steric effects.

More recently, studies using the histidine specific reagent, DEP, have been performed and shown that all five histidine residues of the enzyme can be modified [9]. The modification occurs in at least two identifiable phases, two equivalents reacting rapidly with no effect on activity and three more equivalents reacting at a slower rate. Although the enzyme is inhibited by DEP modification, the loss of activity occurs at the slower rate. The site of action was not identified but total loss of activity did not occur until all five histidine residues had been modified.

In this paper we combine the use of site directed mutagenesis and chemical modification techniques to propose that it is the modification of His-217 by DEP which leads to the loss of enzyme activity.

## 2. MATERIALS AND METHODS

### 2.1. *Preparation of enzyme*

The recombinant enzyme was expressed and purified by the method described for the human enzyme [10] except that the heat treatment step was carried out at 60°C.

*Correspondence address:* M.G. Gore, Dept. of Biochemistry, University of Southampton, Bassett Crescent East, Southampton, S09 3TU, UK.

*Abbreviations:* DEP, diethylpyrocarbonate; IMPase, inositol monophosphatase.

2.2. *Assay of enzyme activity*

The enzyme was assayed using the direct fluorescence assay as described in Gore et al. [11].

2.3. *Protein estimation*

The protein concentration was estimated using the Bicinchinoic acid method of Smith et al. [12].

2.4. *Determination of extinction coefficient for DEP modified histidine residues*

The extinction coefficient for DEP modified histidine depends on the environment [13], and was therefore determined in the buffer system employed in these experiments (20 mM MES, pH 6.5), by the addition of excess DEP to known concentrations of histidine. Under these conditions the extinction coefficient at 240 nm for DEP modified histidine is 2727 $M^{-1}\cdot cm^{-1}$.

2.5. *Chemical modification*

A solution of enzyme (25 $\mu$M) in 20 mM MES buffer, pH 6.5 at 25°C was incubated with 4 mM DEP taken from a stock of 1 M DEP dissolved in anhydrous ethanol. The effective concentration of the DEP solution was determined using the imidazole method [13]. The stoichiometry of the reaction was monitored by following the increase in absorbance at 240 nm ($\varepsilon_{240nm}$ = 2727 $M^{-1}\cdot cm^{-1}$).

2.6. *Site directed mutagenesis*

Oligonucleotide-directed mutagenesis was carried out by the method of Kunkel et al. [14,15]. The plasmid used was the pRSET vector containing the gene coding for the bovine brain inositol monophosphatase [16]. The oligonucleotide 5'ATCCCAGCATTG-GATCCCAT (His-217→Gln) was synthesised on an Applied Biosystems model 380 DNA synthesiser and used in the mutagenesis procedure to generate the mutant. The sequence of the mutant was determined by the dideoxy chain termination method of Sanger et al. [17].

2.7. *Gel permeation studies*

The integrity of the dimeric nature of the enzyme after modification with DEP was determined by use of a Gilson HPLC system equipped with a 250 mm×7.5 mm TOSOH-TSK G3000SW gel permeation column equilibrated 20 mM MES pH 6.5.

## 3. RESULTS AND DISCUSSION

Preliminary studies using DEP to inactivate IMPase showed that the use of a lower concentration of the reagent than that used by Pelton and Ganzhorn [9] permits inactivation of the enzyme without total modification of all five histidine residues. For example, Fig. 1 shows that when IMPase is incubated with 4 mM DEP at pH 6.5 it is approximately 63% inactivated with a second order rate of 14.1 ± 1.6 ($n$=3) $M^{-1}\cdot min^{-1}$ (Table I). Analysis of the stoichiometry of modification monitored by the change in absorption at 240 nm ($\varepsilon_{240nm}$ = 2727 $M^{-1}\cdot cm^{-1}$, see section 2) show that under these conditions three equivalents of histidine per subunit are modified (Table I). The data analysis was carried out as described in Dominici et al. [18] and compensates for the hydrolysis of the reagent during the incubation with enzyme. Two equivalents react with a second order rate of approximately 224 ± 17 $M^{-1}\cdot min^{-1}$ and these reactions have no effect on enzyme activity. A third equivalent reacts at a slower rate of 19.4 ± 1.8 $M^{-1}\cdot min^{-1}$ which is approximately the same rate as that of loss of activity. In the additional presence of 2 mM Ins(1)$P$,

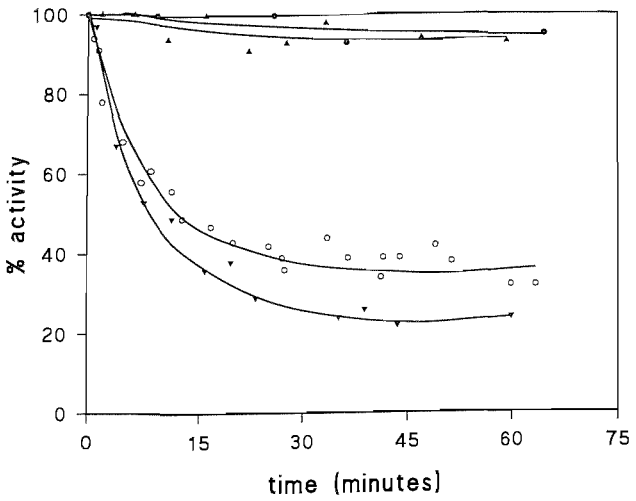


Fig. 1. Inactivation of bovine inositol monophosphatase by DEP. 1.5 ml of enzyme ($M_r$ 30,055) in 20 mM MES, pH 6.5 was incubated at 25°C with 4 mM DEP and 50 l samples taken periodically and assayed for activity by a fluorescent assay [9]. The curves shown represent incubations of DEP with native IMPase (○) or mutated enzymes C218A (▼), H217Q (●) and IMPase +2 mM Ins(1)$P$, 20 mM $MgCl_2$, 100 mM LiCl (▲).

100 mM $Li^+$ and 20 mM $Mg^{2+}$ (as the chloride) the enzyme was not inactivated by DEP ( Fig. 1) and only the 2 fast reacting equivalents of histidine were modified per subunit. These data show that the slowest reacting of the three sites modified under these conditions may be protected by the presence of substrate and $Li^+$ and may therefore be at or near the active site of the enzyme. The enzyme is a dimer of identical subunits and gel-filtration experiments (see section 2) have confirmed that this quaternary arrangement is not perturbed by the modification of these three residues per subunit.

The reagent used in these modification experiments is not always specific for histidinyl residues, sometimes being reactive to cysteinyl, tyrosyl and lysyl side chains [13]. Previous studies have demonstrated that Cys-218 lies at or close to the active site and that modification of this group by *N*-ethylmaleimide causes loss of enzyme activity although mutagenesis studies subsequently demonstrated that this residue is not essential for catalytic activity. In order to eliminate the possibility of DEP reacting at this site, a mutant of IMPase, in which Cys-218 was replaced with Ala, was reacted with the reagent. This mutated enzyme was still inactivated at approximately the same rate as the native enzyme (Table I) and approximately 3 equivalents of histidine were modified per subunit, the same as for wild-type enzyme. It can be concluded therefore that it is not the modification of Cys-218 by DEP that inactivates the enzyme. Furthermore the addition of 1 M hydroxylamine to the modified and inactivated enzyme led to the regain of all control activity indicating that histidinyl residues had been modified by the DEP.

However, the close proximity of His-217 to Cys-218 in the protein sequence suggests that modification of this residue by DEP might result in the inactivation of the enzyme. This possibility was investigated by reacting another mutant of IMPase bearing a His-217→Gln replacement with DEP. This mutated enzyme was only inactivated by 6% (Fig. 1) by the reagent at a rate ($0.23 \pm 0.08$ $M^{-1} \cdot min^{-1}$) which is approximately 100-fold slower than that of the native protein. Significantly only two equivalents of histidine per subunit were modified (Table I) whether substrate and $Li^+$ ions were or were not present. Thus it can be inferred that the slowest reacting of the three sites of modification by DEP is the one associated with loss of activity and that this site is His-217 in the native enzyme. This in turn implies that His-217 is located at or near the active site, a realistic possibility since Cys-218 has been suggested by other experiments to be similarly located.

Ganzhorn and Chanal [19] reported kinetic results which show that catalytic activity of this enzyme depends upon the deprotonation of two groups of $pK_a$ 6.5 and Pelton and Ganzhorn [9] suggested that either or both of these may be due to His residues. The reagent DEP reacts with the unprotonated side chains of histidine and therefore the rate of reaction will depend upon the accessibility of the site to be modified and to the $pK_a$ of the group. Previous studies on the enzyme from human brain have shown that the $pK_a$ of His-217 is higher than would be expected (approximately at pH 7.5) [20] and might therefore be relatively unreactive to the reagent [13] and hence have a slower rate of modification as found in the above experiments.

Further comparison of the sequence of the enzyme from human, bovine and rat brain [10] show that His-150 is unlikely to be catalytically important since it is not conserved in the human or rat enzymes which have a Gln replacement. Previous labelling studies using [$^3$H]-iodoacetic acid [8] have shown that the only histidine residue modified under the conditions used was His-65 and no loss of activity occurred. However, this observation may suggest that His-65 is very exposed or reactive and may therefore be one of the fast reacting sites with DEP.

Stoichiometry experiments showed that when 3 equivalents are modified in the native enzyme the loss of activity is only approximately 63–69% (Table I). Whereas treatment of the native and His-217→Gln mutant enzymes by higher concentrations of DEP (29 mM) results in modification of $4.8 \pm 0.2$ and $4.0 \pm 0.2$ equivalents of histidine per subunit, respectively, we noted little further loss of activity than occurred when only 3 and 2 equivalents (respectively) were modified (see Table I). These observations are in contrast to those of Pelton and Ganzhorn [9].

Finally, previous results of experiments using the human enzyme [20] have shown that like the Cys-218 Ala mutant, the His-217→Gln mutated enzyme is fully active with the same $K^m$ for substrate as the native enzyme but with an apparent $K_m$ for $Mg^{2+}$ approximately 4-fold higher than that of the native enzyme [20]. The latter data, together with the inactivation studies described above, suggest that the His-217 residue lies at or near to the active site of the enzyme but is not involved in the catalytic mechanism. This conclusion is supported by similar results we obtained using *N*-ethylmaleimide to modify Cys-218 [8]. In these studies it was also found that modification of the target residue did not result in full inactivation of the enzyme.

Table I

Modification of Inositol monophosphatase by diethylpyrocarbonate. The table shows the rates of inactivation of inositol monophosphatase enzymes by DEP in the presence or absence of substrate and $Li^+$ ions together with the number of equivalents of histidine modified per subunit.

| Enzyme | % Active loss | $K_{inact}$ $M^{-1} \cdot min^{-1}$ | No. of equivalents modified |
|---|---|---|---|
| Native ($n$=3) | 63.3 ± 0.6 | 14.1 ± 1.6 | 2.95 ± 0.24 |
| Native ($n$=4) | 64.9 ± 9.2 | – | 4.8 ± 0.2 |
| Native + Ins(1) $P$ + $Li^+$ ($n$=2) | 7 ± 3.5 | 0.23 ± 0.08 | 1.90 ± 0.20 |
| His-217→Gln ($n$=2) | 6 ± 1.4 | 0.27 ± 0.12 | 1.85 ± 0.26 |
| His-217→Gln ($n$=4) | 5 ± 4.1 | – | 4.0 ± 0.2 |
| Cys-218→Ala ($n$=2) | 69 ± 8.5 | 14.1 ± 0.5 | 2.81 ± 0.2 |

*Acknowledgements:* We are indebted to the SERC for a studentship to KRM and to the Wellcome Trust for a Fellowship for P.G.

## REFERENCES

[1] Shears, S.B. (1989) Biochem. J. 260, 313–324.
[2] Downes, C.P. and Mitchell, R.H., in: Molecular Mechanisms of Transmembrane Signalling (P. Cohen and M.D. Housley, Eds.), Elsevier, Amsterdam, 1985, pp. 3–56.
[3] Berridge, M.J., Downes, C.P. and Hanley, M.R. (1989) Cell 59, 411–419.
[4] Spector, R. and Lorenzo, A.V. (1975) Am. J. Physiol. 228, 1510–1518
[5] Eisenberg, F. Jr. (1967) J. Mol. Chem. 242, 1375–1382.
[6] Gee, N.S., Ragan, C.I., Watling, K.J., Aspley, S., Jackson, R.G., Reid, G.R., Gani, D. and Shute, J.K. (1988) Biochem. J. 249, 883–889.
[7] Hallcher, L.M., Sherman, W.R. (1980) J. Biol. Chem. 255, 10896–10901.
[8] Knowles, M.R., Gee, N., McAllister, G., Ragan, C.I., Greasley, P.G. and Gore, M.G. (1992) Biochem. J. 285, 461–468.
[9] Pelton, P.D. and Ganzhorn, A.J. (19920 J. Biol. Chem. 267, 5916–5920.
[10] McAllister, G., Whiting, P.J., Hammond, E.A., Knowles, M.R., Atack, J.R., Bailey, F.J., Maiggetler, R. and Ragan, C.I. (1992) Biochem. J. 284, 749–754.
[11] Gore, M.G., Greasley, P.J. and Ragan, C.I. (1992) J. Biochem. Biophys. Methods. 25, 55–60.
[12] Smith, P.K., Krohn, R.I., Hermanson, G.T., Mallia, A.K., Gartner, F.H., Provenzano, M.D., Fujimoto, E.K., Goeke, N.M., Olson, B.J. and Klent, D.C. (1985) Anal. Biochem. 150, 76–85.

[13] Miles, E.W. (1977) Methods Enzymol. 47, 431–442.
[14] Kunkel, T.A. (1985) Proc. Natl. Acad. Sci. USA 82, 488–492.
[15] Kunkel, T.A., Roberts, J.D. and Zakour, R.A. (1987) Methods Enzymol. 154, 367–382.
[16] Diehl, R.E., Whiting, P., Potter, J., Gee, N., Ragan, C. I., Linemeyer, D., Schoepfer, R., Bennett, C. and Dixon, A.F. (1990) J. Biol. Chem. 265, 1–4.
[17] Sanger, F., Nicklen, S. and Coulson, A.R. (1975) Proc. Natl. Acad. Sci. USA 74, 5463–5467.
[18] Dominici, P., Tancini, B. and Voltattorni, C.B. (1985) J. Biol. Chem. 260, 10583–10589.
[19] Ganzhorn, A.J. and Chanal, M.C. (1990) Biochemistry 29, 6065–6071.
[20] Greasley, P.J., McAllister, G., Ragan, C.I. and Gore, M.G., Biochem. J., submitted.